FINAL REPORT

MEMS
Micro Electro-Mechanical Systems for
Wirelessly Monitoring the Health of
Transportation Related Structures

Infrastructure Technology Institute

Northwestern University

Principal Investigator: Charles H. Dowding

SAFETEA-LU: 3/7/2008 – 8/31/2012

NU-ITI Project 60020780 (A224)

MEMS Micro Electro-Mechanical Systems for Wirelessly Monitoring the Health of Transportation Related Structures: Summary

C.H. Dowding, M. Kotowsky, D. Meissner, T. Koegel

This project report begins with this overarching summary of the project and is followed by full reports of the details of the five principal phases of the project. Each of these phase reports begins with a summary that describes the objective, context, work and the major findings. The longer, full phase reports contain detailed findings and supporting information. References are presented at the end.

Introduction

This report on Micro Electro-Mechanical Systems (MEMS) describes the development of small, wireless systems to monitor the response of cracks for structural health monitoring on and near transportation related structures. Developed were two types of wireless structural health monitoring (SHM) systems to record characteristics of cracks over long periods of time: Autonomous Crack Monitoring (ACM) and Autonomous Crack Propagation Sensing (ACPS). ACM seeks to correlate changes in widths of cosmetic cracks in structures to nearby blasting or construction vibration activity for the purposes of litigation or regulation. ACPS seeks to track growth of cracks in steel bridges, supplementing regular inspections and alerting stakeholders if a crack has grown.

The ever decreasing size and increasing performance of computer technology suggest that expensive, labor-intensive, and intrusive wired SHM systems may be replaced by a similarly capable, easier to install, yet less expensive and intrusive wireless SHM systems based on existing, commercially available wireless sensor networks. The implementation of a wireless SHM system with all the functions of a standard, wired, AC powered system, no requirement for an on-site personal computer for system operation, a small enough footprint such that it will not disturb residents of the instrumented structure, or interfere with the operation of a transportation related structure, a sensor suite that can be operated with minimal power use, and system operation for at least six months without a battery change or any other human intervention, is fraught with obvious and non-obvious challenges.

Description of the Technology and Context for Transportation Related Need

Wireless sensor networks (WSNs), which form the foundation for MEMS systems, consist of a network of miniature nodes, or “motes,” that communicate with one or more base stations via 420 to 450 megahertz radio links as shown in Figure 1. This radio communication then allows transportation structures and those nearby to be to be wirelessly monitored remotely from a powered base station connected to the internet. In general, motes are designed to be small, low-cost, relatively interchangeable, and in many cases, redundantly deployed. Wireless systems eliminate the need to string wires across large, complex, and potentially dangerous facilities such as bridges, highway and railroad rights of way, and other structures.

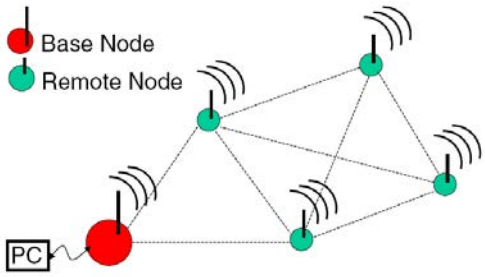

Figure 1: Sensor nodes, placed within the monitored structure, communicate wirelessly with the base node through multiple pathways. Each node operates as both a sensing as well as a data transmission node.

Each mote is made up of a processing unit, a radio transceiver, a power unit, and a sensing unit. The two main components within the sensing unit are an analog-digital converter (ADC) and software-switchable power sources to activate and deactivate sensors. The sensors, ADCs, and switchable power supplies are either integral to the mote itself or added by means of an external sensor board that is physically attached to the mote. In none of the WSNs described in this project does any data processing occur on the motes themselves – all data is transmitted back to the base station before any data processing might occur. For more detail on motes, nodes and their components, see Ozer (2005) and Kotowsky (2010). Nodes consist of the "mote" plus sensing transducers.

Two principal sensors have been developed and or field qualified in this project that operate optimally with wireless systems for SHM of structures associated with transportation facility construction or operation: string potentiometer displacement sensors for the ACM systems and ladder-patterned crack propagation sensors for the ACPS systems. By using a low voltage to power the ACM system potentiometer, power consumption can be lowered significantly to increase battery life sufficiently for use with wireless SHM systems. Crack propagation sensors in ACPS systems inherently operate in low power environments as they measure crack length by change of resistance, which is an inherently lower power operation.

ACM systems

There are two modes of operation for ACM systems. Mode 1 only requires measurement at definable intervals of time (e.g. every 15 to 60 minutes). Mode 2 requires measurement of short, random events. Blasting, passage of vibratory rollers, large trucks, trains, and earthquakes are examples of such random events. Current wireless systems operate optimally in mode 1. They can operate in a sleep mode at all times except for the few seconds required for measurement, which requires little power. Mode 2 requires operation at all times, which consumes large

amounts of power and frequent exchange of batteries. A low power consumption trigger device can overcome this inherent weakness in current MEMS devices that are designed primarily to provide mode 1 information.

A new hardware device, Shake 'n Wake, was developed to trigger ACM mode 2 operation of wireless SHM systems. Shake 'n Wake has proven to:

(1) not significantly increase the power consumption of a mote (Phase A)
(2) not contaminate the output signal of its attached sensor (Phase C)
(3) provide a predictable and repeatable trigger threshold (Phase C)
(4) awaken the mote in time to record the highest amplitudes of the motion of interest (Phase C)

The Shake 'n Wake triggering device can trigger any wireless SHM device and is not limited to ACM systems described herein.

An ACM mode 2 triggering device requires the ability to determine whether a vibratory event has occurred and is of sufficient magnitude to be deemed an event of interest. Traditional wired ACM systems make this determination by continuously sampling the output of a velocity transducer (geophone) at a high frequency, typically one thousand times per second, and comparing the sampled value to a predetermined threshold value. Should the sampled value exceed the trigger threshold, the ACM system begins recording at one thousand samples per second from the geophone and all crack displacement sensors. This process of continuous digital comparison, while possible to implement using a wireless sensor network, is not practical if the system is to operate for months without replacing or recharging its batteries. The continuous process of sampling, converting the signal to a digital value, and comparing that signal with a stored threshold value requires constant attention from the ACM system, which consumes significant amounts of battery power.

ACPS Systems

Autonomous Crack Propagation Sensing (ACPS) is a measurement technique designed to record the propagation of slow-growing structural cracks over long periods of time. In contrast to ACM, ACPS, does not seek to directly correlate crack extension to any other physical phenomena; rather ACPS seeks to record quantitatively, repeatedly, and accurately the extension of cracks in structures, specifically to supplement regular inspections of bridges. An ACPS system could alert structural stakeholders of crack extensions with ample time to ensure the safety of the structure and its users.

Though ACPS techniques can be applied to any structure that exhibits cracking over time, the primary motivation in the development of this technique is to supplement the in-service inspection of fatigue cracks in steel bridges. Fatigue cracks in steel tend to grow slowly over time, and when found during routine inspection of steel bridges, they are cataloged according to procedures laid out in the Bridge Inspector's Reference Manual (USDOT, FHWA 2006) . These cracks are then re-examined at the next inspection and compared to records to determine whether the crack has grown. ACPS, especially on bridges, is an ideal application for a wireless sensor network. Running wires across bridges between different points of interest is

usually cost-prohibitive and is often impossible due to superstructure configuration and access restrictions. Since access can be difficult and expensive, it is desirable to minimize installation time and maximize time between maintenance visits, so long-lasting solar-powered nodes are ideal. Furthermore, power management strategies implemented by the manufacturers of existing wireless sensor networks are well-suited to the low sampling rate required by ACPS.

Field Qualification

While laboratory qualification is an important step in development of new instruments, field testing in actual operation is also important for commercialization and adoption by the construction industry. The wireless ACM system (based upon commercially available, weather rugged motes) developed in this MEMS project was installed in a residential test structure adjacent to an aggregate quarry. Quarries like this supply road aggregate, and their continuous operation is important in controlling the cost of constructing transportation infrastructure. The residential structure is typical of structures that are found adjacent to transportation facilities under construction and operation. The wireless ACM system was installed alongside a traditional wired ACM system to compare its performance.

Field performance the weather rugged ACM wireless system was based upon ability to measure long term (mode 1) response of an interior cosmetic crack in a residential structure. Wireless data loggers managed the response of low power draw potentiometers that measured micrometer changes in crack width. Assessment criteria included: fidelity of the measured crack response, ease of installation, cost, resolution of structural health measurement, length of operation under a variety of conditions without intervention, and ease of display and interpretation of data.

Synopsis of Findings

Major findings of this MEMS project to develop small wireless sensor network systems (WSNs) to measure crack response are summarized below by phase. Each of these five (5) phases (A through E) begins with a summary which describes the objective, context, work and major finding. The longer, full reports contain all detailed findings and supporting information. These phases follow one another, but may summarize several years of effort and thus overlap. This overlapping occurs because the multiple stages of field work: conception, installation, operation, synthesis, report writing, and summary article writing may require a few years to complete.

Final Report for Phase A:
Determination of Battery Performance of Wireless Sensors when Adding Shake 'n Wake (SnW) Random Event Trigger to MICA-2 Wireless Sensor Network[1]

M. Kotowsky and C. Dowding

Summary

Objective of this phase of the MEMS project
Determine the battery life of a wireless system when coupled to a low power consuming system that is capable of being triggered by random vibratory events near transportation facilities under construction or operation.

Context
Battery life of wireless systems is a key consideration. If batteries must be switched out too often, the advantage of automated, remote monitoring is lost. This consideration is especially critical for systems that monitor random dynamic events in transportation related structures. The traditional – and currently only ---means of guaranteeing capture of an event lasting only 10ths of a second is to record continuously and then save a prerecorded signal if the system is triggered. Recording continuously drains battery power so rapidly that battery life of current small MEMS wireless systems may last only a handful of days. The Shake 'n Wake (SnW) system adds a velocity transducer to awaken the wireless sensor network (WSN) so it can measure a random dynamic event without constant sensing and thus consuming large amounts of battery power.

Summary of Work
The combined SnW-WSN system was placed in a test structure to determine the power consumption and thus battery life in a field setting. Figure AS-1 shows one of the nodes (mote plus sensor). Assessment of these field measurements showed that the SnW trigger allowed the wireless motes to respond to randomly occurring events without sacrificing power. Figure AS-2 compares the wirelessly monitored temperature, humidity, crack responses, and vibration produced interrupts over a 75 day interval. While suitability of the SnW system was determined with MICA-2 wireless system, it can be ported to any wireless system that allows access to the interrupt lines. Thus SnW can be employed to monitor vibratory structural health of transportation related structures and not require additional power or batteries provided the WSNs samples at a sufficiently high rate of data acquisition.

Continued on next page.

[1] DISCLAIMER
The contents of this report reflect the views of the authors, who are responsible for the facts and the accuracy of the information presented herein. This document is disseminated under the sponsorship of the Department of Transportation University Transportation Centers Program, in the interest of information exchange. The U.S. Government assumes no liability for the contents or use thereof.

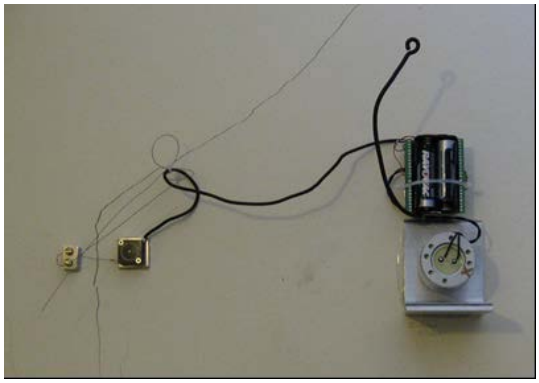

Figure AS-1 Photograph of (from left to right) string potentiometer across crack with MICA-2 mote with aerial, and Shake ‘n Wake velocity transducer below the mote. The small size of the mote can be understood by the two AAA batteries that completely cover the footprint of the mote. The string potentiometer is the size of quarter.

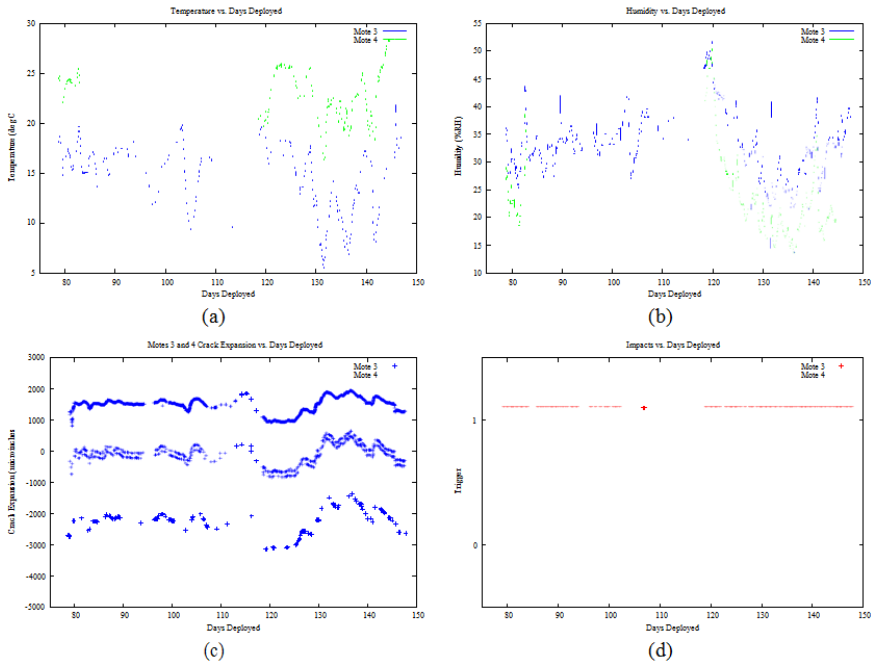

Figure AS-2: Time histories of (a) temperature (b) humidity (c) crack displacement and (d) Shake ’n Wake triggers recorded by the Version 3 of the wireless ACM system over the 75-day period of interest.

Major Finding:

Shake ‘n Wake system can be employed without significantly increasing power consumption and could allow wireless sensor networks (WSNs) to be employed to detect vibratory events associated with transportation facilities under construction or operation provided the WSNs support high sample rate data acquisition. More detailed findings are presented in the following full report.

Final Report for Phase A:
Determination of Battery Performance of Wireless Sensors when Adding Shake 'n Wake (SnW) Random Event Trigger to MICA-2 Wireless Sensor Network

M. Kotowsky and C. Dowding

Introduction

This Phase A report describes the field trial of the Shake 'n Wake system to determine its ability to trigger a Mica 2 wireless sensor network (WSN) to measure random dynamic events (mode 2 operation) with a minimal reduction in WSN battery power. Mode 2 recording requires an ACM system to have the ability to determine whether a vibratory event has occurred and is of sufficient magnitude to be deemed an event of interest. Traditional wired ACM systems make this determination by sampling continuously the output of a geophone at a high frequency, typically one thousand times per second, and comparing the sampled value to a predetermined threshold value. Should the sampled value exceed the trigger threshold, the ACM system begins recording at one thousand samples per second from the geophone and all crack displacement sensors. Figure A-1 shows this process.

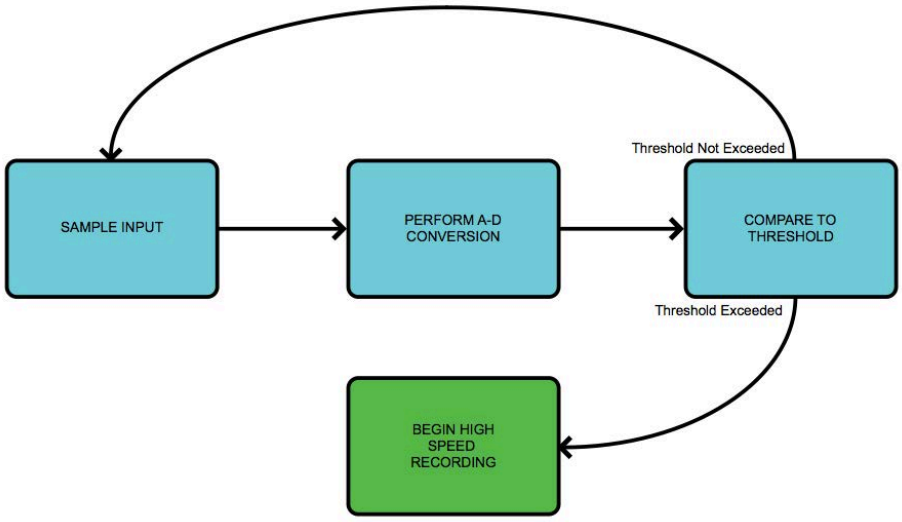

Figure A-1: Traditional wired ACM system's determination of threshold crossing

This process of continuous digital comparison, while possible to implement using a wire- less sensor network, is not practical if the system is to operate for months without replacing or recharging its batteries. The continuous process of sampling, converting the signal to a digital value, and comparing that signal with a stored threshold value requires constant attention from the control processor, signal conditioners, and analog-to-digital conversion circuitry. Implementation of Mode 2 recording with a WSN therefore required the design and fabrication of a new hardware device to process the input from a geophone and determine whether or not it has detected an event of interest, all without overtaxing the limited energy supply of a typical mote. This new hardware device, Shake 'n Wake, was conceived with the following design criteria:

(1) It must not significantly increase the power consumption of a mote.

(2) It must not contaminate the output signal of its attached sensor.
(3) Its trigger threshold must be predictable and repeatable.
(4) It must wake up the mote in time to record the highest amplitudes of the motion of interest.

Each of these criteria were proven to have been met by the Shake 'n Wake design. The results of the experiment to verify criterion 1 are detailed below (see Analysis of Power Consumption). The rest of the results of the experimental verification are detailed in Phase C.

Shake 'n Wake System Design (Version 3)

Geophone Selection

Though the Shake 'n Wake will operate with any type of sensor that produces a voltage output, a passive, or self-powered, sensor is necessary to realize practical power savings. A geophone, a passive sensor that produces output voltage using energy imparted to it by the very motion that it measures, is an ideal sensor to pair with the Shake 'n Wake. Two geophones were experimentally tested with the Shake 'n Wake: a GeoSpace GS-14-L3 28 Hz 570Ω geophone, pictured in Figure A-2a and a GeoSpace HS-1-LT 4.5 Hz 1250Ω geophone, pictured in Figure A-2b. Response spectra for these geophones can be found in Kotowsky (2010).

To maximize the signal-to-noise ratio of the output of the geophones, shunt resistors were not installed at the geophone output terminals.

(a)
(b)

Figure A-2: (a) GeoSpace GS 14 L3 geophone (b) GeoSpace HS 1 LT 4.5 Hz geophone

McKenna (2002) showed that the dominant frequencies of the walls and ceilings in a wide variety of residential structures are between 8 and 15 hertz. The HS-1 geophone has a minimum defined non-shunted response frequency of approximately 1.5 hertz and is therefore well-suited to measuring the expected structural response. The GS-14 geophone, with a minimum defined non-shunted response frequency of 12 hertz, is not as well suited but its smaller size makes it more attractive for installation in an occupied residential structure.

Shake 'n Wake Design

The Shake 'n Wake board, shown in Figure A-3, implements the same modular design and is the same size is the commercially available sensor boards manufactured by Crossbow. It can therefore be attached to any MICA-based wireless sensor mote by way of its standard 51-pin connector. Shake 'n Wake implements the hardware portion of the Lucid Dreaming strategy for event detection in energy constrained applications introduced by Jevtic et al. (2007a).

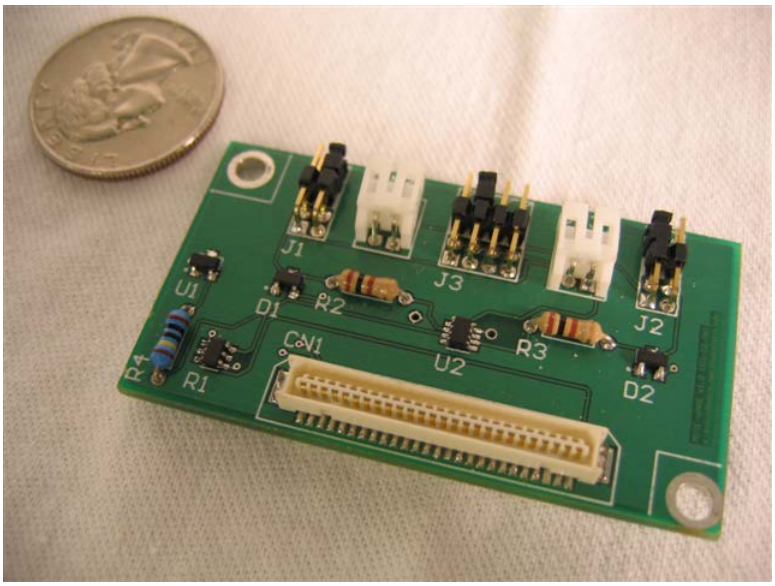

Figure A-3: The Shake 'n Wake sensor board, after Jevtic et al. (2007a)

Because of the single-ended design of the low-power analog comparator on which the Shake 'n Wake hardware is based, the device cannot inspect both the positive and negative portions of any geophone output waveform using a single comparator. To avoid ignoring either half of an input waveform, the Shake 'n Wake board has two comparators and provides the user with two sensor input connectors: CN3 and CN4. The output leads from the geophone are wired simultaneously to CN3 and CN4, but the connectors have opposite polarities. This wiring ensures that both the positive and negative portions of the geophone output will be considered in determining whether the triggering threshold is crossed.

CN3 passes its input signal directly to a comparator that compares the positive portion of the input waveform to the user-specified threshold while ignoring the negative portion; CN4 passes the inversely polarized input signal to a second, identical comparator which compares the negative portion of the input waveform to the threshold while ignoring the positive portion. The same user-supplied threshold is applied to both signals. Either connector can be disabled using the jumper switches J1 and J2. Jumper J3 provides the ability to select the interrupt controller address on the MICA2's processor over which the Shake 'n Wake can communicate the occurrence of a threshold crossing, thus ensuring compatibility with other sensor boards that might also need to interrupt the mote's processor (Jevtic et al., 2007a).

The voltage input threshold at which the Shake 'n Wake board will wake up the mote's main control processor can be set in software by the user both before and after deployment

of the mote. The variability of the trigger threshold is achieved by using a programmable potentiometer with a 32-position electronically reprogrammable wiper which is placed in series with a precision 1.263 V DC reference and a 1 MΩ precision resister (Jevtic et al., 2007a). Figure A-4 shows a simplified diagram of the voltage comparison circuitry. V_{comp}, the reference voltage to which the geophone output is compared, is directly determined by the position of the wiper, x, which is an integer between 0 and 31, inclusive. Thus, the threshold voltage to which the input voltage is compared is:

$$Vcomp = 3.558 * x$$

where Vcomp is the threshold voltage (in millivolts) and x is the setting (0-31) of the potentiometer.

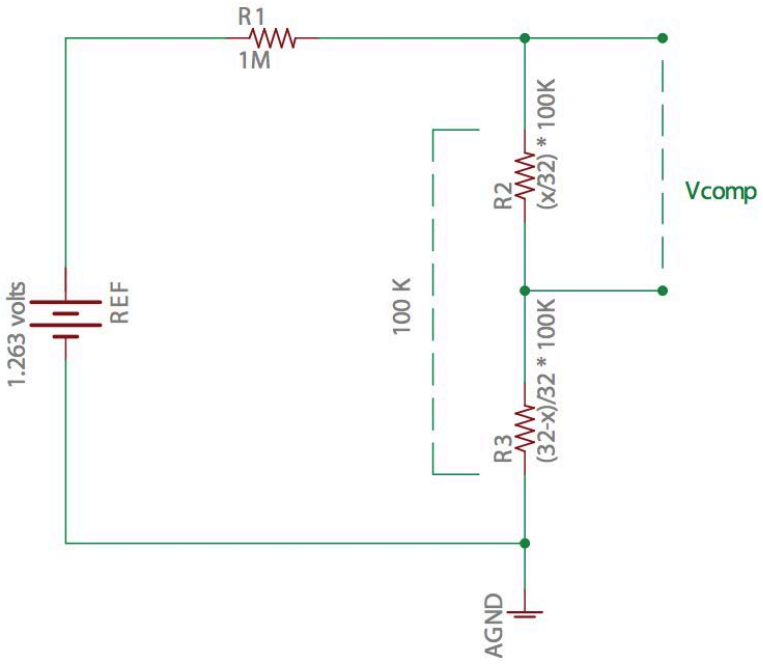

Figure A-4: Simplified Shake 'n Wake reference circuit diagram

Hardware

Like Versions 1 and 2 described in Ozer (2001), Dowding et al. (2007) and Kotowsky (2010), Version 3 consisted of several MICA2 motes equipped with MDA300CA sensor boards, string potentiometers, and two AA batteries. Version 3 nodes also included a single Shake 'n Wake board and a geophone. Figure A-5 shows a photograph of a fully- assembled Version 3 node.

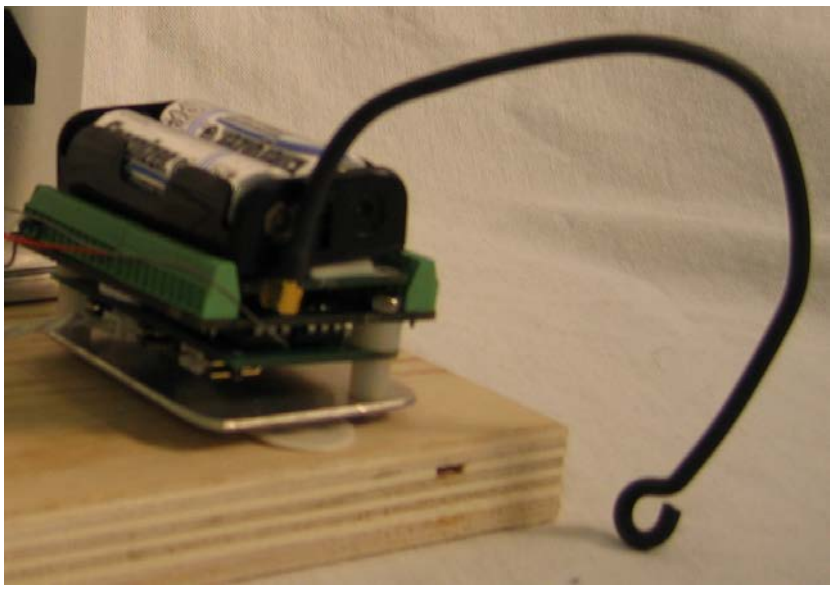

Figure A-5: Photograph of a Version 3 wireless ACM node

The base station was significantly changed from the base station used with Version 2. First, the Stargate was replaced with a commercially available Moxa UC-7420 RISC-based GNU/Linux embedded computer. The Stargate was found to be too physically fragile for practical use without the creation of a fully-customized enclosure. The UC-7420 ships from the factory in a rugged metal enclosure designed for industrial use. Because the UC-7420 was not designed to connect to a mote via the mote's 51-pin connector, an MIB510CA serial interface board was used to connect the base mote to one of the serial ports on the UC-7420. Detailed specifications of the UC-7420 can be found in the separate publication by Kotowsky (2010).

Second, instead of relying on a locally available Internet connection to connect back to the laboratory, the Version 3 base station includes a 3G cellular router and antenna. The inclusion of the cellular router allows placement of the base station at any location in an instrumented structure as long as that location has available cellular signal and 110 V AC power. Figure A-6 shows a photograph of the base station.

Figure A-6: Photograph of the base station of Version 3 of the wireless ACM system, including UC-7420, MIB510CA, cellular router, power distributor, and industrially-rated housing

Physical installation of Version 3 of the MICA2-based wireless ACM system is an extension of Versions 1 and 2: the MICA2/MDA300CA/string potentiometer combination is mounted to the wall in the same manner as in Version 1. The geophone, as it needs to be coupled closely with the wall or ceiling to be monitored, requires rigid attachment to the wall using epoxy, but the mote and sensor boards may be fastened to the wall only hook-and-loop fasteners. The HS-1 geophone features a threaded protrusion for ease of installation on mechanical equipment, so installation was made easier through the fabrication of an aluminum bracket that could accept the protrusion and provide a flat surface for the epoxy-wall interface. Figure A-7 shows a Version 3 wireless ACM node installed on a wall with a string potentiometer over a crack and an HS-1 geophone in a mounting bracket.

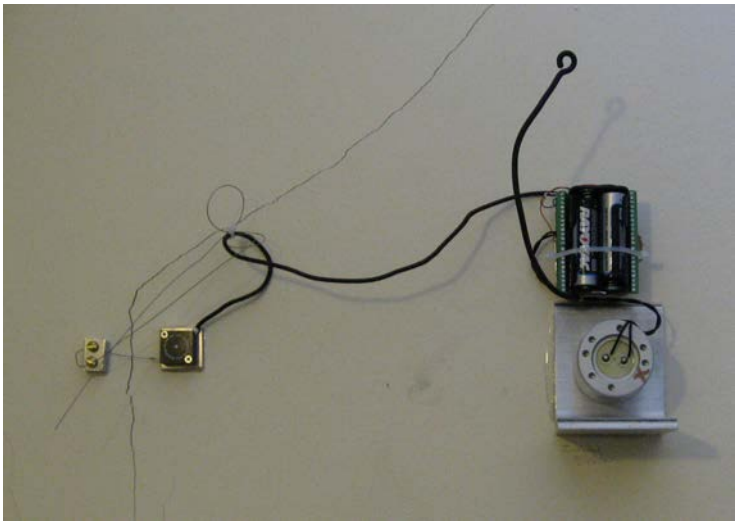

Figure A-7: Photograph of a Version 3 wireless ACM node with string potentiometer and HS-1 geophone with mounting bracket installed on a wall

Software

The software portion of Version 3 of the MICA2-based wireless ACM system is an extension of the software of Version 2 with two significant additions: the ability to allow a hardware interrupt from an external device to bring the mote out of low-power sleep mode and the ability for each mote to receive and relay commands broadcast from the base station. These two new features allow a MICA2 mote to interact with the Shake ’n Wake hardware and for a user to change the Shake ’n Wake triggering threshold, node sampling rates, and node identification numbers while the system is deployed.

Implementation of Version 3 required modification and cross-compilation for the UC-7420 of the xlisten and xcmd applications provided with the Crossbow MICA2 system. xcmd, the application that allows a PC to send commands to the wireless sensor network, was modified to allow the sending of ACM-related commands to modify sampling rates, accelerate the formation of the mesh network, and change the triggering threshold of the Shake ’n Wake devices. xlisten, the application that allows a PC to read data coming back from the network, was modified to understand threshold-crossing messages and messages acknowledging receipt of commands. This modified software can be found in the separate publication Kotowsky (2010).

Implementation of Version 3 also required modification of the software that runs on each MICA2. This modification activates an interrupt request channel on the MICA2 and instructs the mote to send back a “trigger received” message upon activation of that interrupt. The mote will also send back its most recent data readings from the MDA300CA upon receiving a Shake ’n Wake trigger. Additionally, the on-mote code was modified to accept the receiving of and responding to commands from a PC. This modified software can be found in the separate publication Kotowsky (2010).

Operation

The addition of the ability to send commands to the sensor network from the base station substantially changes the installation procedure after the mote and sensors have been attached to the structure. Rather than using a physically separate calibration mote to center the string potentiometer, an engineer can center the potentiometer using only the Version 3 software. Once the motes are powered on, the engineer can connects to the base station using any 802.11-capable PC. He logs into the UC-7420 using secure shell and issues a command to the network to enter quick-mesh mode in which the rate of packet transmission is significantly increased such that a mesh network forms in under one minute instead of in 30-40 minutes. The engineer uses the xlisten program on the UC-7420 to monitor the network output until he sees that all sensors have acknowledged receipt of the quick-mesh command, then he issues another command to disable quick-mesh mode. He then chooses a mote, issues a command to that mote to sample once per second, and uses the increased sampling rate and his computer to center the string potentiometer in the middle of its active range. He then decreases the sample rate of that mote and moves on to the next node until all potentiometers are centered.

When the motes are first powered on, the trigger threshold on each Shake ’n Wake is set by default to 31, the least sensitive setting. By issuing a command from the base station, either at install-time or at any later time by connecting to the base station over the Internet, the trigger threshold may be adjusted to suit the needs of the site. Table A-1 details the ACM-

related commands that are made available with Version 3 of the MICA2-based wireless ACM software.

set_rate X	X is an integer [1,30]. X specifies frequency, in seconds, of ticks.
set_ticks X	X is an integer [1,200]. A sample is taken every X ticks.
set_quick X	X is either 0 or 1. If X is 0, the default settings for mesh formation are used. If X is 1, the motes will transmit mesh formation information much more quickly, allowing a mesh to me be formed quickly.
set_pot X	X is an integer [1,31]. X = 1 is the most sensitive.

Table A-1: ACM-related commands added to xcmd by Version 3 of the MICA2-based wireless ACM software

Analysis of Power Consumption

To analyze the power consumption of a Shake 'n Wake-enabled mote, a simple ammeter circuit was implemented by placing a 10-ohm resistor in series with the positive terminal of the battery on the mote. By reading the voltage across this resistor, the current draw of the mote can be calculated, recorded and compared to the total theoretical power capacity of a pair of lithium AA batteries in series: 3000 mAh at 3 V DC (Energizer Holdings (2010b); Appendix B.7). Figure 3.11 shows the current draw profile of a single mote.

The current readings were recorded at 10 hertz and averaged to determine the average cur- rent used by the mote during a period of 18 hours. The average current draw when the mote is sampling once per hour is 325 μA. Since the total current capacity of the battery pack is 3000 mAh, the total estimated lifespan is estimated to be approximately 384 days, assuming the first hour of higher-frequency sampling is ignored.

Figure A-8 shows the current draw of a mote with Shake 'n Wake installed as compared with a Version 2 mote. Figure A-8b clearly indicates that during the crucial sleep-state of the mote, the current draw varies between 0.03 and 0.05 milliamps – very similar to the sleep-mode current draw of the Version 2 wireless ACM system without Shake 'n Wake, shown in Figure A-8a. Thus it can be concluded that the Shake 'n Wake does not draw a significant amount of additional power.

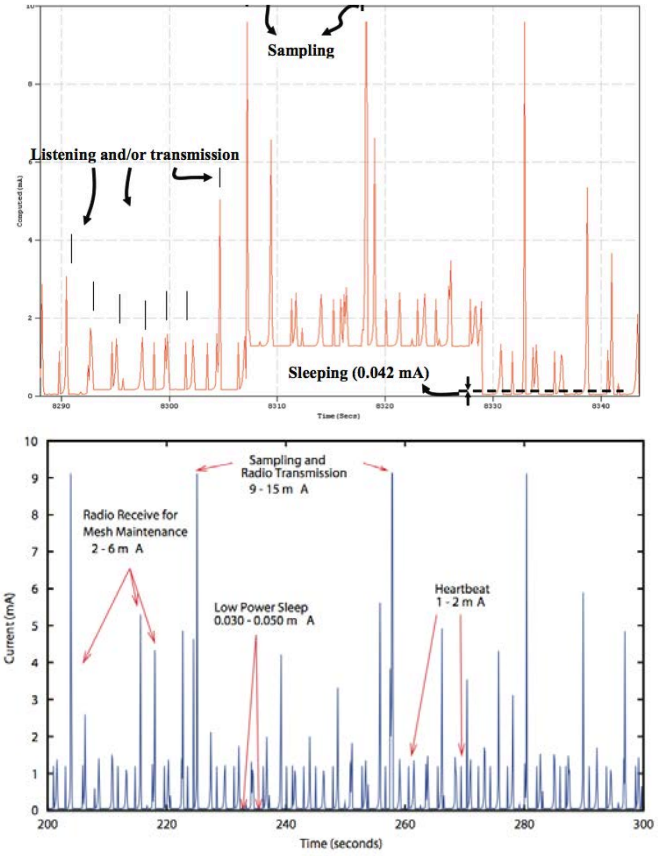

Figure A-8: Current draw of (a) wireless ACM Version 2 mote with no Shake 'n Wake, after Dowding et al. (2007) (b) Version 3 mote with Shake 'n Wake

Deployment in the Test Structure

A deployment test of Version 3 of the MICA2-based wireless ACM system was conducted in the main building of the test structures near the Northwestern campus described in Kotowsky (2010) between September 2007 and February 2008. The objective of the test was to determine the degree of difficulty of the installation of the system, the effectiveness of the Shake 'n Wake in detecting vibration events, and further assurance that Shake 'n Wake does not significantly decrease deployment lifetime of the system.

Sensor nodes were deployed through only one of the structures, as shown in Figure A-9. Two geophone-only nodes (with no MDA300CA or string potentiometer) were installed on the underside the service stairway leading from the basement to the kitchen, as pictured in Fig- ure A-10a. One of these motes was connected to a GS-1 geophone, the other was connected to an HS-1 geophone. Two motes, each equipped with a MDA300CA sensor board, a Shake 'n Wake sensor board, an HS-1 geophone in a mounting bracket, and a string potentiometer were in- stalled over existing cracks in the structure: one over the doorway leading from the kitchen into the service stairway to the second floor, shown in Figure A-10b, and one on the wall of the main stairway leading from the second floor to the third floor, shown in Figure A-10c. These two motes were installed alongside optical crack measurement devices used for a different project. The base station, shown in Figure A-10d, was deployed in the basement underneath the

kitchen.

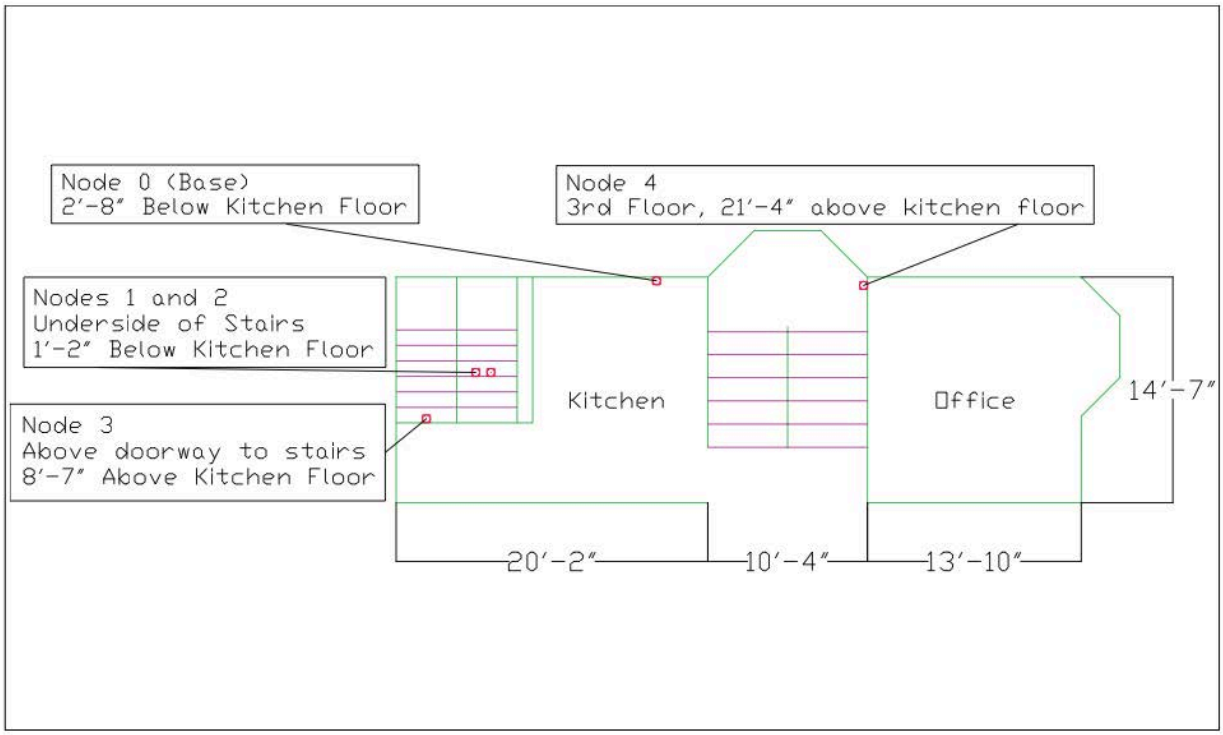

Figure A-9: Layout of nodes in Version 3 test deployment

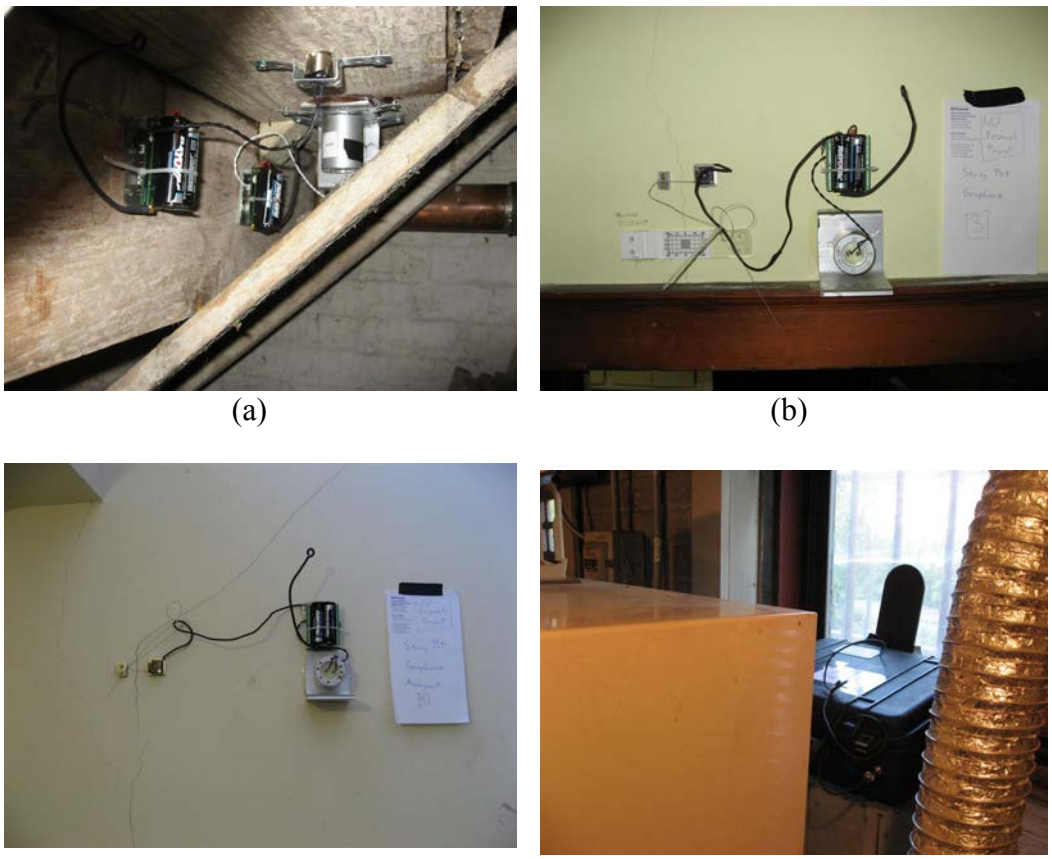

(a) (b)

(c) (d)

Figure A-10: Version 3 wireless ACM nodes located (a) on the underside of the service stairs (b) over service stair doorway to kitchen, and (c) on the wall of the main stairway – (d) the base station in the basement

Results

Figure A-11 shows plots of temperature, humidity, battery voltage, and parent mote over the entire deployment period. Only Motes 3 and 4 transmit this data – they are the only motes with an MDA300CA attached. The plots indicate that after approximately 25 days of deployment, the system ceased to take data. Later examination indicated that this failure was due to an unforeseen software condition that caused the monitoring to stop prematurely. At approximately day 75, a workaround was implemented: each night, the base station would automatically rebroadcast the correct sampling interval. Data transmission was restored immediately. Mote 4 ceased taking data between days 85 and 115 for a reason that is not yet understood but thought to be an issue with the mesh networking protocol – Figure A-11d shows that Mote 4 used Mote 3 as an intermediary, which was the only difference between those motes.

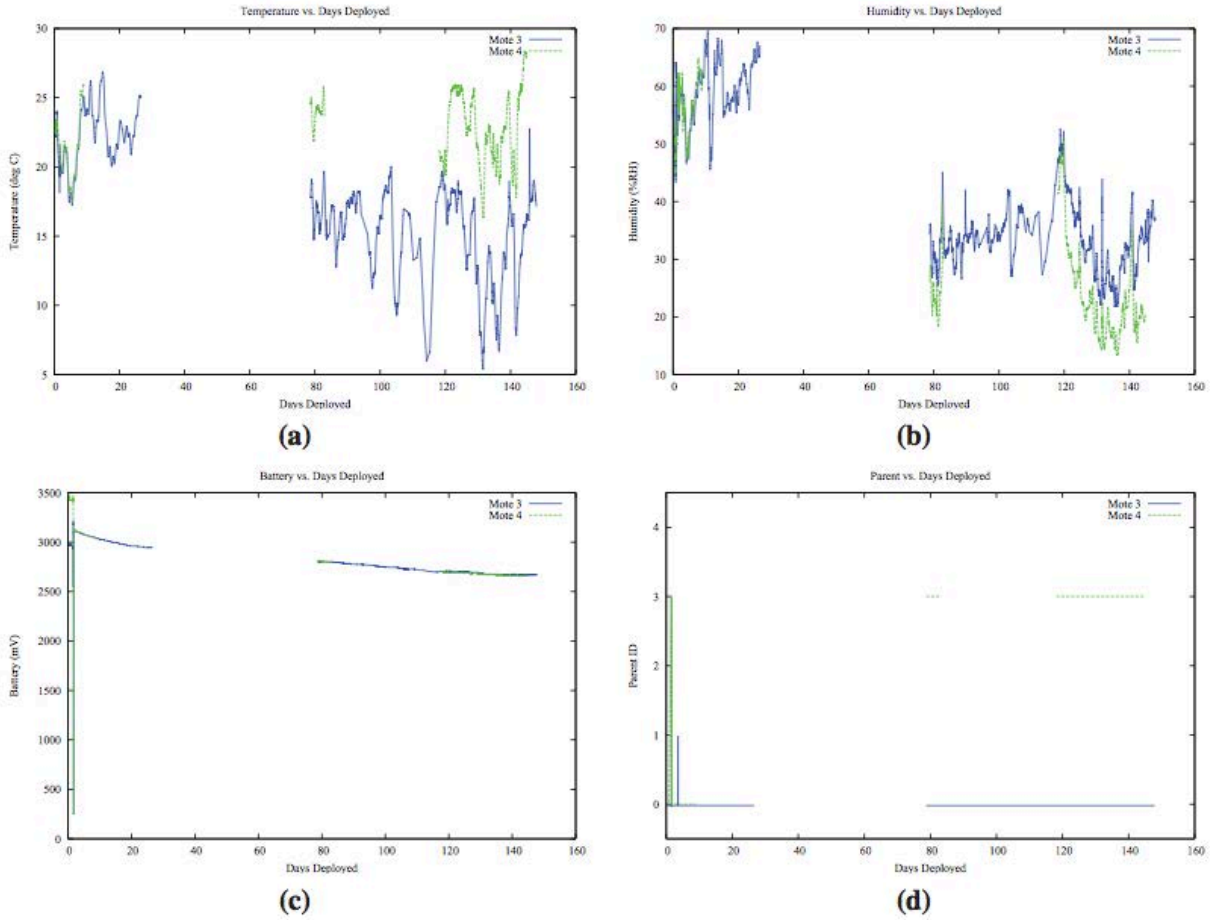

Figure A-11: Plots of (a) temperature (b) humidity (c) battery voltage and (d) parent mote address recorded by Version 3 of the wireless ACM system over the entire deployment period

Diagnostic logs on the base station showed that Motes 1 and 2, the motes underneath the service staircase with no MDA300CA sensor boards, did not reply when the sampling interval workaround was implemented near day 75. The most reasonable explanation for this behavior is that the lack of MDA300CA attached to these motes caused the XMesh power management algorithm to fail causing the batteries to deplete after only two days, approximately the same expected lifetime of a MICA2 with no power management. Figure A-11d does show that Mote 1 was functioning as a parent mote for Mote 3 before it failed.

Figure A-12 shows the data recorded over the period from day 75, when the base station workaround was implemented, through the time the system was removed from the test structure. Figure A-12d shows when a Shake ’n Wake trigger signal was received at Motes 3 or 4.

Discussion

Figure A-11c shows the alkaline battery voltage versus deployment time for Version 3 of the MICA2-based ACM system. Figure A-13 compares the battery voltage versus time of Ver-

sions 2 and 3 of the two MICA2-based wireless ACM systems. The two Version 3 motes with MDA300CA boards installed lasted approximately 150 days. The graph indicates, however, that battery voltage decay curve of the more economical batteries used in Version 3 did not match those used in Version 2. This evidence, added to the similar current consumption profiles shown in Figure 3.11, indicates that Version 3 can operated for at least six months when high-quality alkaline batteries are used.

Figure A-12c shows that the MDA300CA reported what appear to be three different sets of string potentiometer readings, each separated by an approximately 1800 μin pseudo-constant offset. In post processing, it is possible to filter the three sets of data into three regions, as shown in Figure A-14, under the assumption that each region represents the same physical reading with constant 1800 μin offsets. 84% of the data points fall into the region with an absolute value above 760 μin. The high region, as outlined Table A-2, contains the majority of the recorded points. Figure A-15 shows plots of temperature and humidity versus the high region of measured crack width.

Phase A Findings & Conclusions

This phase report has described the final version (3) of a wireless ACM system built on the MICA2 plat- form. Version 1 was a proof-of-concept designed to demonstrate the viability of a MICA2-based implementation of ACM by implementing Mode 1 recording. Version 2 incorporated new wire- less mesh networking and power management libraries to implement Mode 1 recording with more reliability and system longevity. Version 3 incorporated the design and manufacture of a new sensor board, the Shake 'n Wake, to allow data to be taken at random times rather than scheduled times without sacrificing system longevity. The following conclusions can be drawn:

- The MICA2 WSN platform combined with MDA300CA sensor boards and string potentiometers is capable of performing Mode 1 recording for approximately 30 days. The MDA300CA is essential, as the internal ADC on the MICA2 does not have sufficient resolution or front-end gain for the expected potentiometer output.
- Intelligent power management software based on the XMesh routing layer can be used with the MICA2/MDA300CA/potentiometer system to operate a fully functional Mode 1 system for six to twelve months.
- Battery longevity is dependent on the ambient temperature and humidity of the deployment environment.
- A robust, industrially-rated and fully enclosed GNU/Linux embedded computer can be combined with an MIB510CA board to create a reliable and secure Internet-accessible base station that can continue to collect data even while the Internet connection might be off-line. Such a base station can also be used to modify the WSN operating parameters, either automatically or on demand.
- The inclusion of a cellular modem in the base station allows a MICA2-based ACM system to be deployed anywhere with 110 V AC power within radio range of the sensor network.
- Installation time is decreased with the added ability to put the motes into quick-mesh mode to form the initial mesh network. Installation is further simplified by the added

ability to individually increase the sampling rate of a mote in order to more easily center the string potentiometer over a crack.

- Shake ’n Wake adds the ability for a MICA2-based wireless ACM mote to respond to a randomly occurring event of interest without sacrificing power.
- A MICA2-based wireless ACM node should not be deployed without a MDA300CA sensor board, even if the node does not need to measure the width of a crack.
- The MDA300CA board and its drivers prevent the MICA2-based ACM system from fully implementing Mode 2 recording, even when paired with Shake ’n Wake, as its drivers do not fully support sampling rates of 1000 hertz.
- Installation of a string potentiometer would be made less difficult if the MDA300CA had a software-programmable front-end gain; the active range of the potentiometer decreases by 99% due to the front-end gain on the MDA300.
- Software incompatibilities between the MDA300CA drivers and the Shake ’n Wake drivers cause the MDA300CA to take readings from the string potentiometer with a DC offset approximately 15% of the time. These anomalous readings can be filtered out in post-processing.
- The Shake ’n Wake hardware design and a software implementation of the Lucid
- Dreaming strategy for random event detection in energy-constrained systems are not uniquely compatible with the MICA2-MDA300CA system described in this appendix; they can be ported to any wireless sensor network that allows for direct physical access to the interrupt lines on the control processor and proper access to the low-level software. Unfortunately, many commercially available systems designed for ease of use for novice users do not provide such access, thus Shake ’n Wake/Lucid Dreaming integration must be performed at the factory and not by the end user.

Final Report for Phase B: Techniques for Wireless Autonomous Crack Propagation Sensing (ACPS) in Steel Bridges with Weather Rugged Mote[1]

M. Kotowsky and C. Dowding

Summary

Objective of this phase of the MEMS project
Determine the viability of weather rugged wireless network systems (WNSs) to measure fatigue crack propagation through failure of resistive ladder patterns bonded to steel

Context
Though ACPS techniques can be applied to any structure to measure crack extension over time, the primary motivation in the development of this technique is to supplement the in-service inspection of fatigue cracks in steel bridges. Fatigue cracks in steel tend to grow slowly over time, and when found during routine inspection of steel bridges are reported. ACPS, especially on bridges, is an ideal application for a wireless sensor network. Running wires across bridges between different points of interest is usually cost-prohibitive and is often impossible due to superstructure configuration and access restrictions. Since access can be difficult and expensive, it is desirable to minimize installation time and maximize time between maintenance visits, so long-lasting solar-powered nodes are ideal.

Summary of Work

A Weather rugged wireless sensor network was employed in the laboratory to monitor fracture propagation in a steel test specimen. This system wirelessly relayed measurements of crack growth. Crack growth is monitored with several commercially available ladder-pattern crack propagation gauges shown in Figure BS-1. The response of the wireless mote system is shown in Figure BS-2. These laboratory measurements demonstrate the viability of combining a weatherized wireless mote and a resistance based ladder-pattern crack propagation gauge to measure growth of fatigue cracks in steel transportation structures such as bridges. Further work demonstrated the viability of a painted ladder-pattern propagation gauge to circumvent the problem of bonding commercial ladder gauges in the field.

Continued on next page.

[1] DISCLAIMER

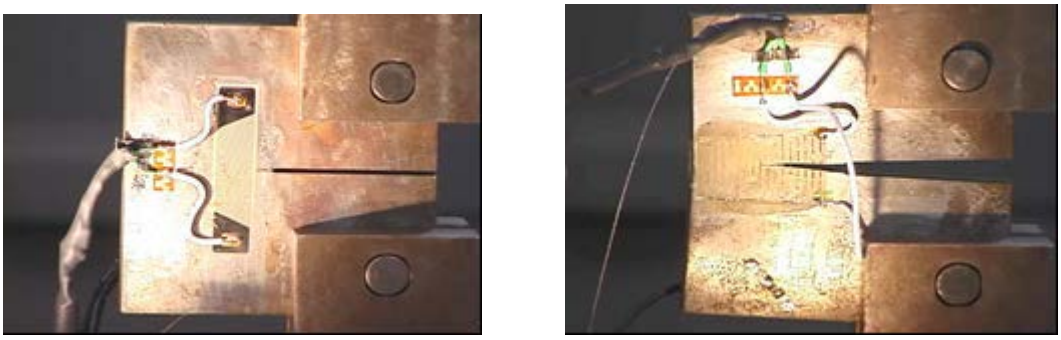

Figure BS-1: Ladder-pattern crack propagation gauges with an advancing fatigue crack

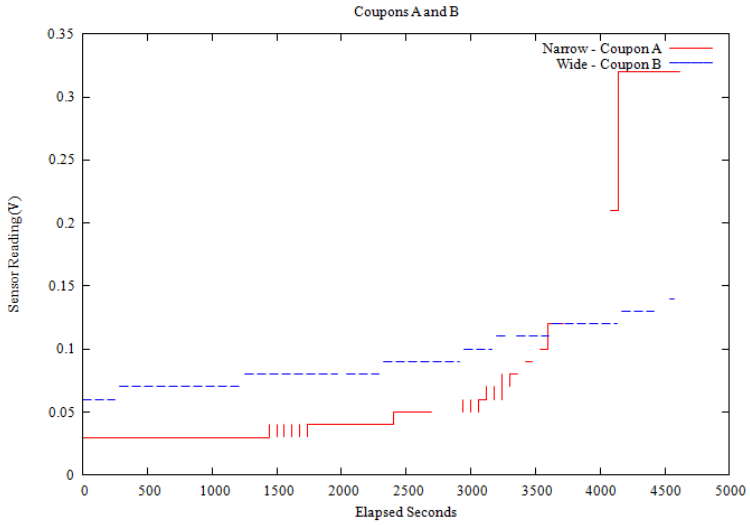

Figure BS-2: Changes in voltages measured wirelessly showing the jumps as the fatigue crack extended. These responses demonstrate the viability of the approach.

Major Finding:

Combination of a weather rugged wireless sensor network and a commercial ladder-pattern crack propagation gauge (or painted ladder gauge) has been shown in the laboratory to be a viable system to measure crack propagation in steel bridges.

Final Report for Phase B: Techniques for Wireless Autonomous Crack Propagation Sensing (ACPS) in Steel Bridges with Weather Rugged Mote

M. Kotowsky and C. Dowding

Introduction

This Phase B report describes the qualification of a wireless Autonomous Crack Propagation Sensing (ACPS). ACPS is a measurement technique designed to record the propagation of slow-growing structural cracks over long periods of time. In contrast to ACM, ACPS, does not seek to directly correlate crack extension to any other physical phenomena; rather ACPS seeks to record quantitatively, repeatably, and accurately the extension of cracks in structures, specifically to supplement regular inspections of bridges. An ACPS system allows structural stakeholders to be alerted to crack extensions with ample time to ensure the safety of the structure and those using it.

Though ACPS techniques can be applied to any structure that exhibits cracking over time, the primary motivation in the development of this technique is to supplement the in-service inspection of fatigue cracks in steel bridges. Fatigue cracks in steel, such as those shown in Figure B-1, tend to grow slowly over time, and when found during routine inspection of steel bridges, are cataloged according to procedures laid out in the Bridge Inspector's Reference Manual, or BIRM (United States Department of Transportation: Federal Highway Administration, 2006). These cracks are then re-examined at the next inspection and compared to records to determine whether the crack has grown.

ACPS, especially on bridges, is an ideal application for a wireless sensor network. Running wires across bridges between different points of interest is usually cost-prohibitive and is often impossible due to superstructure configuration and access restrictions. Since access can be difficult and expensive, it is desirable to minimize installation time and maximize time between maintenance visits, so long-lasting solar-powered nodes are ideal. Furthermore, power management strategies implemented by the manufacturers of existing wireless sensor networks are well-suited to the low sampling rate required by ACPS.

Visual Inspection

Visual inspection is the most common mechanism by which the growth of cracks is recorded quantitatively. By federal law, every bridge in the United States over 20 feet in length must be inspected at least once every two years by specially trained bridge inspectors. This inspection frequency can be increased based on the design, past performance, or age of the bridge. A key part of these routine bridge inspections is identification of fatigue cracks, or cracks due to cyclic loading, in steel bridge members. These cracks tend to grow slowly over time depending on the volume of truck traffic, load history, weld quality, and ambient temperature (United States Department of Transportation: Federal Highway Administration, 2006).

Fatigue cracks are commonly cataloged by recording the method by which they were dis- covered, date of discovery, crack dimensions, current weather conditions, presence of corrosion, and other factors that may contribute to the form or behavior of the crack. The BIRM indicates that the inspector should: "Label the member using paint or other permanent markings, mark the ends of the crack, the date, compare to any previous markings, be sensitive to

aesthetics at prominent areas. Photograph and sketch the member and the defect." Figure B-2 shows an example from the BIRM of how a fatigue crack should be marked.

Figure B-1: Fatigue crack at coped top flange of riveted connection, after United States Department of Transportation: Federal Highway Administration (2006)

Figure B-2: Fatigue crack marked as per the BIRM, after United States Department of Transportation: Federal Highway Administration (2006

The tracking of crack growth by visual inspection has several drawbacks, the most obvious of which is that documentation of the conditions of cracks can only be updated during inspections which may occur as infrequently as once every two years. Less obviously, photographic records of crack length tend not to be repeatable due to changes in photography angle, ambient light, photographic equipment, and inspector.

Other Crack Propagation Detection Techniques

Several other techniques exist for the detection, classification, and monitoring of fatigue cracking in structures. Acoustic emission monitoring, as described in Hopwood and Prine (1987) can be used to determine whether a crack is actively growing or has extinguished itself. Stolze et al. (2009) describe a method to detect and monitor the progression of cracks using guided waves. ACPS with wireless sensor networks has several distinct advantages over these structural health monitoring techniques when applied to in-service bridges:

- ACPS is designed to be deployed for months or years on an actively utilized structure. The other techniques are not designed to be used in the field for more than a few days.
- ACPS using commercially available wireless sensor networks is an order of magnitude less expensive than acoustic emission or guided wave equipment.
- ACPS sensors on a wireless network do not require power or signal cables to be installed on a bridge.
- ACPS using a wireless sensor network may not require special software or programming skills.

The Wireless Sensor Network

The eKo Pro Series Wireless Sensor Network (WSN), shown in Figure B-3, commercially produced by Crossbow Technology, Inc., is specifically designed for environmental and agricultural monitoring. Each eKo mote is water and dust resistant, capable of operating in wide temperature and humidity ranges, and will operate for over five years with sufficient sunlight (Crossbow Technology, Inc., 2009a). The eKo base station, which must be connected to 110 V AC power and a network connection, can transmit e-mail alerts when sensor readings cross programmable thresholds. The eKo WSN's robust design makes it an attractive platform for deployment in the harsh operating environment of an in-service highway bridge. It is equally important to note that an eKo mote end-user need not manually program the system to function properly, which is attractive to bridge engineers. The eKo motes record data every thirty seconds for the first hour after activation. Thereafter they record once every fifteen minutes.

(a) (b)

Figure B-3: (a) eKoPro Series WSN including base station, after Crossbow Technology, Inc. (2009a) (b) Individual eKomote with a 12-inch ruler for scale

ACPS Using Commercially Available Sensors

Direct measurement of the elongation of a crack can be measured with a crack propagation pattern, a brittle, paper-thin coupon on which a ladder-like pattern of electrically conductive material is printed. This coupon is glued to the surface of the material at the tip of the crack, as shown in Figure B-4. When the crack elongates and breaks the rungs of the pattern, the electrical resistance between the sensor's two terminals will change. This resistance is be read using an eKomote to record the distance the crack has propagated.

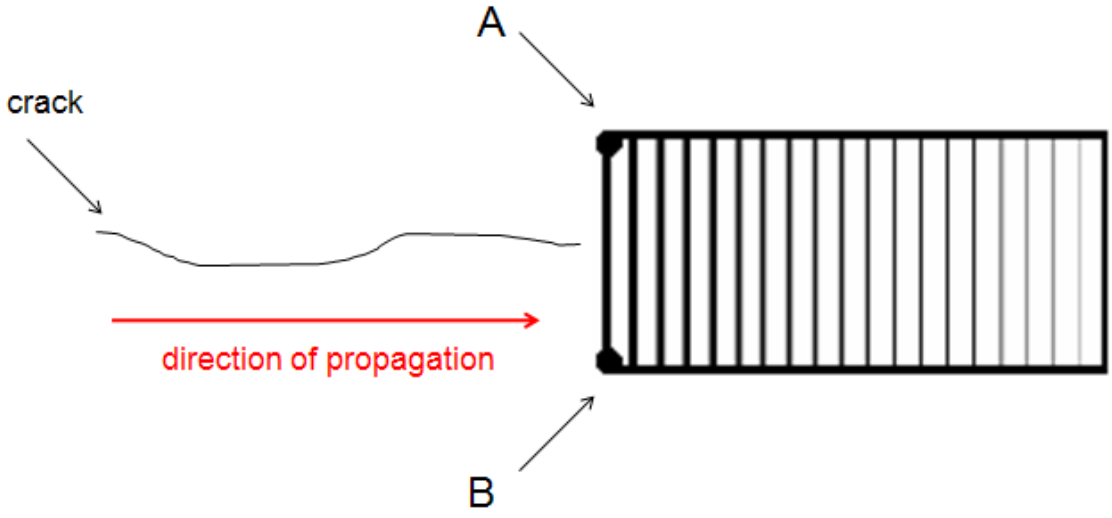

Figure B-4: Cartoon of a crack propagation pattern configured to measure the growth of a crack: resistance is measured between points A and B.

Vishay Intertechnology, Inc. manufactures commercially a series of these crack propagation patterns. Two of these sensors were chosen for use in an ACPS system: the TK-09-CPA02-005/DP, or "narrow gauge," shown in Figure B-5a and the TK-09-CPC03-003/DP, or "wide gauge," shown in Figure B-5b. Both sensors allow for the measurement of twenty distinct crack lengths with their twenty breakable grid lines. The narrow gauge's grid lines are spaced 0.02 inches apart, while the wide gauge's grid lines are spaced 0.08 inches apart. Additionally, the narrow gauge's resistance varies non-linearly with the number of rungs broken, as shown in Figure B-6a, while the wide gauge's resistance varies linearly with number of rungs broken, as shown in Figure B-6b. This linear behavior occurs because each rung of the wide gauge has a resistance specifically de- signed such that when it is broken, the change in the overall resistance of the sensor is linear, not exponential. The narrow gauge's rungs are all approximately the same width and therefore have the same resistance. This behavior becomes significant when signal resolution is considered, as explained in the following section.

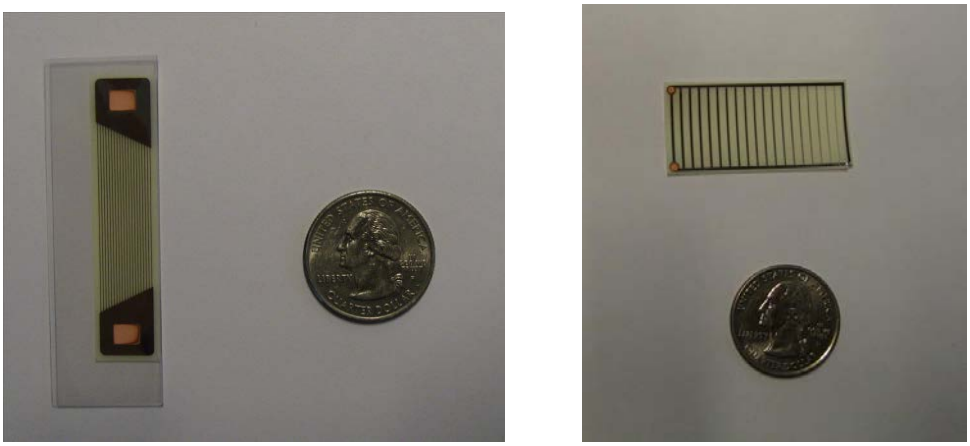

(a) (b)

Figure B-5: Crack propagation patterns (a) TK-09-CPA02-005/DP (narrow) (b) TK-09-CPC03-003/DP (wide)

Integration with Environmental Sensor Bus

The eKoPro Series WSN is designed to be used with sensors that communicate over Crossbow's Environmental Sensor Bus (ESB). The ESB protocol (Crossbow Technology, Inc., 2009c) describes a specific connector type, power supply, and digital interface scheme that must be im- plemented by the sensor manufacturer if that sensor is to be used with an eKomote. The crack propagation patterns are not compliant with the ESB, so a customized interface cable was de- signed, built, and installed.

The custom interface cable is composed of a Maxim DS2431 1024-Bit 1-Wire EEPROM, a Switchcraft EN3C6F water-resistant 6-conductor connector, a length of Category 5e sold- conductor cable, one 374Ω precision resistor and one 49.9Ω precision resistor. The EEPROM was soldered into the water-tight connector housing as shown in Figure B-7. The EEPROM allows a sensor to respond with a unique sensor identifier when queried by an eKomote such that the sensor will be properly identified and configured automatically by any mote to which hit is connected. After the EEPROM was mounted in the connector housing, the

individual cable leads were attached and the water-tight cable assembly was completed as shown in Figure B-8. This cable can be connected to any input port on any eKomote once the EEPROM is programmed with the appropriate information to operate the sensor.

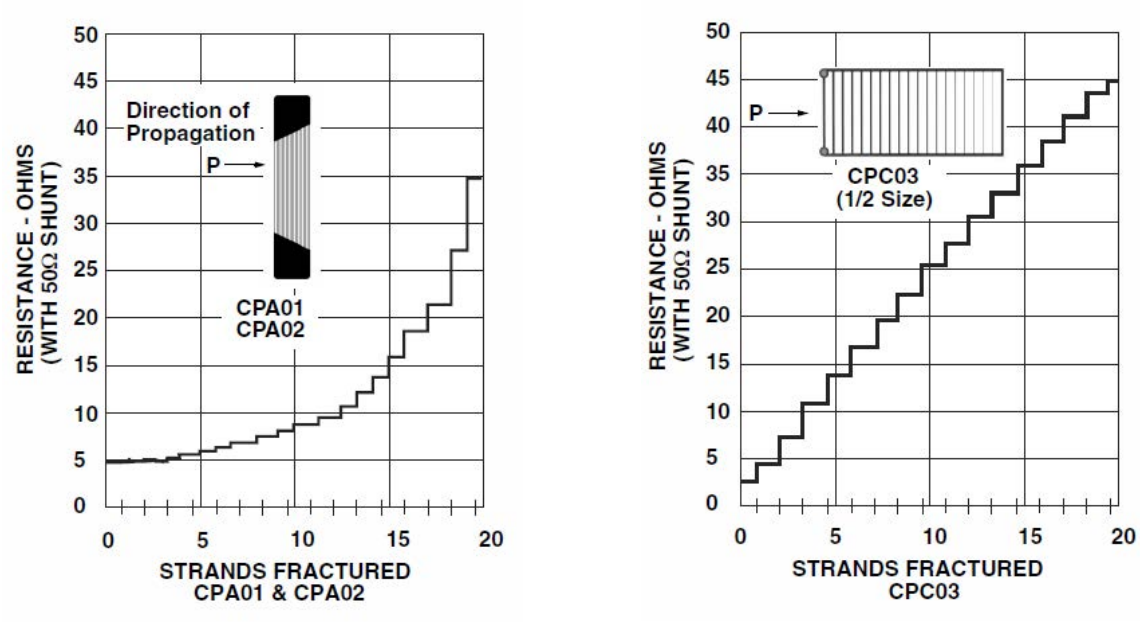

(a) (b)

Figure B-6: Crack propagation resistance versus rungs broken for (a) TK-09-CPA02-005/DP (narrow) (b) TK-09-CPC03-003/DP (wide), after Vishay Intertechnology, Inc. (2008)

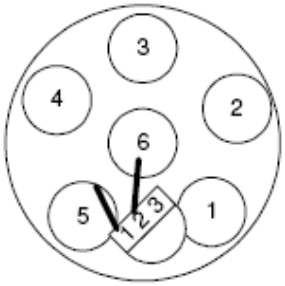

Figure B-7: Schematic of the EEPROM mounted in the watertight connector assembly, after Crossbow Technology, Inc. (2009c)

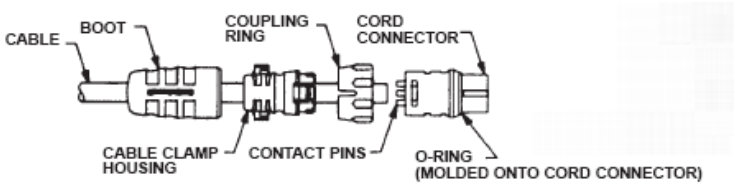

Figure B-8: Watertight ESB-compatible cable assembly, after Switchcraft Inc. (2004)

When fully intact, the narrow and wide crack propagation patterns have a 5Ω and 3Ω resistance, respectively, which will increase as their rungs are broken, acting as open circuits when all rungs have been broken. Because the crack propagation patterns are purely resistive sensors and the eKomote is only able to record voltages, two precision resistors were used to create a circuit to convert the resistance output into a voltage. The 49.9Ω resistor was placed in parallel with the two terminals of the crack propagation pattern while the 374Ω a resistor was placed in series with the mote itself. Figure B-9 shows a schematic of this circuit.

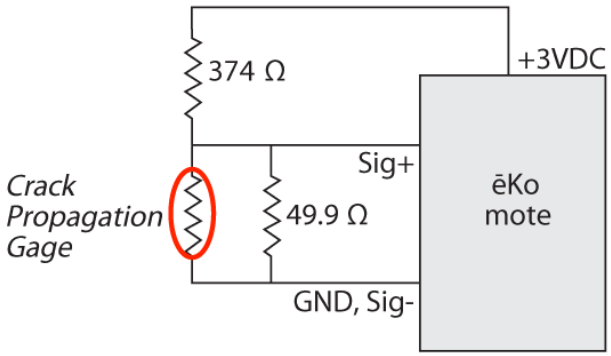

Figure B-9: Diagram of sensor readout circuit, adapted from Vishay Intertechnology, Inc. (2008)

This circuit can be connected to either the narrow or wide gauge, and will cause each rung break of a wide pattern to register an increase of approximately 10 millivolts on the eKomote. Because the resistance change is so small, the first rung breaks of a narrow sensor will register no measurable voltage difference on the eKomote, but the last several rungs broken will register a significantly higher voltage change than the rungs of a wide gauge. The circuit was placed within the custom cable so that two exposed leads at the opposite end of the cable from the watertight connector may be soldered to the two terminals of the crack propagation pattern after it has been mounted on the target material.

In addition to the fabrication of the custom ESB interface cable, a customized data interpretation file for each type of crack propagation sensor was created and stored on the eKobase station. These files, found in the separate document Kotowsky (2010), need only to be created once by the sensor manufacturer and do not need to be created or maintained by the end-user of the ACPS system.

Proof-of-Concept Experiment

A proof-of-concept experiment was designed to test both the effectiveness of the crack propagation gauges in measuring fatigue cracking in steel and the eKomotes' ability to reliably and accurately read the sensors. Three 3.5 in by 3.5 in by 0.5 in ASTM E2472 compact tension test coupons A, B, and C, a schematic of which is shown in Figure B-10, were fabricated from A36 steel. These coupons were placed in a mechanical testing apparatus to apply cyclic tensile forces at their circular attachment points to propagate a crack through the specimens and the gauges. Before each coupon was instrumented with a crack propagation pattern, a fatigue crack was initiated in each one under the assumption that any crack to be instrumented in the field would have begun to grow before the sensor is affixed. During the pre-cracking procedure, the relative displacement of the attachment points was cycled between 0.24 inches and 0.0016 inches at a frequency of 10 hertz until a crack was observed to be growing from the tip of the wire-cut notch. Approximately 10,000 cycles were required to initiate crack growth.

Coupon A was instrumented with a narrow crack propagation pattern on one face, as shown in Figure B-11a. Coupon B was instrumented with a wide crack propagation pattern on one face, as shown in Figure B-11b. The wide pattern was too long to fit on the test coupon, so the three rungs farthest away from the crack tip were removed before testing. The initial reading would therefore indicate three rungs already having been broken before crack propagation began.

The crack propagation patterns on both Coupons A and B were affixed using the manufacturer's recommended solvent-thinned adhesive cured at a temperature of at least +300◦ F. This elevated temperature cure is not practical in the field, so Coupon C was instrumented with a narrow pattern on one face and a wide pattern on the other face using epoxy cured at room temperature to determine if this would have a detrimental effect on ACPS functionality.

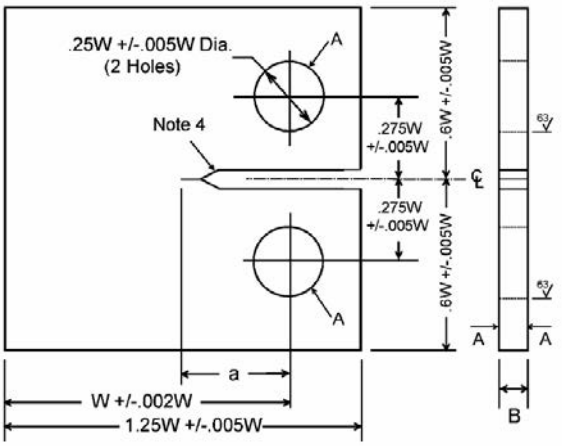

Note 1 - A Surfaces shall be perpendicular and parallel as applicable to within 0.05 mm (0.002 in.) T.I.R.
Note 2 - Intersection of crack starter notch tip shall be equal distance between top and bottom of specimen edges within 0.5 mm (0.02 in.).
Note 3 - Integral or attached knife edges for clip gage at crack mouth may be used.
Note 4 - For starter-notch and fatigue-crack configuration see Fig. 7.
Note 5 - Loading pins are of 0.24W (+0.000W/-0.005W) diameter.

FIG. A1.1 Compact-Tension Specimen for CTOA and δ_5 Testing

Figure B-10: Schematic of compact test specimen: W=3.5 in, B=0.5 in, after for Testing and Materials (2006)

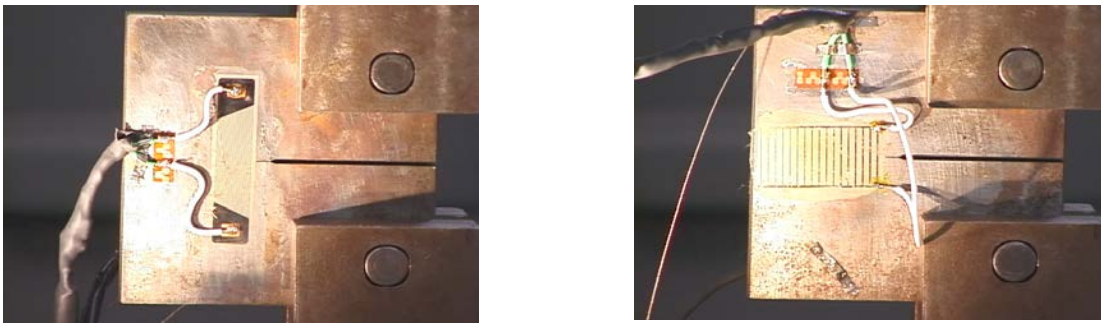

(a) (b)

Figure B-11: Test coupon with (a) narrow gauge and (b) wide gauge installed

Experimental Procedure

After the fatigue cracking procedure was performed and the gauges were affixed to the coupons, each coupon was loaded into the mechanical testing machine and wired to either an eKomote the case of Coupons A and B, or a general-purpose data logger and bench-top power supply in the case of Coupon C. The experiments on coupons A and B were designed to verify functionality of both the gauges and the eKomotes, but the experiment on Coupon C was designed solely to verify the performance of the sensor adhesion procedure. Figure B-12 shows a photograph of the experimental setup.

Figure B-12: Photograph of experiment configuration for pre-manufactured crack propagation gauges

During the approximately 80-minute tests, the coupons were cyclically loaded between 0.07 kip and 2.5 kip at decreasing frequencies. The crack in Coupon A propagated through all twenty rungs of the narrow gauge, as shown in Figure B-13a, while the crack in Coupon B propagated through eight rungs of the wide gauge, as shown in Figure B-13b

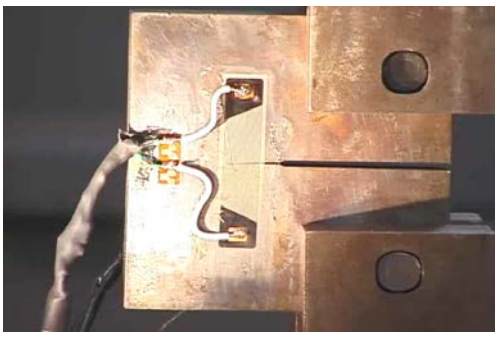

(a)

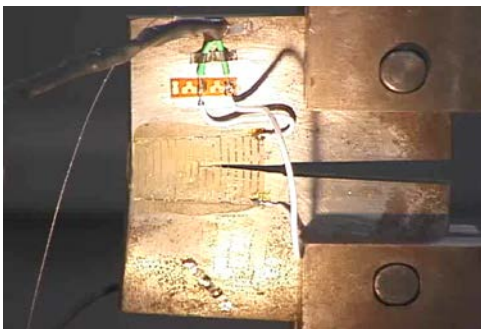

(b)

Figure B-13: Test coupons with crack propagated through (a) narrow gauge and (b) wide gauge affixed with elevated-temperature-cured adhesive

Coupon C was subjected to the same testing procedure as were Coupons A and B, but the testing was aborted when it was observed that the room-temperature-cured adhesive had failed before the gauge itself, as shown in Figure B-14.

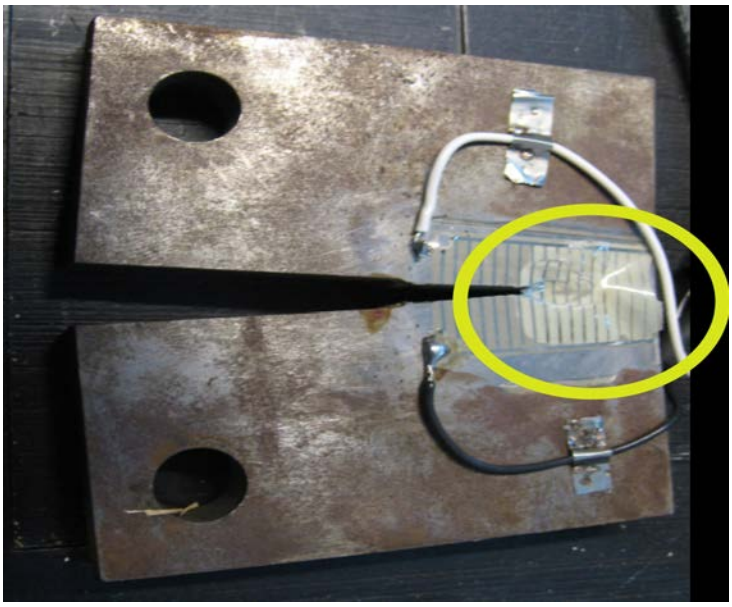

Figure B-14: Photograph of glue failure on wide gauge affixed with room temperature-cured adhesive: the indicated region shows the glue failed before the gauge.

Results and Discussion

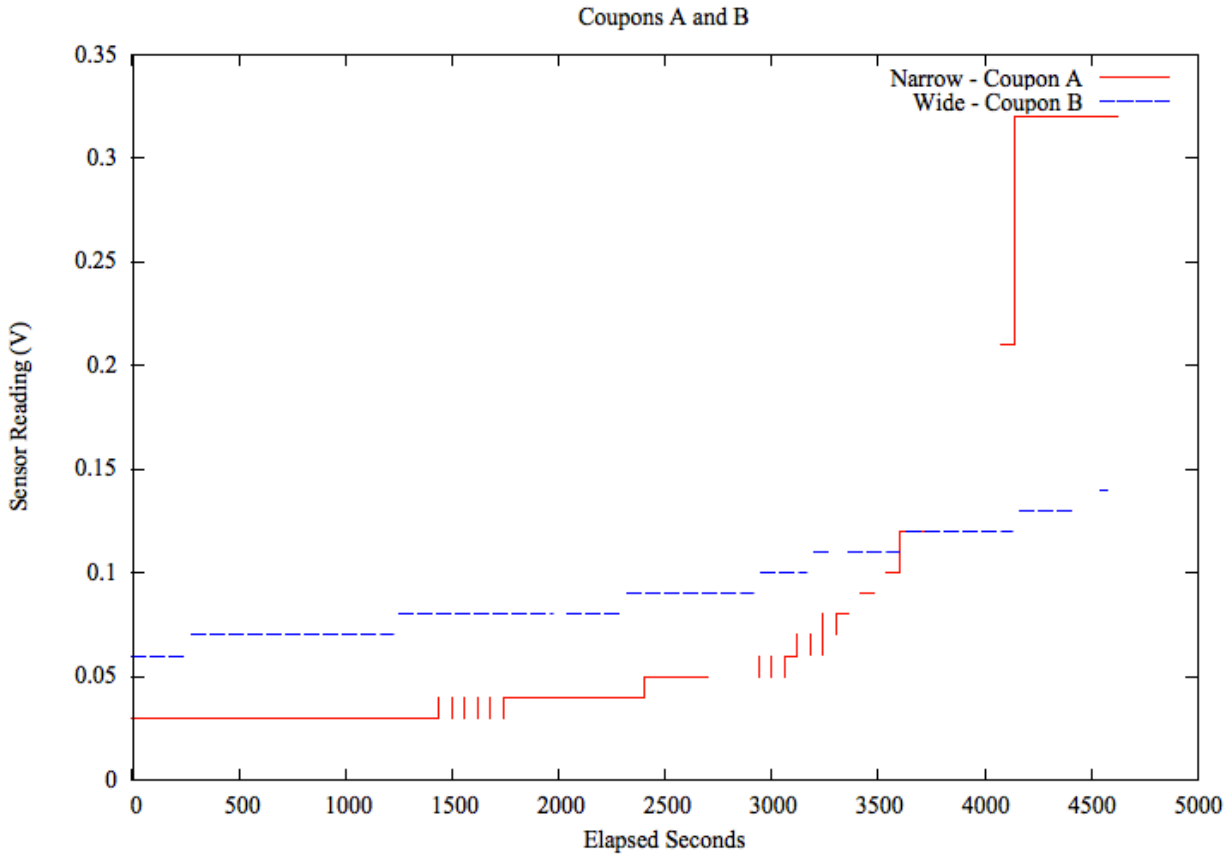

Figure B-15: Data recorded by eKomote during tests of Coupons A and B

Figure B-15 shows the data recorded by an eKomote during tests of Coupons A and B. The wide gauge showed a linear change of voltage versus number of broken rungs. Eight rung-breaks are easily identifiable. The narrow gauge showed a non-linear change of voltage versus number of broken rungs. Figure B-13a clearly indicates that all twenty rungs have been broken by the crack, but Figure B-15 only shows ten discernible increases in voltage. This result is not unexpected: the 10-bit analog-to-digital conversion unit and the 3 V DC precision excitation voltage on the eKomote combine to limit the minimum-viewable change in voltage output of any sensor to approximately 3 mV. This resolution is suitable for measuring a rung-break on the wide gauge but it is not suitable for measuring the breakage of the first 10-12 rungs of the narrow gauge. Figure B-6a shows that the resistance change exhibited by a narrow gauge for the first 10-12 rung-breaks is significantly lower than that for the last 8-10 rung-breaks, therefore the voltage change exhibited by the readout circuit will also be lower for the first 10-12 rung-breaks.

Two times over the course of the test, the eKomote read momentary jumps in the voltage output of the wide gauge and its readout circuit. This same phenomenon was observed eleven times with the narrow gauge. This behavior is explained by noting that for any voltage input to the eKomote's analog-to-digital conversion unit that falls on or near one of the 3 mV thresholds, a small amount of electromagnetic interference is capable of increasing or decreasing the voltage of the observed signal such that it could appear to have

fallen into either of the two adjacent conversion regions. It is also possible that since the crack, and therefore the conductive portions of the gauge, were loaded cyclically, intermittent contact may occur just before or after a rung had been broken.

Figure B-14 shows that the adhesive cured at room temperature was not able to withstand the cyclic strains imposed by the fatigue test. The lightly colored region indicated in Figure B-14 shows where the adhesive holding the gauge to the steel coupon has released and allowed air to fill the gap between the coupon and the substrate of the crack propagation gauge. Once the brittle substrate of the gauge separates from the surface on which it is mounted, the gauge will not only fail to reflect accurately the position of the crack tip beneath it, but it will become extremely fragile and likely to fail due to some other physical phenomenon than crack propagation.

Custom Crack Propagation Gauge

An implicit assumption made in the use of crack propagation gauges is that the engineer has a priori knowledge at the time of sensor installation of the direction in which the crack is going to propagate. In cases where such knowledge does not exist, several of these mass-produced gauges would be necessary to track the crack in all of its possible propagation directions. For the best results, an impractical installation method involving elevated-temperature-cured adhesive must be employed to utilize these gauges.

A solution to both of these problems is a so-called custom crack propagation gauge. This type of gauge is drawn, rather than glued, near the crack to be monitored, using commercially available conductive material. This material, combined with a more sophisticated network of signal conditioning resistors, creates a gauge that can be any shape or size.

Theory of Operation of Custom Crack Propagation Sensor

The basic principles on which custom crack propagation gauges function are similar to their pre- fabricated counterparts: an existing crack in a structure grows, propagating over time through one or more rungs of the sensor. As each rung breaks, the resistance of the entire sensor increases by a known value. Using a precision excitation voltage and precision resistors of a known value, each rung break can be observed by an eKomote or any other data logger as an increase in voltage. Figure B-16 shows a schematic of a custom crack propagation gauge.

Sensor Design

Figure B-16 indicates that the design calls for several resistors wired in parallel. Though this could be implemented with individual precision resistors, pre-manufactured bus resistors, an example of which is shown in Figure B-17, provide a simpler and more reliable implementation. Each bus resistor has ten pins. One of the pins, designated by a mark on the resistor housing, is the common pin. The measured resistance between each of the other nine

pins and the common pin is always identical, regardless of what is connected or not connected to any of the other pins. This resistor configuration is ideal to simplify fabrication and deployment of a custom crack propagation sensor.

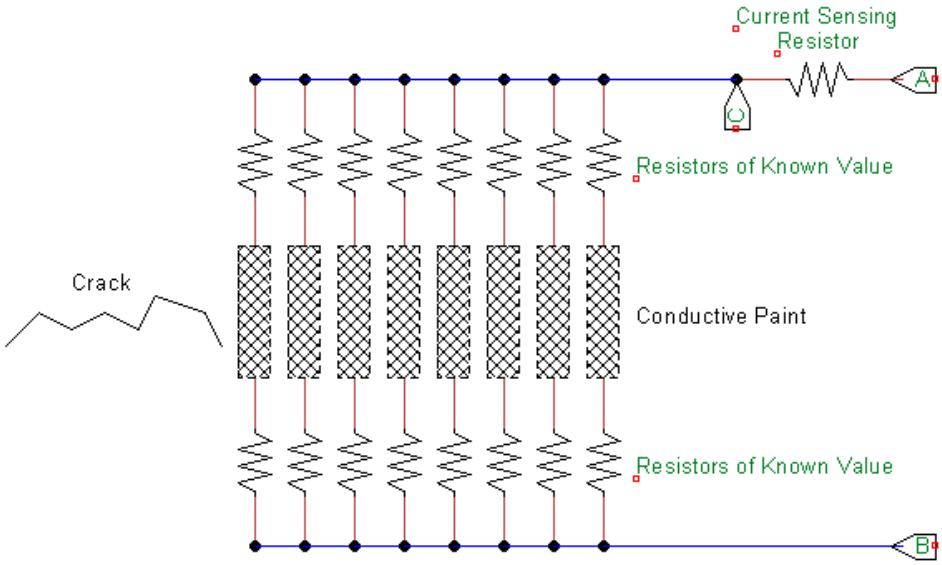

Figure B-16: Schematic of a custom crack propagation gauge; crack grows to the right, 3 V DC is applied between A and B, sensor output is measured between C and B.

Figure B-17: Photograph of a commercially available bus resistor, after Bourns (2006)

The values of the bus resistors and the current-sense resistor must be selected such that each rung-break may be reliably detected by an eKomote's 10-bit analog-to-digital converter and 3 V DC precision excitation voltage. Because the combined resistance of resistors wired in parallel is equal to the reciprocal of the sum of the reciprocals of each resistors' value, the change in resistance of the entire sensor will be smallest for the first rung break and increase non-linearly for each subsequent rung break. The change in resistance, and therefore voltage output, for the first rung break must be maximized while ensuring that the current draw of the sensor never exceeds 8 mA, the maximum current output of the eKomote's precision excitation voltage. Table B-1 shows, for each possible combination of available bus resistor

and current- sense resistor, the analog-digital conversion steps for the first rung break. Ohm's Law indicates that the fully-intact resistance of the gauge would need to be less than 375Ω before the sensor would draw more than 8 mA at 3 V. None of the resistor combinations listed in Table B-1 can combine to form gauge with an intact resistance of 375Ω or less.

		Bus Resistor Value				
		1KΩ	10KΩ	100KΩ	220KΩ	470KΩ
CS Resistor Value	49.9Ω	17	2	0	0	0
	374Ω	29	14	2	1	0
	1KΩ	19	25	5	2	1
	11KΩ	2	18	26	17	10
	20KΩ	1	11	30	24	16
	49.9KΩ	1	5	26	30	26

Table B-1: Change in eKoADC steps for first rung break for each combination of bus resistor and current-sense resistor values

Table B-1 shows that two resistor combinations yield the largest possible analog-to-digital step change for breakage of the first rung. The larger resistor combination, the 220KΩ bus resistors and the 49.9KΩ current-sense resistor were chosen because the larger resistors will draw less current from the same voltage supply. Figure B-18 shows the theoretical change in sensor output voltage as each of its nine rungs break. It is important to note that the predicted behavior of the voltage output as the rungs break is non-linear. This is, like in the case of the narrow gauge sensor, due to the fact that equivalent resistance of resistors in parallel is equal to the reciprocal of the sum of the reciprocals of all of the resistors' values.

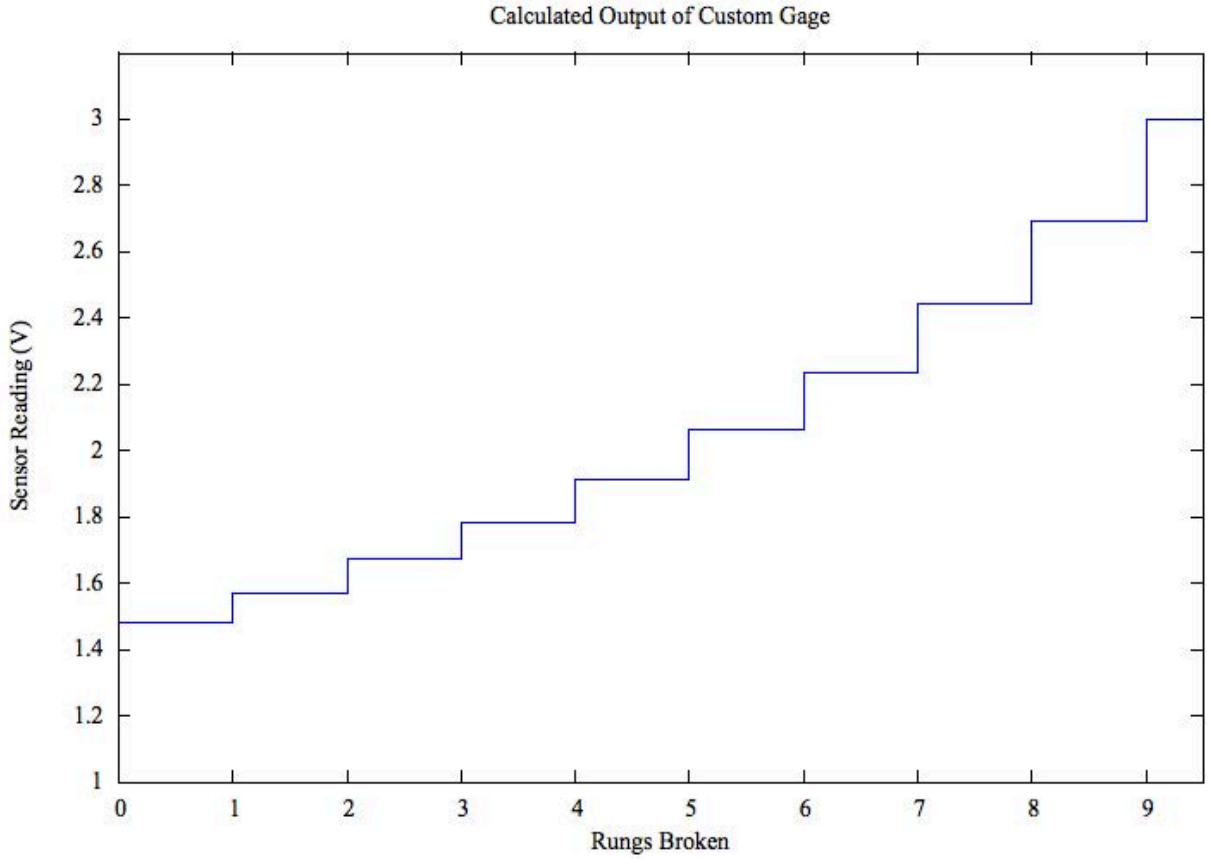

Figure B-18: Predicted change in output voltage of custom crack propagation sensor with rungs broken

Calculated Output of Custom Gauge

The rungs of the crack propagation gauge can be any conductive material. For the sensor prototype, a CircuitWorks Conductive Pen was used to connect the individual rungs on the two sides of the custom crack propagation sensor. The pen draws a highly conductive silver trace which sets and cures in approximately thirty minutes (ITW CHEMTRONICS, 2009).

While the commercially manufactured crack propagation patterns were designed to be glued to bare steel, the custom crack propagation gauges must be affixed to a non- conductive material for proper functionality. In a field deployment of this sensor, which would likely be on an in-service steel highway bridge, the existing bridge paint system would insulate the conductive traces from the conductive steel substrate. Sherwin-Williams MACROPOXY 646 Fast Cure Epoxy paint was chosen to most closely simulate existing bridge paint (Hopwood, 2008). Industrially-rated quick-setting epoxy adhesive was used to affix the bus resistors to the steel before application of the conductive traces. Sensor application was performed at room temperature. Figure B-19 shows an engineer applying the gauge to a test coupon.

Proof-of-Concept Experiment

A single A36 steel coupon was painted with the simulated bridge paint. Two custom crack propagation sensors were then affixed to the coupon, one on either side. Figure B-20 shows the test coupon with a custom crack propagation gauge installed. Because of the small size of the coupon relative to the size of the sensor, not all pairs of terminals were connected with conductive paint. As such, it was expected that the output of the sensor would behave as though it started with several rungs broken.

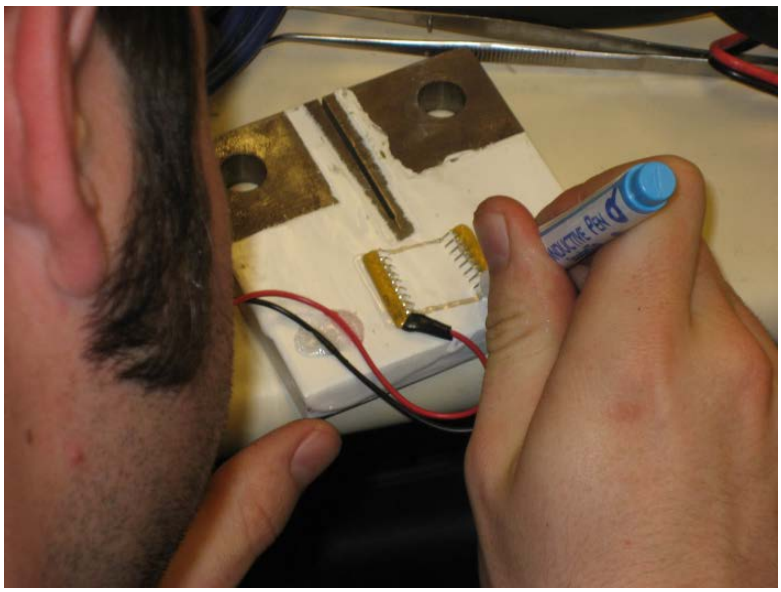

Figure B-19: Photograph of an engineer applying a custom crack propagation gauge

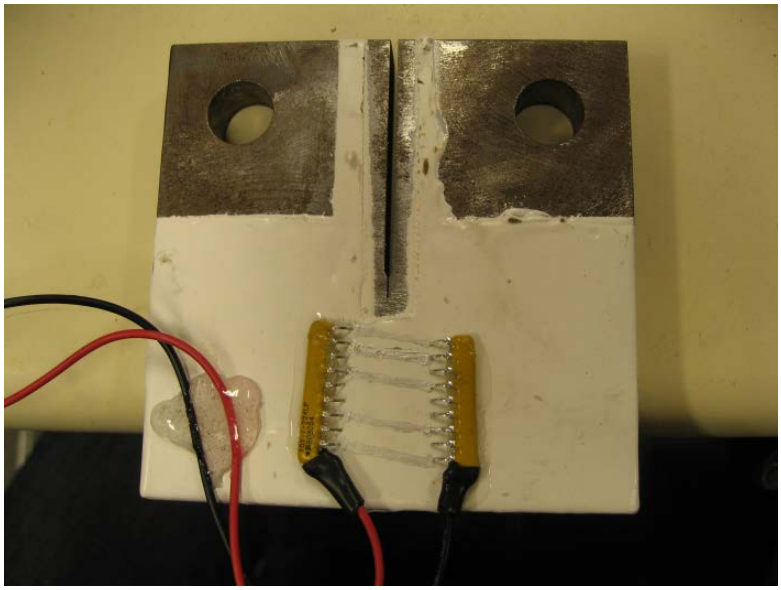

Figure B-20: Photograph of coupon with attached custom crack propagation gauge

The experimental procedure to test the custom crack propagation gauge was also identical to that for the others. The coupon was fatigued with no sensors or paint until the crack propagation was initiated. Then, cyclic tension between 0.07 kip and 2.5 kip at 10 hertz was applied to the specimen until failure.

Results and Discussion

After approximately one hour of fatigue testing, the crack propagated through the entirety of the region covered by the custom crack gauge. Figure B-21 shows that all four painted rungs are cleanly broken. Figure B-22a shows a plot of the gauge output versus time. Because this data was taken with a wired data logger, it is more susceptible to the electromagnetic interference generated by the test apparatus. Figure B-22b shows the results of the application of a 0.1 hertz low-pass Butterworth filter to the data. The data clearly show four distinct rung-breaks.

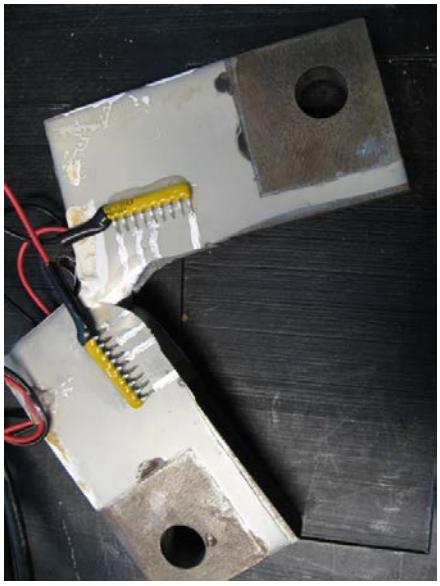

Figure B-21: Coupon with custom gauge after all rungs broke

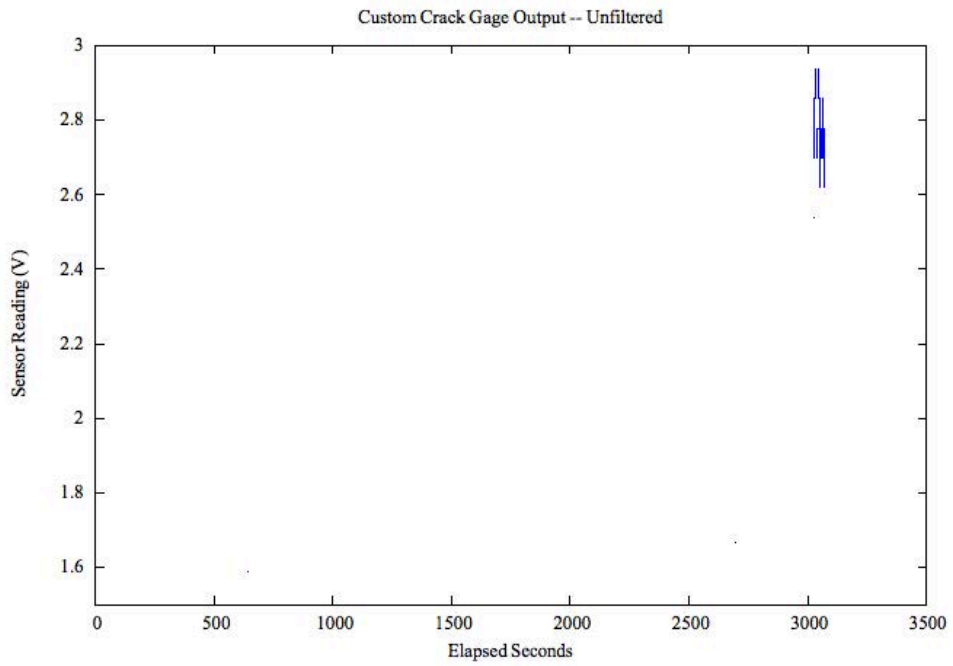

(a)

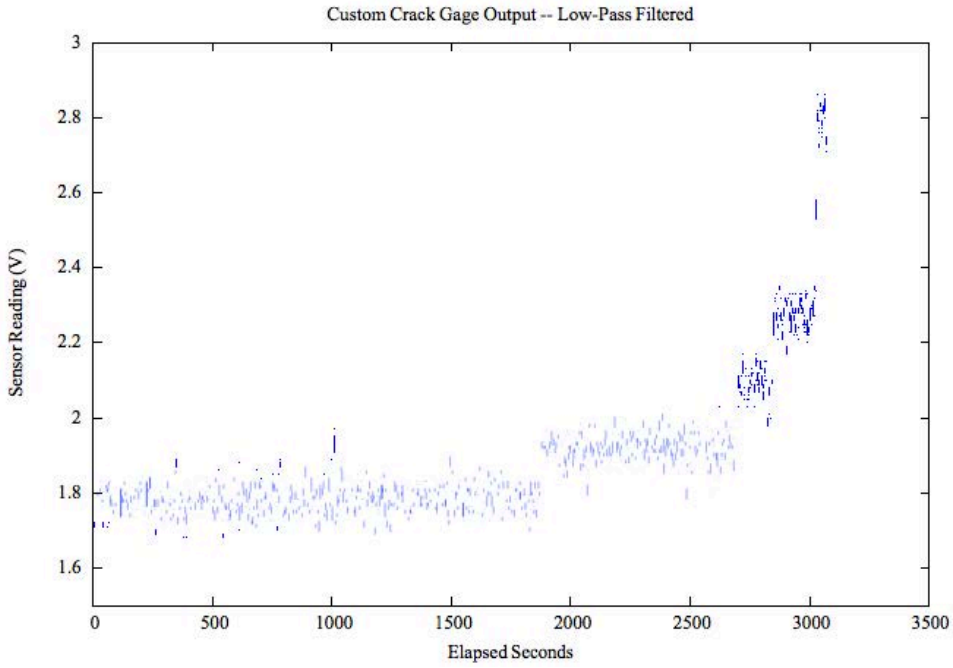

(b)

Figure B-22: Custom crack gauge output versus time (a) unfiltered, and (b) with 0.1 hertz low-pass filter

Phase B Findings & Conclusions

This phase has introduced Autonomous Crack Propagation Sensing (ACPS) and evaluated two types of commercially available crack propagation gauges and a newly invented crack propagation gauge for ACPS. It has also examined the potential of the Crossbow eKoPro Series Wireless Sensor Network for use in ACPS. The following conclusions can be drawn:

- The eKoPro Series Wireless Sensor Network is suitable for use in ACPS provided care is taken to accommodate its limited on-board analog-to-digital conversion hardware.
- Both types of the evaluated commercially available crack propagation pattern may be used for ACPS, however, each has its disadvantages: The TK-09-CPA02-005/DP can track crack tip position with a finer resolution, however, its non-linear output causes the first 40-50% of its rung breaks to be undetectable by an eKo mote. The remaining 50-60% of its rung breaks, however, are easily detected. The TK-09-CPC03-003/DP, conversely, is a larger gauge with coarser resolution for crack to position. This gauge's linear output characteristics enable each of its individual rung breaks to be detected by the eKo mote.
- When applied to bare steel using the manufacturer-specified elevated-temperature-cured adhesive, both types of traditional crack propagation patterns are capable of functioning as ACPS sensors using eKo motes. When applied with a more field- practical room-temperature-cured adhesive, the adhesive has been shown to fail before the gauge can break. These gauges are therefore only usable in field conditions where elevated-temperature-curing adhesive can be employed.
- Customized crack propagation gauges made from conductive ink and commercially-available bus resistor networks can track crack propagation and conform to the eKomotes' strict analog specifications. These gauges can be applied at room temperature without adversely affecting sensor functionality. Customized crack propagation gauges allow for a single gauge to track the propagation of a crack whose direction of propagation might be unknown or difficult to characterize.

Final Report for Phase C:
Qualification of Shake 'n Wake's (SnWs) Ability to Activate Wireless Networks Systems (WSN) to Detect Random Transient Vibratory Events[1]

M. Kotowsky and C. Dowding

Summary

Objective of this phase of the MEMS project:
To determine the effectiveness of a SnW velocity transducer actuated voltage pulse to appropriately trigger a wireless sensor into activity. This SnW triggering system will save large amounts of power and extend battery power of WSN's that must record random vibratory events at high sampling rates.

Context
Cessation of sensing to conserve battery life is acceptable for measuring at predetermined time intervals; unfortunately detection of random dynamic events like blasting, pile driving, or passage of large vehicles does not allow such cessation. In the current state of commercially-available wireless sensor networks, there is no immediate solution to this problem. One must sacrifice battery life for constant awareness of the physical state of the structure being monitored. The Shake 'n Wake (SnW)system allows systems to be triggered into a state of measurement.

Summary of Work
In this phase the triggering effectiveness of the combined SnW velocity transducer and MICA-2 wireless mote was studied by controllably vibrating the combined systems in the laboratory. Effectiveness was determined in terms of excitation frequency and amplitude of random events that would trigger the system. Response time of the combined system was determined in Phase A.

The combined system is shown mounted on a vibrating cantilever in Figure CS-1. The combination SnW velocity gauge trigger and WSN mote responded quickly enough to awaken the mote in time to digitally record a random transient signal at both low and high frequencies that span the range of typical ground motions produced by the construction or operation of transportation facilities. Figure 7 illustrates the SnW trigger timing in conjunction with the vibratory excitation. Larger (HS1) velocity gauges are required for the widest range of possible motions.

[1] DISCLAIMER

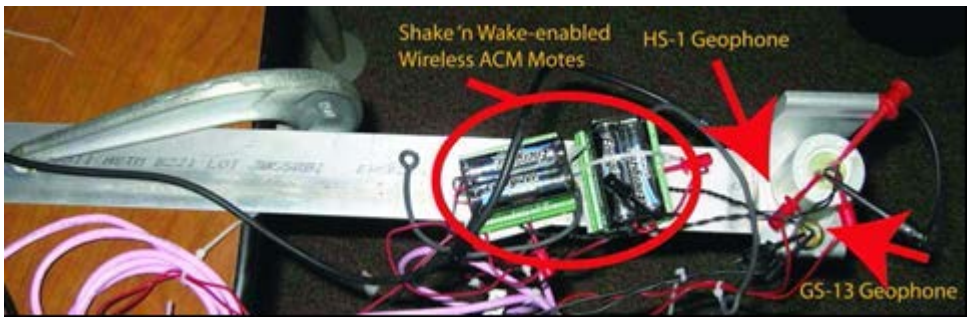

Figure CS-1: Test apparatus to produce controllable transient excitation to assess response of Shake ‘n Wake triggering system

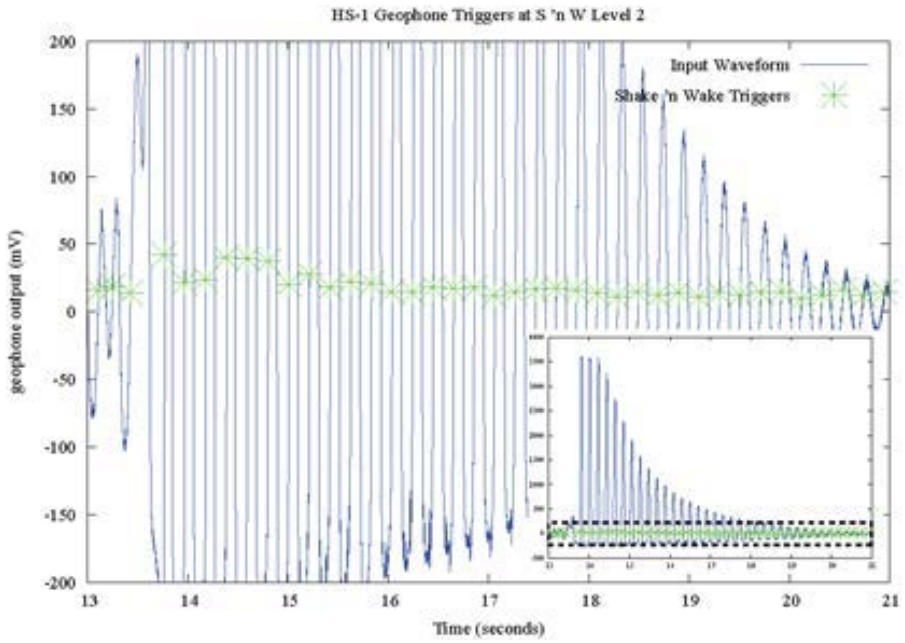

Figure CS-2: Comparison of dynamic excitation (blue) with the SnW trigger signals (green x’s) demonstrates that the SnW system triggers the mote in time to detect the amplitude of the first arriving pulse.

Major Finding:

Shake ‘n Wake system can trigger the wireless sensor network system (WSNs) mote to measure crack response to a random vibratory event in time to detect the first arriving pulse, and thus could be employed as a vibratory Structural Health Monitoring system for transportation facilities under construction or operation when combined with a WSNs with high sampling rate data acquisition.

Final Report for Phase C:
Qualification of Shake 'n Wake's (SnWs) Ability to Activate Wireless Networks Systems (WSN) to Detect Random Transient Vibratory Events

M. Kotowsky and C. Dowding

Introduction

This Phase C Report describes experimental verification of the design criteria of the Shake 'n Wake board. The design criteria of the Shake 'n Wake board are as follows:

(1) It must not significantly increase the power consumption of a mote.
(2) Its trigger threshold must be predictable and repeatable.
(3) It must not contaminate the output signal of its attached sensor.
(4) It must wake up the mote such that the mote has time to record during the peak of the motion of interest.

Criterion 1 is addressed in Phase A (see Analysis of Power Consumption). Verification of design criteria 2), 3) & 4) are described in the following sections.

Transparency of Shake 'n Wake

Because Shake 'n Wake is intended to be attached in parallel an analog-to-digital conversion unit on the mote, the output of the geophone must not be affected by the presence of the Shake 'n Wake. To determine whether the Shake 'n Wake hardware meets this design criterion, the output of the test geophones attached to Shake 'n Wake boards were compared to control geophones while subjected to identical physical excitation. Figure C-1 shows the experimental setup on which all four geophones – an HS-1 test geophone, an HS-1 control geophone, a GS-14 test geophone, and a GS-14 control geophone, were placed on the end of a cantilevered aluminum springboard at an identical distance from the fulcrum.

By measuring the responses of the geophones connected to Shake 'n Wake boards and comparing them to the responses of the control geophones, it can be determined whether or not the Shake 'n Wake circuitry will contaminate the waveform. Figure C-2 clearly indicates that the positive portion of the output of a test geophone follows the positive portion of the output of its equivalent control geophone. The negative portion of the output of the test geophone is clipped at a value of -200 millivolts. The negative portion of the output of a geophone attached to a Shake 'n Wake is clipped by reverse-current-limiting diodes that prevent voltage of inappropriate polarity from damaging the board's internal electronics. When the same geophone is attached to the opposite connector on the Shake 'n Wake, similar clipping of the positive portion of the waveform can be observed. These results show that the Shake 'n Wake satisfies the requirement of not corrupting the output of the geophone.

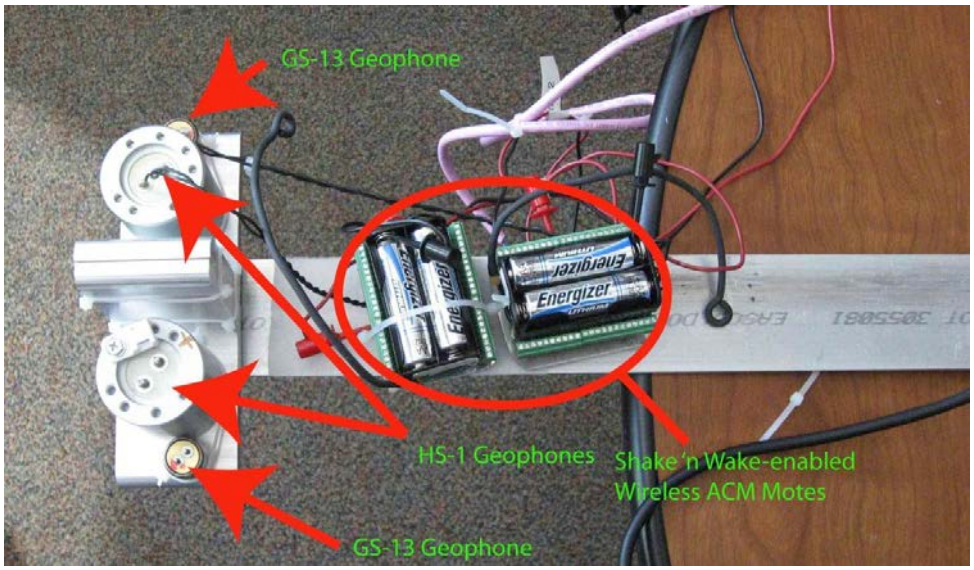

Figure C-1: Shake 'n Wake transparency test apparatus

Verification of Trigger Threshold

Idealized analysis of the Shake 'n Wake's adjustable trigger circuit, pictured in Figure 3.24, indicates that for any trigger setting, x, the threshold, V_{comp} at which the Shake 'n Wake will bring the mote out of its low-power sleep state is $3.558mV * x$. To verify the validity of this idealized analysis, the output of an HS-1 geophone is recorded on the same time scale as the output of the Shake 'n Wake to which it is attached, and the output of a GS-14 geophone is recorded on the same time scale as the output of the Shake 'n Wake to which it is attached. Both geophones were placed on a cantilevered aluminum springboard with identical distances from the fulcrum. Figure C-3 shows this experimental setup.

The length of the springboard was decreased successively to produce response frequencies of 5, 10, 15, and 20 hertz, thereby spanning the frequency range of interest for structural motion in response to a vibration event. The Shake 'n Wake was set to level 2 of 31, the most sensitive level that could be used while avoiding false triggers from ambient vibration of the springboard. Figures C-4 and C-5 show the voltage level at which each Shake 'n Wake triggers with a threshold setting of level 2 when the geophones are moved at a frequency of 5 hertz.

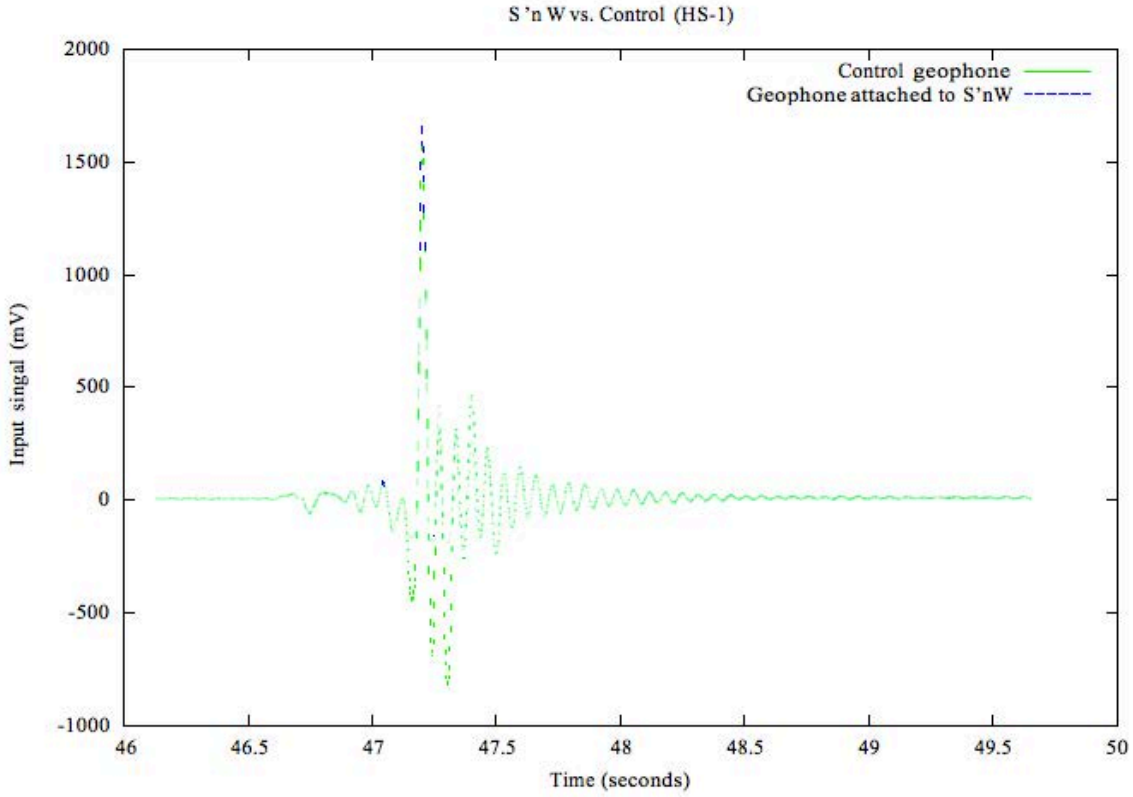

Figure C-2: Shake 'n Wake transparency test results for HS-1 geophone

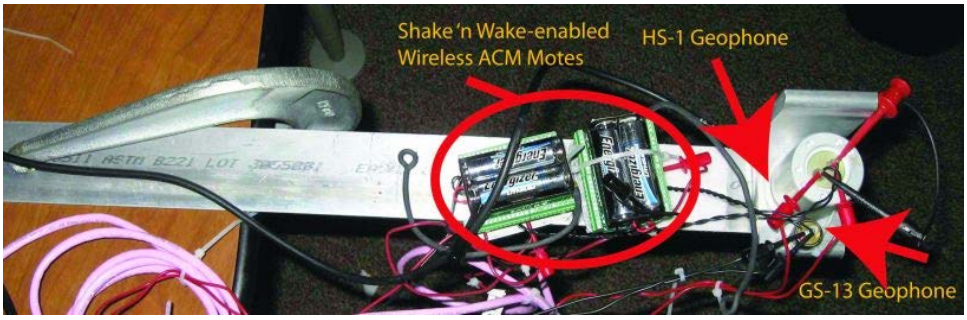

Figure C-3: Shake 'n Wake trigger threshold test apparatus

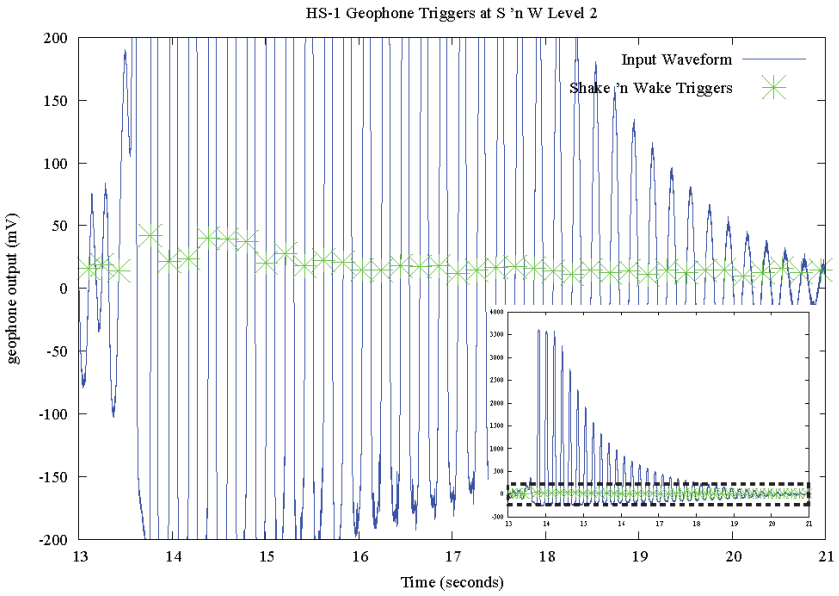

Figure C-4: Shake 'n Wake Level 2 trigger threshold test results for HS-1 geophone at 5 hertz

For each of the set of test frequencies, averages of the voltage level at which the Shake 'n Wake triggered were computed. Figure C-6 graphically summarizes these results. Based on the anal- ysis of the idealized trigger threshold reference circuit in Figure 3.24, the theoretical value at which the Shake 'n Wake should trigger – regardless of the sensor to which it is attached – is 7.116 millivolts. Figure C-6 indicates that the Shake 'n Wake is actually triggered at a higher voltage threshold than predicted, and the actual trigger threshold varies with frequency of the output of the geophone.

These results indicate that the idealized analysis is not adequate to determine the actual volt- age threshold at which the Shake 'n Wake will trigger; frequency also must be taken into account when determining this voltage. The dependence of the Shake 'n Wake's comparators on the frequency of their input voltage can be attributed to the hysteresis of the comparator, described in detail in the comparator's product data sheet in Maxim Integrated Products (2003). In order to accurately determine the threshold voltage, the Shake 'n Wake must be calibrated by the user with the desired sensor over the range of desired input frequencies. Though Figures C-4 and C-5 do indicate that though the trigger threshold varies with frequency, it is predictable; in each pe- riod of the input waveform, the trigger occurs at approximately the same input voltage. This satisfies the requirement that the trigger threshold be both predictable and repeatable, though sensor- and frequency-specific calibration is required for precise predictions.

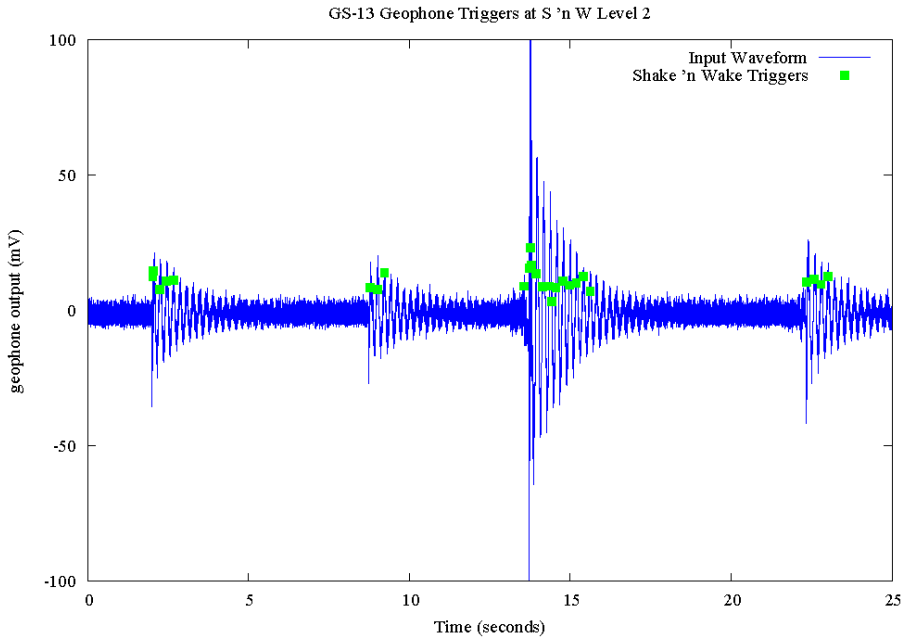

Figure C-5: Shake 'n Wake Level 2 trigger threshold test results for GS-14 geophone at 5 hertz

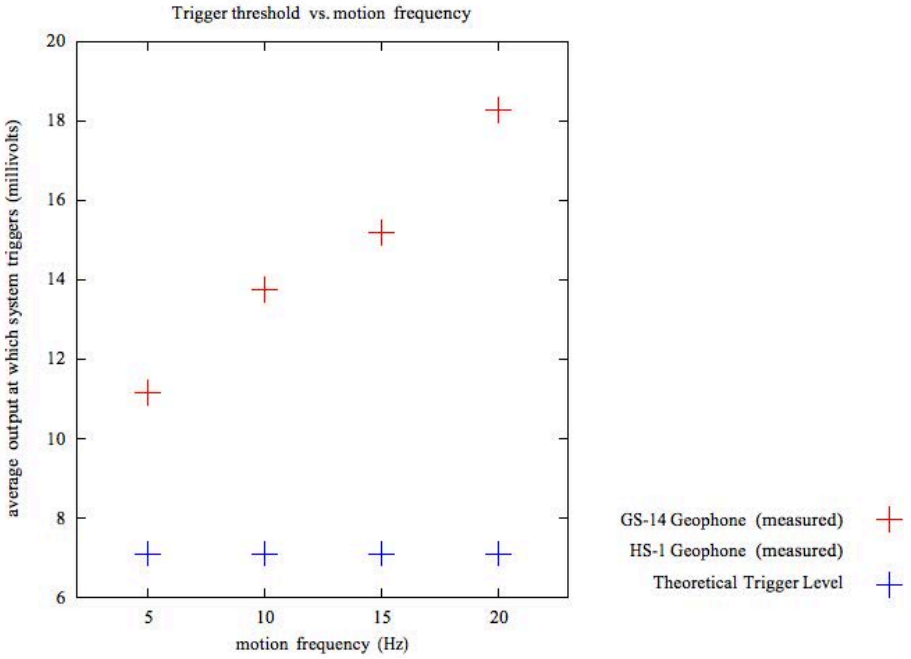

Figure C-6: Summary of Shake 'n Wake level 2 trigger threshold voltages

Physical Meaning of Trigger Threshold

The HS-1 and the GS-14 geophones each have a different characteristic response to vibration phenomena. These responses are shown graphically in Kotowsky (2010). Figure C-7 shows the

trigger levels derived from the springboard experiment translated into terms of particle velocity. Over the frequency range of interest, the response of an undamped HS-1 geophone can be determined using the factory calibration sheet included in Kotowsky (2010). The GS-14 geophone, however, is not typically used for detection of low-frequency motion, so the relationship between its voltage and frequency has not been included in the factory calibration curve in Kotowsky (2010). Its low-frequency response can be extrapolated from the factory-provided curve using a power law formula as follows:

The cantilever vibration displacement δ can be held constant during the experiment by applying identical tip displacement. Its velocity is then equal to $2\pi f\delta$. Even with a constant δ, the velocity increases linearly for the portion of the GS-14's response curve where frequency is less than 20 hertz. Therefore, the portion of the GS-14's response curve can be described with the following power law formula:

$$v = 2\pi\delta k f$$

where f is the frequency of motion, k is a constant that depends on the damping of the geophone, n is the slope of the response curve on a logarithmic plot, and v is the voltage per inch per second of geophone output at frequency f. For the undamped response curve (A), used in this experiment to provide the largest signal-to-noise ratio to the Shake 'n Wake board, this portion of the response curve can be approximated as:

$$v = 2.455 * 10^{-5} * f^{3.106}$$

Speed of Response

The Shake 'n Wake board does not have the ability to digitally record the readings from the sensor to which it is attached. It is therefore crucial to the operation of a system performing Mode 2 recording that the mote to which the Shake 'n Wake is attached begins to operate and execute user code as quickly as possible, as it will be the user code that is responsible for recording the event. If a wireless ACM system were deployed to measure dynamic response of a residential structure, the highest frequency input signal to which the Shake 'n Wake must respond is 20 hertz; this is the highest expected frequency of motion of an instrumented wall.

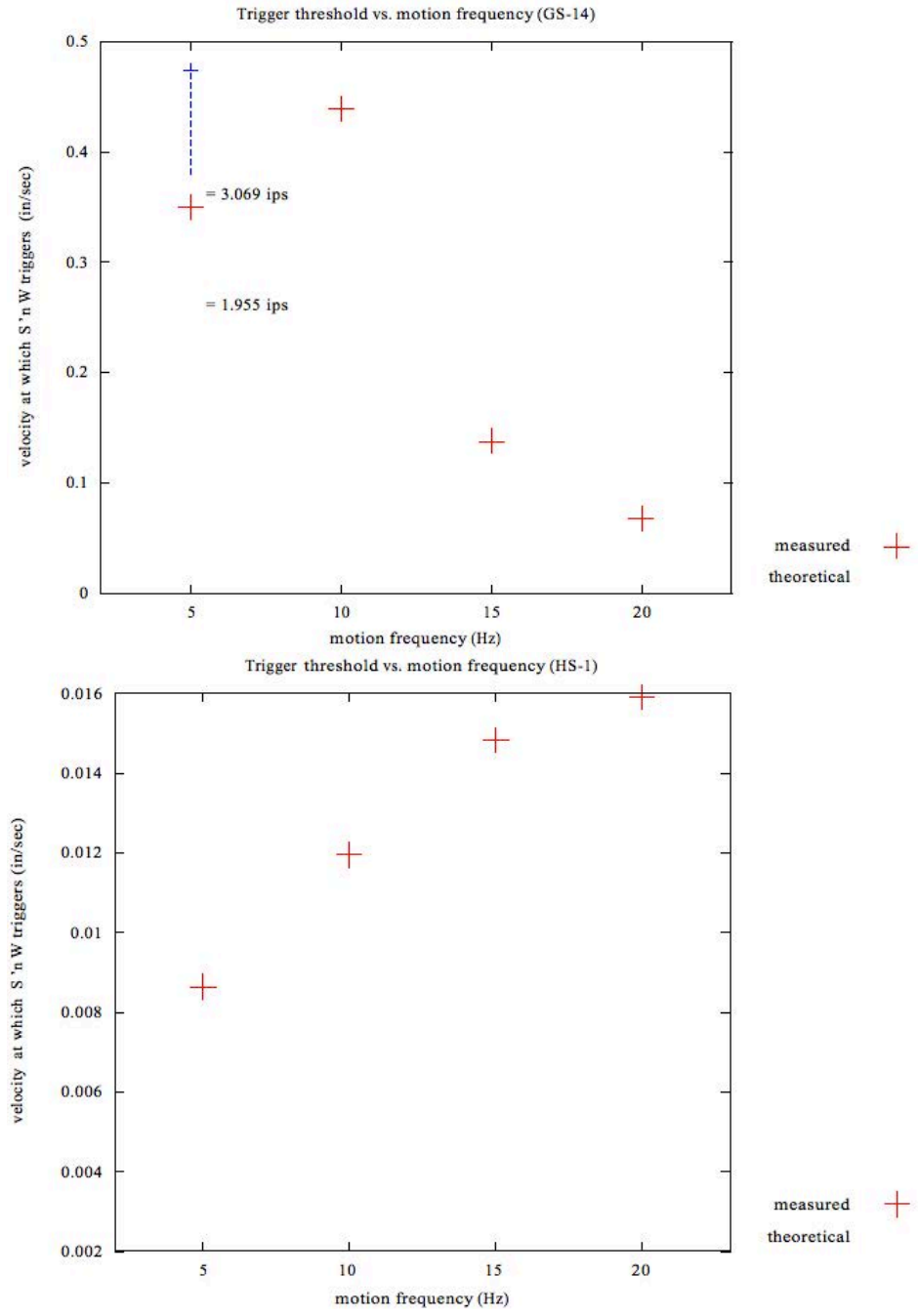

Figure C-7: Summary of Shake 'n Wake level 2 trigger threshold velocities

Figure C-8 shows that a 20 hertz zero-centered sinusoidal input signal will reach its peak absolute amplitude after 12.5 milliseconds.

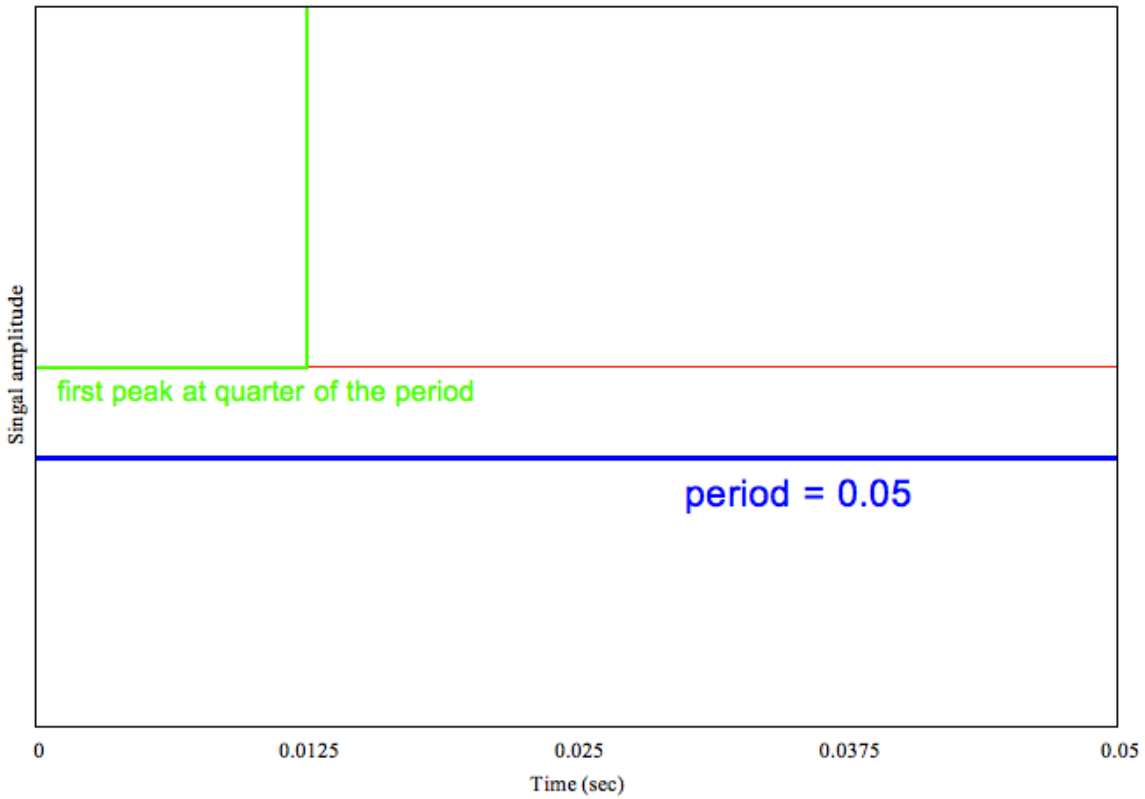

Figure C-8: 20 hertz sinusoidal input signal with rise time of 12.5 milliseconds

If it is assumed that the mote must be awake for at least one full sample length before the peak of interest and that it will be sampling at 1000 hertz, then it follows that the time from Shake ’n Wake event detection to the execution of user code by the mote must be less than 11.5 milliseconds.

Output from an oscilloscope connected to various components of a wireless ACM node, shown in Figure C-9, illustrates signal propagation delay from the geophone through the components of the Shake ’n Wake and finally into the mote’s processor. At time $t_1 = 60\mu s$, the out- put voltage of the geophone, shown in yellow, crosses the threshold V_1 which corresponds to the software programmable threshold residing in the Shake ’n Wake’s memory. 58µs later, at time t_2, the Shake ’n Wake’s hardware interrupt request line (IRQ), shown in green, changes to logic low. This change in state of the IRQ is the “wakeup” signal passing from the Shake ’n Wake to the mote. The mote, which is asleep until t_2, has already been programmed by the user with an instruction to turn on an LED. The LED active-low hardware line, shown in purple, activates at t_3, 31µs after the signal from the Shake ’n Wake is sent to the mote. The activation of the LED indicates that the mote has executed its first line of user code. In a real event detection system, this first post-wakeup instruction would be to immediately begin sampling at a high frequency. The power draw of entire system, shown in pink, begins to increase from its sleep level as soon as the Shake ’n Wake sends its “wakeup” signal.

This timing diagram shows that the interval between the moment the input signal reaches the theoretical trigger threshold and the moment the Shake ’n Wake signals a “wakeup” is 58 µs and the time interval between when the Shake ’n Wake signals a “wakeup” and the

time the first line of user code is executed on the mote is 31 µs. Since this 89 µs is well within the specified 11.5 millisecond window, it follows that the Shake 'n Wake can perform within the timing requirements.

Discussion

These experiments have served to quantify the abilities of the Shake 'n Wake hardware relative to the requirements of a random-event detection scenario. The suitability of the geophones is limited on one end by amplitude: if the vibration frequency is not high enough, the required output amplitude for the Shake 'n Wake to trigger at its most sensitive setting becomes unreachable. On the other end of the frequency range, the limit of functionality is the response speed of the Shake 'n Wake hardware. Table C-1 summarizes the practical limits of the Shake 'n Wake with respect to frequency of geophone output.

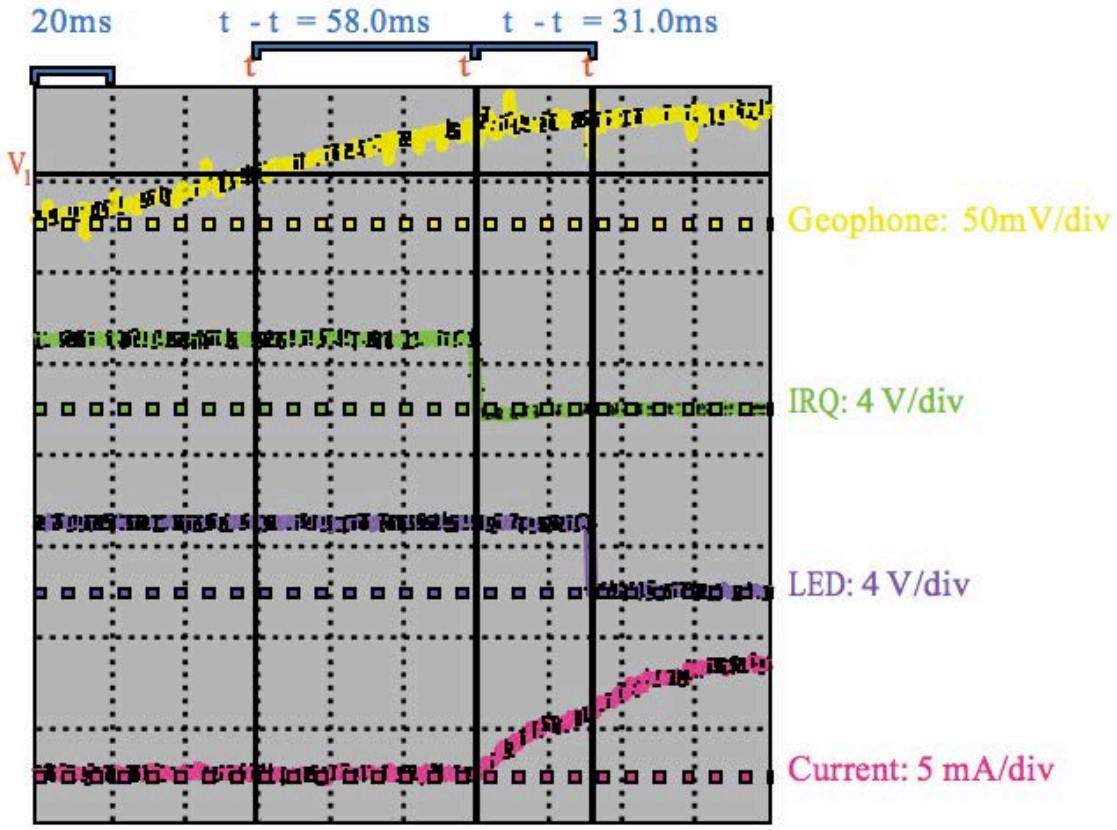

Figure C-9: Scope readout indicating the mote can execute user code within 89 µs of a signal of interest, after Jevtic et al. (2007b)

Upper Frequency Limit: Shake 'n Wake Response Time

A mote attached to a Shake 'n Wake will be executing user code 89 µs after a geophone voltage of

interest. Using the same assumption that the mote must be awake for at least one full sample period before the peak of interest and that it will be sampling at 1000 hertz once it wakes up, the minimum time between the "wakeup" signal and the arrival of the peak of the event is 1.089 milliseconds. Figure C-8 indicates that the rise time of an idealized sinusoidal input signal is 25% of its period. If the rise time must be at least 1.031 milliseconds, then the period must be at lest 4.356 milliseconds and the frequency must be at most 230 hertz. Thus, in order for a node to be executing user code in time to catch the first peak of a dynamic event of interest, the maximum frequency of the event is 230 hertz.

Lower Frequency Limit: Geophone Output Amplitude

The GS-14 and HS-1 geophones' output amplitude for a given input velocity varies with frequency, as shown in the response spectra in Kotowsky (2010). Figure C-7 shows that for the GS-14 geophone, the frequency of motion must be greater than 20 hertz be- fore a 0.05 inch per second velocity can be detected by the Shake 'n Wake at level 2. However, if the amplitude of motion is great enough, the GS-14 can produce sufficient amplitude at low frequencies. For the HS-1 geophone, the frequency of motion can be as low as 2 hertz and still provide a large enough amplitude to trigger the Shake 'n Wake at level 2, no matter what the amplitude of the motion.

input velocity	＞1ips	0.05ips
GS-14	2－230Hz	20－230Hz
HS-1	2－230Hz	2－230Hz

Table C-1: Summary of functional ranges for Shake 'n Wake event detection at level 2

Phase C Findings & Conclusions

The above experiments verify that the Shake 'n Wake:

- does not contaminate the sensor output
- provides a predictable and repeatable threshold voltage
- responds quickly enough to allow the mote to wake up in time to digitally record the signal of interest
- can be used with a GS-14 geophone to detect motions with a frequency 20 hertz and 230 hertz at amplitudes of 0.05 ips, down to 2 hertz if amplitude is sufficiently large
- can be used with an HS-1 geophone to detect motions with a frequency between 2 hertz and 230 hertz regardless of amplitude

Final Report for Phase D:
Design and Installation of Wireless System within and outside Sycamore Test House[1]

J. Meissner and C. Dowding

Summary

Objective of this phase of the MEMS project

Design and install a weather rugged wireless sensor network Autonomous Crack Measurement (ACM) system in typical structure adjacent to an operating quarry to measure long term crack response.

Context

The test house is adjacent to a road aggregate quarry. It is typical of residential structures that often surround such quarries or are adjacent to road construction that requires blasting or pile driving. When residents of these homes complain that the blasting vibration induces cracks, the regulatory vibration limits can be lowered by local municipal entities, which raise the cost of producing road aggregate or the cost of construction. Instrumentation of these homes can and does show that climatological changes produce far greater crack response than typical blast induced ground motions. Such comparisons are useful to reduce anxiety of those near-by residents who feel vibrations, which results in lower cost of road aggregate and or construction or operation of transportation infrastructure.

Summary of Work

The weather rugged, solar powered wireless sensor network system (WNSs) was designed to be deployed to monitor crack response and transmit data between two structures to connect to the internet. It was then installed both within the test house adjacent to an operating aggregate quarry to monitor crack response inside and outside (as shown in Figure DS-1) to transmit data to the other structure. The weather rugged, solar powered mote system was combined with the string potentiometer micro inch displacement transducer to measure crack response. Weather ruggedness and provision of solar power allowed the WSN to be deployed outside to transmit data from the test house to the internet connected house by multi hopping. Performance of the system in comparison to a wired, research grade system is described in Phase E.

Continued on next page.

[1] DISCLAIMER

Figure DS-1: Installation of the weatherized motes for transmission of data from the test house to the structure with the internet connection. Yellow device below the mote on left is a temperature probe that accesses the mote from a port that also allows attachment of the crack response gauge, which illustrates the flexibility of these newer designs.

Major Finding:

A weather rugged, solar powered, wireless sensor network to measure both crack response and climatological data can be designed, installed and connected to the internet by typical engineers, which facilitates use of these devices by engineers monitoring response of transportation facilities under construction or operation.

Final Report for Phase D:
Design and Installation of Wireless System within and outside Sycamore Test House

J. Meissner and C. Dowding

Introduction

This phase D report describes the design and installation of a weather rugged wireless sensor network (WSN) at a test house adjacent to an aggregate quarry. The system follows the Remote Autonomous Monitoring [RAM] paradigm pictured in Figure D-1 below: Data are autonomously collected and stored short-term at the test house, transmitted to the QC house, uploaded to an ITI server, and then broadcast over the web for viewing.

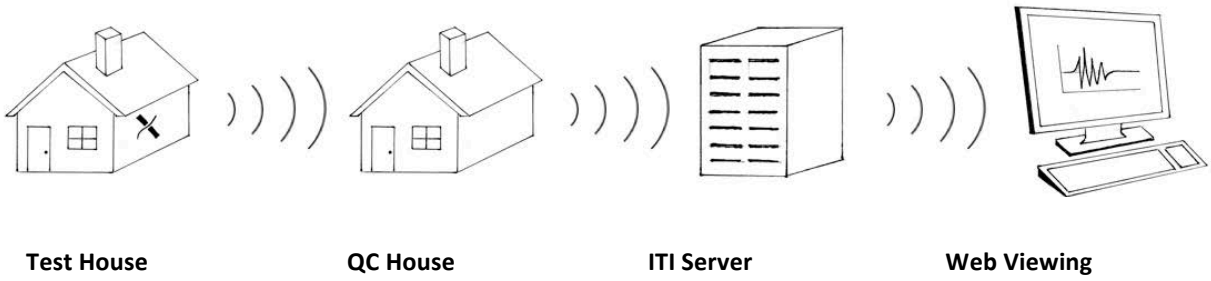

Figure D-1. Remote Autonomous Monitoring paradigm

Location

The test house and quarry are located west of Chicago is shown in Figure D-2 below. The house is approximately 300 feet away from the edge of the blasting zone.

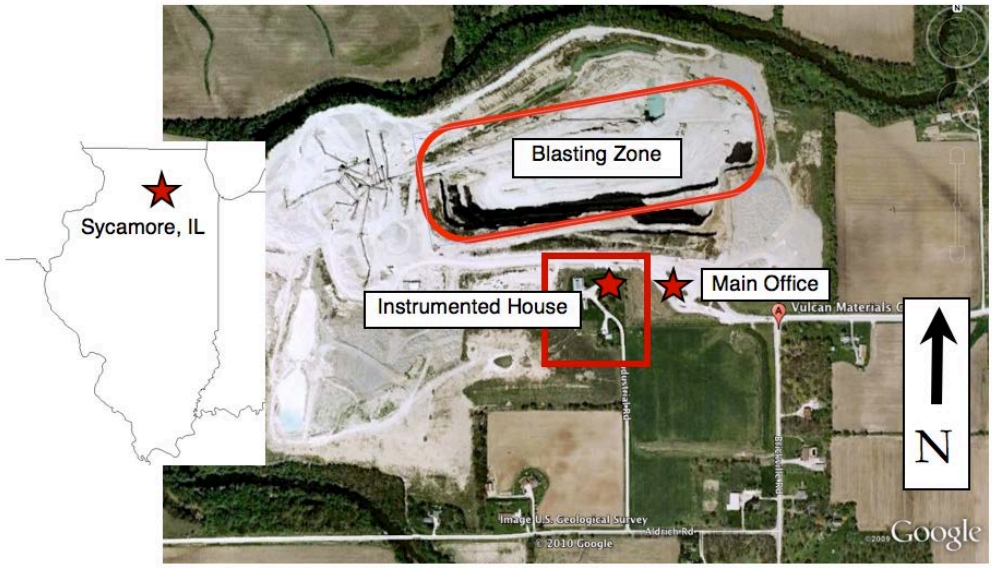

Figure D-2. Overall view of the aggregate quarry showing location of the test house in relation to the blasting zone.

Test Structures

Figure D-3 shows the aerial layout of the instrumented test house and the QC House (where the internet connection is located). The actual houses are also shown in the photographs below. The test house is a two-story wood-framed structure with a basement foundation. However, there is an addition section of the house that is shallowly founded.

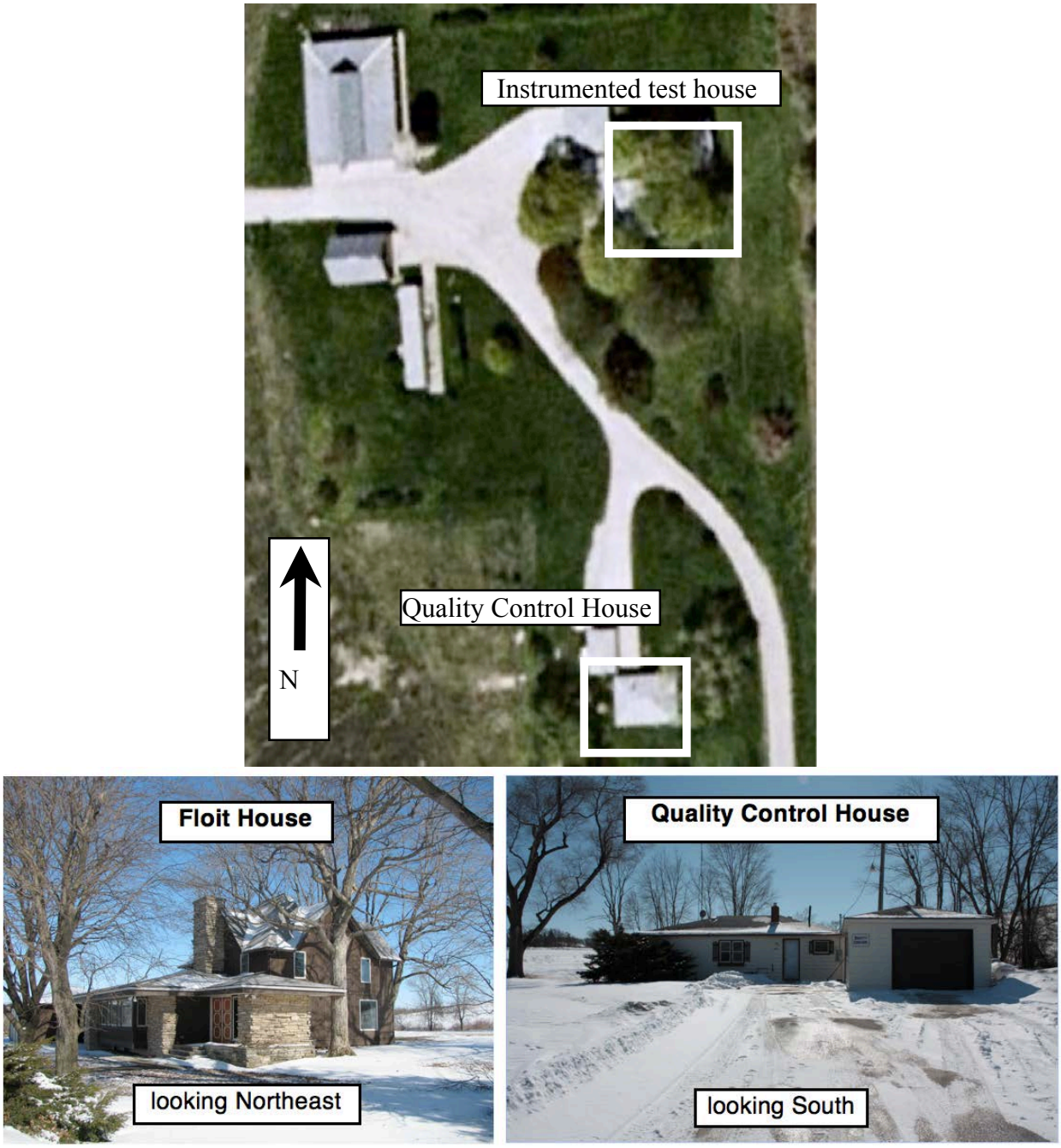

Figure D-3. Aerial layout and pictures of both the test house (instrumented) and the Quality Control House (internet connection)

Wireless eKo Mote System

The test house is instrumented with a wireless ēKo Mote system (Memsic, Corp.) to monitor structural and crack response as well as environmental conditions like temperature and humidity.

The REG installed a wireless sensor network (WSN) to monitor long-term changes in two cracks at the test house in conjunction with temperature and humidity. The WSN is a multi-hop system that consists of 4 nodes (motes) and a base station at the QC house. Data is collected from the sensors at the nodes and is then relayed back to the base station. Figure D-4 shows the location of the nodes within the wireless mesh network. Figures D-5 through D-9 also show detailed photographs of the mote locations.

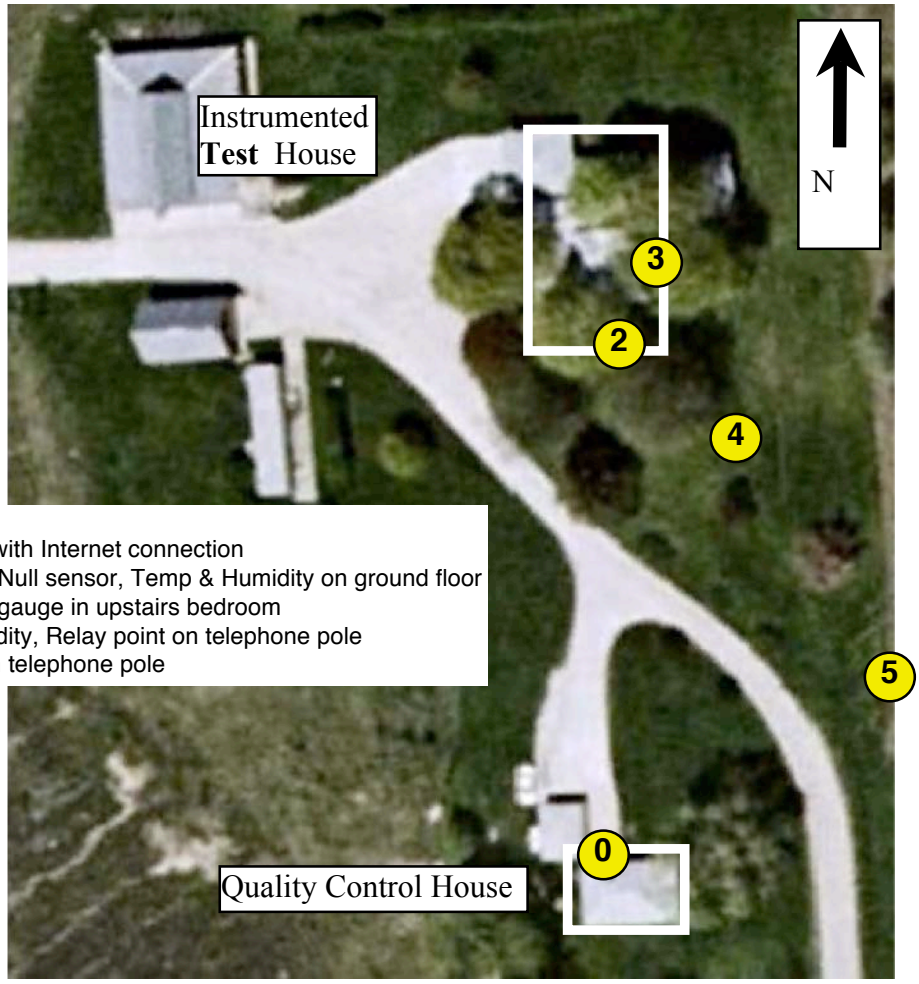

Figure D-4. Layout of nodes in the Wireless Sensor Network. Motes 2 and 3 have crack gauges, Motes 2 and 4 have temperature and humidity probes. Mote 5 is simply a relay point.

Mote Locations

Figure D-5. Exterior view of southwest corner of instrumented test house, showing where Node 2 is inside.

Figure D-6. Exterior view of east wall of instrument test house, showing where Node 3 is inside.

Figure D-7. Node 4 as relay point on telephone pole.

Figure D-8. Node 5 as relay point on telephone pole.

Figure D-9. Node 0 is base station inside QC house.

Sensor Locations and Nomenclature

The test house is outfitted with 3 high-precision String Potentiometer (Firstmark Controls 150 series). S1 and S3 measure, while S2 is a null gauge. Figure D-10 shows the exact sensor locations within the house and Figures D-11 through D-13 show photographs of the installed equipment.

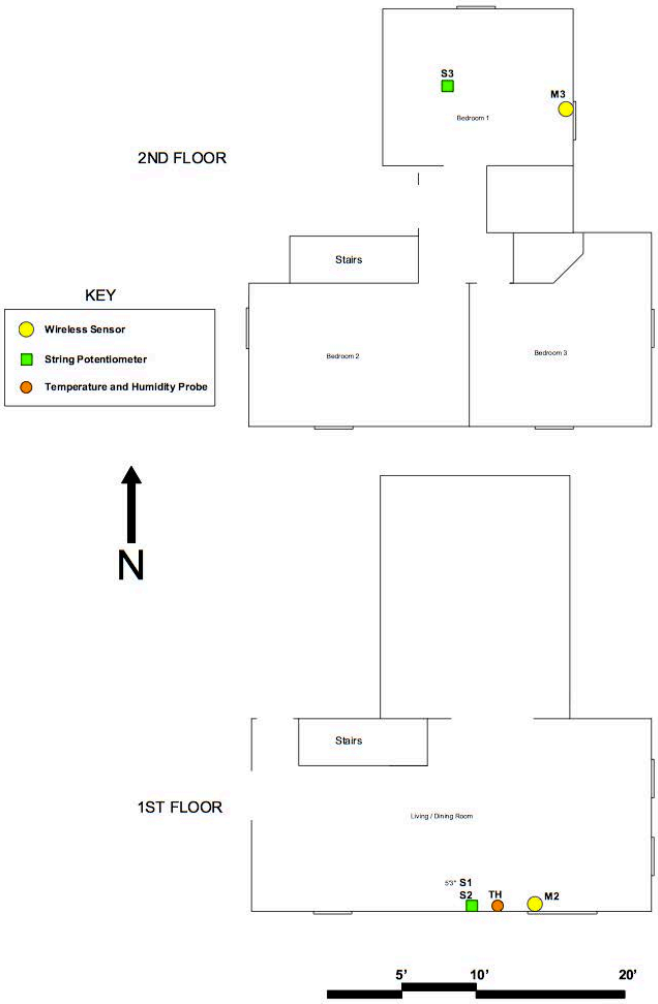

Figure D-10. Exact sensor and equipment locations within house.

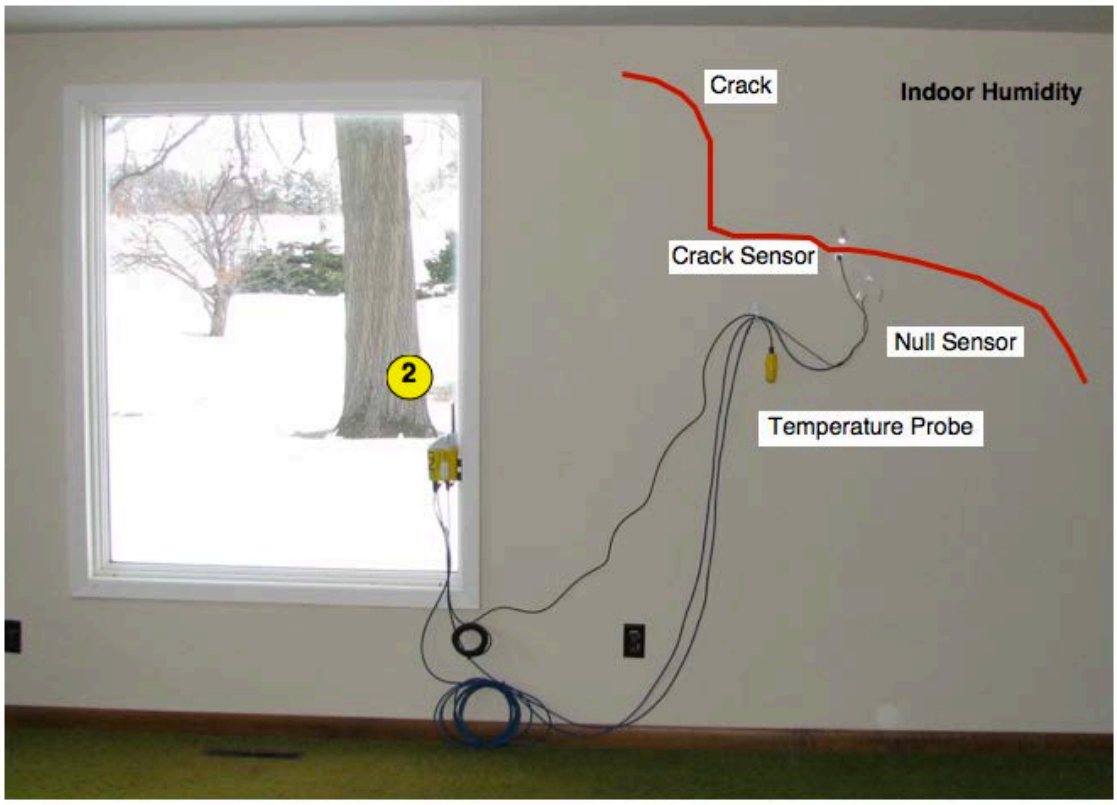

Figure D-11. Interior view of Node 2 in living room. Crack sensor, null sensor, and temperature probe connected to eKo Mote.

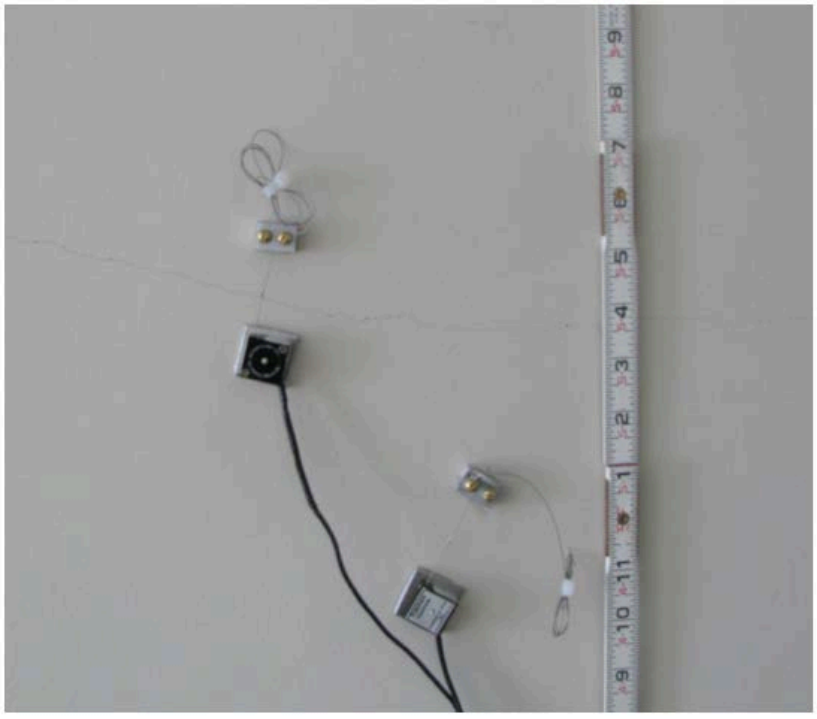

Figure D-12. Close-up of crack sensor and null sensor. Both instruments are string-potentiometers.

Figure D-13. Interior view of Node 3 in upstairs bedroom. Crack sensor connected to eKo Mote.

Figure D-14. Close-up of string potentiometer across ceiling crack.

Design of wireless eKo Mote System

The wireless ēKo Mote system is designed to monitor long-term crack responses in conjunction with temperature and humidity measurements both inside and outside. The string potentiometers record data every 15 minutes. The motes relay that data from node to node back to the base station where it is then uploaded to ITI's server in Evanston.

Location Details

Details and context of the nodal locations are shown in the close up photographs. External nodes 4 and 5, shown in Figure D-15, were attached to poles and were faced to the south to maximize solar exposure. Node 5 was employed to measure external temperature and humidity, and the manufacturer's temperature and humidity probe can be seen attached below the node. It was located between node 4 and the base station, node 0, to provide a shorter path between node 4 and the base station. Node 4 employed no external measurement devices, and was positioned to facilitate transmission from the house to the base station. The need for 4 and 5 will be discussed later in the performance section.

Figure D-15. Installation of exterior nodes. Left installation includes temperature and humidity sensor module below the node.

Locations of the interior nodes 2 and 3 and the associated monitoring gauges are shown in the building plan view in Figure D-10. Node 2 was configured to monitor interior temperature and humidity as well as crack response of the large shear crack identified in the photograph in Figure D-16. The node itself was mounted on the window frame of the south facing living room window such that its solar cells could achieve maximum solar exposure, while the temperature

and humidity gauge module as well as the crack and null displacement gauges were mounted some 1.5 meters away. Node 3 was responsible for monitoring response of the crack in the second floor bedroom ceiling some 2-2.5 meters away as shown in Figure D-13. It was installed on the window frame of the east-facing window.

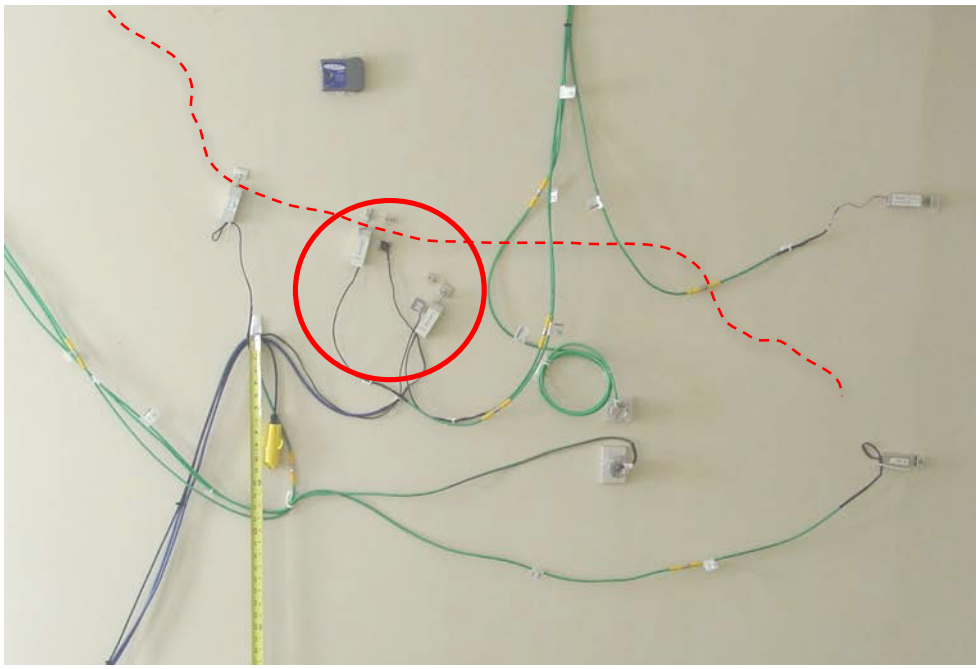

Figure D-16. Red circle shows the potentiometer crack sensors attached to wireless node by blue lines. The crack, which transects the upper two displacement sensors in the inset red circle, is underlined by a dashed line.

System Components and Design Details

The Wireless Network System (WSN) employed is designed for environmental and agricultural monitoring. As shown in Figure D-15, each node is water and dust resistant, capable of operating in wide temperature and humidity ranges, and is advertised to operate for over five years with sufficient sunlight. Its weatherproof design makes it an attractive platform for deployment in exterior as well as interior locations.

Nodes are the principal components of the WSN. Its energy-efficient radio and sensors are designed for extended battery-life and performance, and integrates IRIS family processor/radio board and antenna that are powered by rechargeable batteries and a solar cell. A node is capable of an outdoor radio range of 500ft to 1500ft depending on deployment. Since the nodes form a wireless mesh network, the range of coverage can be extended by simply adding additional nodes. The nodes come pre-programmed and configured with a low-power networking protocol.

The base station, which must be connected to 110 V AC power and a network connection, can transmit e-mail alerts when sensor readings cross-programmable thresholds. Though the base station can be connected directly to the Internet, the test deployment described herein employed a secure virtual private networking system to traverse corporate firewalls and protect the system and the data.

The base station provides multiple methods for viewing and manipulating recorded data: One may use the base stations built-in web interface to perform simple plotting operations. One may also connect to the base station using FTP or SFTP to retrieve raw data for further, more sophisticated processing and Web display. The latter method was employed in the described test deployment.

A unique feature of this system is that the node end-user need not manually program the system to function properly, which is attractive to those with normal computer skills. The nodes record data every thirty seconds for the first hour after activation. Thereafter they record once every fifteen minutes. These data are automatically stored, retrieved once daily, processed, and graphically displayed on a secure Web site.

During every sampling cycle, each node records its internal temperature, battery voltage, and solar input voltage, along with data from up to four external sensors to which it is attached. For instance, external temperature and humidity, soil moisture, and other agriculturally interesting phenomenon can be recorded using sensors supplied by the manufacturer. Two nodes in this demonstration were fitted with temperature and humidity probes supplied by the manufacturer, as shown in the left photograph in Figure D-15.

Nodes that were deployed to measure crack response were supplemented with an signal conditioning board, available from the manufacturer, to amplify excitation voltage and sensor output voltage, effectively increasing the resolution of the system. As configured by the manufacturer, the signal conditioning board increases the resolution of the crack displacement sensor by approximately ten times. The module was not packaged in a weather proof enclosure and was placed in a plastic container using non-weatherproof components to facilitate indoor deployment.

Crack response was determined by measuring the opening and closing of cracks shown in Figure D-16with a miniature string potentiometer, shown in Figure D-17. Potentiometer-based displacement sensors with their very low power consumption, no warm up time, and excitation voltage flexibility are prime candidates for wireless structural health monitoring. The potentiometer chosen for wireless sensing is a subminiature position transducer which requires no additional electronics to operate. With the signal conditioner installed, the effective resolution is increased by a factor of approximately 10, for about 3.8 μm, implying that the sensing system is approximately 38 times less sensitive than a system employing an LVDT.

Figure D-17. Details of the potentiometric proximity sensor spanning the ceiling crack.

Phase D Findings & Conclusions

The weather-rugged eKo mote system can be designed and installed to

1) Measure crack width response inside a structure
2) Connect to the internet
3) Operate as signal transmitters exterior to structures in variable weather

These findings are important for installation of systems to monitor the behavior of transportation structures without being connected by wire.

Final Report for Phase E:
Field Qualification of Wireless Autonomous Crack Measurement (ACM) System to Measure Long Term Crack Response[1]

T. Koegel & C. Dowding

Summary

Objective of this phase of the MEMS project

Qualify the performance of a weather rugged wireless sensor network as an ACM system by comparing its performance with research grade wired systems in the same test facility. Both of these systems autonomously measure long term crack response.

Context:

Comparisons of crack response to vibratory and climatological effects are useful to reduce anxiety of those feeling vibrations, which can result in lower cost of road aggregate and transportation construction. Anxiety can be reduced when those affected can visually compare vibratory with climatological response of cracks. These comparisons can be made by measurements with wired and wireless systems that convey information to a computerized database from which the comparative graphs are made. While it is assumed that wireless systems are less costly and less intrusive, side-by-side comparisons between wired and wireless systems are rare to non-existent.

Summary of Work

Field performance of the combined micro-inch string potentiometer crack sensor and solar panel powered wireless mote (shown in Figure ES-1) was documented by comparing its performance with a typical wired system. Both of these systems were installed in a test structure adjacent to an aggregate quarry, which produced vibratory ground motions and air overpressures. This test house is typical of residential structures that often surround such quarries or transportation construction. Weather ruggedness, solar panel recharge capability, and built in internet communication and graphics of the WSN employed for this comparison were critical to its success. This weather ruggedness is a critical attribute for any wireless system for

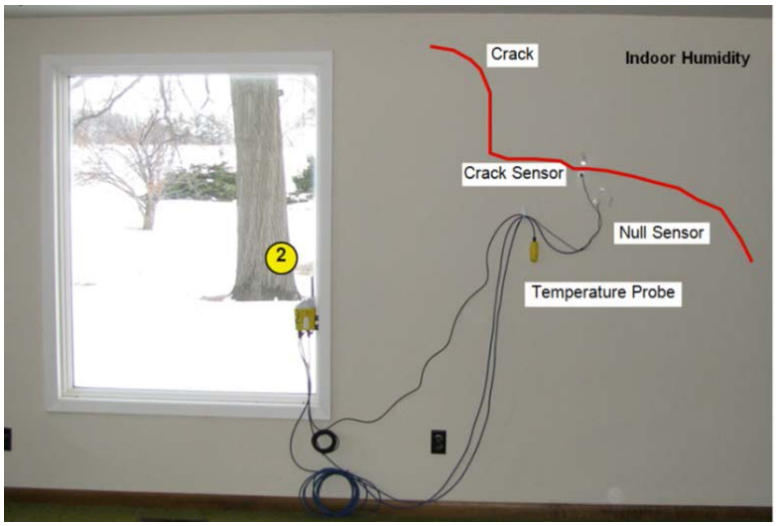

Figure ES-1: Wireless mote (2) installed in the window of the test structure to obtain solar power for continuous operation. Shown also are 2 crack sensors and a temperature probe on the right that are monitored by the mote for wireless transmission to another structure. The wired system was installed later and is described in the full report.

[1] DISCLAIMER

transportation infrastructure use. Integration of the string potentiometer and the solar panel allowed the system to be deployed inside as well to monitor crack response for almost a year.

Comparison is based upon measurement of mode 1 or long term crack response. Long term response can be monitored with measurement made every 15 to 60 minutes. Measurements are made of both crack response and climatological (temperature and humidity) effects. Comparison of these measures underscores the importance of temperature and humidity on crack behavior. Performance of the wireless system when compared to that of a research grade wired system in Figure 10 was found to be similar to that of wired systems, even though it was less costly, required less time to install, and was less intrusive. This comparison demonstrates the viability of such wireless systems to measure long term response of transportation related structures as well as those that are near-by.

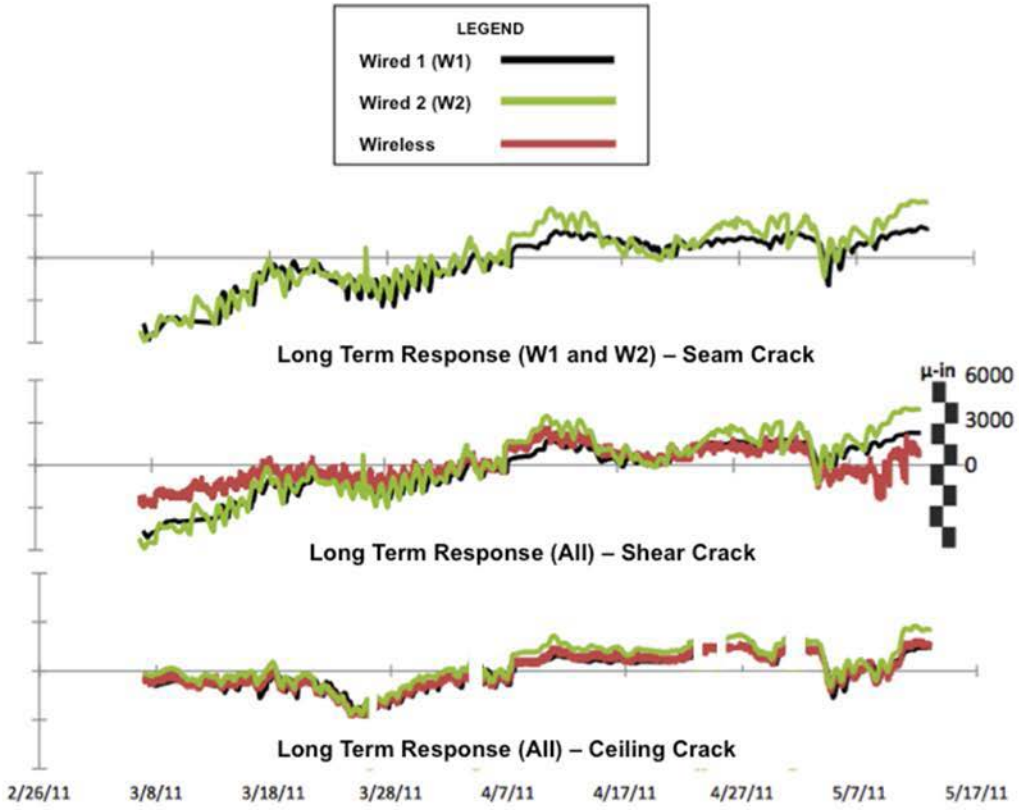

Figure ES-2: Comparison of the long-term responses of the cracks as provided by the Wired (W1 & W2) and wireless node systems from February to May. The shear crack is shown in Figure ES-1.

Major Finding:

Crack monitoring performance of the wireless sensor network (WSN) was shown to be similar to a research grade wired system even though it was less costly, required less time to install, and was less intrusive. Use of the WSNs has the potential to lower the cost of monitoring transportation facilities under construction or operation.

Final Report for Phase E:
Field Qualification of Wireless Autonomous Crack Measurement (ACM) System to Measure Long Term Crack Response

T. Koegel & C. Dowding

Introduction

This Phase E report substantiates the ability of wireless sensor network systems (WSNs) to measure remotely and autonomously the performance of any component of a constructed facility that involves existing cracks such as bridges, building facades, etc over long periods of time. One of the first systems to move wireless technology from the research lab to the field serves as the example of this class of wireless systems. While there are and will be other wireless systems, this system was chosen as a typical example of the wireless class for comparison with wired systems. For some time, wireless systems have been on the verge of being usefully deployed in the field for structural health monitoring (SHM). These systems, such as that described in this report, have now matured to the point that the data logging and communication nodes can be sustainably deployed in the field in robust enclosures at an affordable price. In addition, the process of data logging, internet transmission and graphical data display have also matured to the point that display of data can be accomplished by the average engineer.

Structural health is monitored in this example by the measurement of micro-meter opening and closing of cracks on the interior walls of structure. This response and the associated climatological data are transmitted via a secure internet connection in an adjacent structure back to a central server where they are made available via the World Wide Web. While the nodes themselves are weather proof, the displacement sensors are not. Since there are other, more weather proof micro-meter displacement transducers, this interior case can also serve as an example for exterior deployment. Development of inexpensive, climatologically robust displacement transducers has lagged development of inexpensive data logging nodes because these systems have been developed for the larger agricultural market where the emphasis is on recording environmental and soil moisture conditions. The much smaller market for structural health monitoring through crack displacement, the basis of this comparison, is dependent upon other markets to drive accessory development.

This report is organized about considerations for field qualification. They include fidelity of the measured crack response, ease of installation, resolution of the measurements, length of operation under a variety of conditions without intervention, and ease of display and interpretation of data. The article first describes the components of the system and the measurement plan. It then closes with an evaluation of the considerations for field qualification.

Instrumentation Deployment

Site

The wireless system was installed in a test house adjacent to a limestone aggregate quarry near Sycamore, IL shown nestled in the trees immediately south of the quarry in Figure E-1. The two-story house, an elevation view of which is shown in the inset to Figure E-1, is typical of farm homes that have seen many additions. A visit to the basement shows that there are at least two additions to the house: one to the two-story frame structure and the most recent single story wrap

around on the west side. The house consists of a wood frame with composite wood exterior siding and gypsum drywall for the interior wall covering.

Figure E-1: Instrumented house located just south of the quarry with aerial photograph of quarry showing the location of the house.

Qualification plan and instrument locations

Four wireless nodes were deployed within and around the test structure to assess the wireless system's behavior by comparing its behavior under a variety of field conditions with that of research grade wired systems (Meissner, 2010). Assessment involves fidelity of the measured crack response, ease of installation, resolution of structural health measurement, length of operation under a variety of conditions without intervention, and ease of operation. The placement of nodes shown in Figure E-2 was chosen to maximize the variety of operational conditions. Two interior nodes (3 and 2) were chosen to compare performance of the solar cells for an east and south facing window exposure as response of different cracks. Exterior nodes (4 and 5) were located at variable distances from the house, where the base station was deployed and the base station (0) in structure that housed the Internet connection. The objective of the variable distances of exterior nodes between the house and base station was to determine the occurrence and necessity of multi-hopping to reach the base station. Multi-hopping describes a process where nodes closer to the base station relay messages from other nodes that would not otherwise be able to communicate with the base station directly.

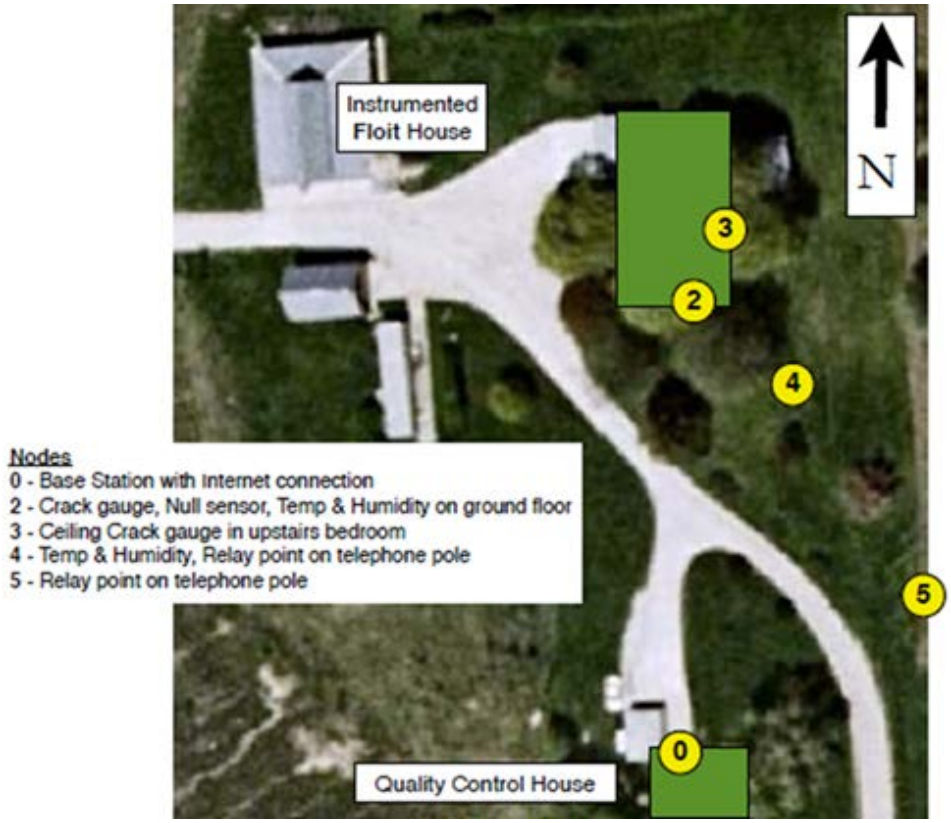

Figure E-2: Location of the nodes showing the relation of the instrumented house (nodes, 2 & 3) and the location of the internet connection (node 0)

Installation Details

Details and context of the nodal locations are shown in the close up photographs. External nodes 4 and 5, shown in Figure E-3, were attached to poles and were faced to the south to maximize solar exposure. Node 4 was employed to measure external temperature and humidity, and the manufacturer's temperature and humidity probe can be seen attached below the node. Node 5 was located between node 4 and the base station, node 0, to provide a shorter path between node 4 and the base station.

Figure E-3: Installation of exterior nodes. Left installation includes temperature and humidity sensor module below the node.

Locations of the interior nodes 2 and 3 and the associated monitoring gauges are shown in the building plan view in Figure E-4. Node 2 was configured to monitor interior temperature and humidity as well as crack response of the large shear crack identified in the photograph in Figure E-5. The node itself was mounted on the window frame of the south facing living room window such that its solar cells could achieve maximum solar exposure, while the temperature and humidity gauge module as well as the crack and null displacement gauges were mounted some 1.5 meters away. Node 3 was responsible for monitoring response of the crack in the second floor bedroom ceiling some 2-2.5 meters away as shown in Figure E-6. It was installed on the window frame of the east-facing window.

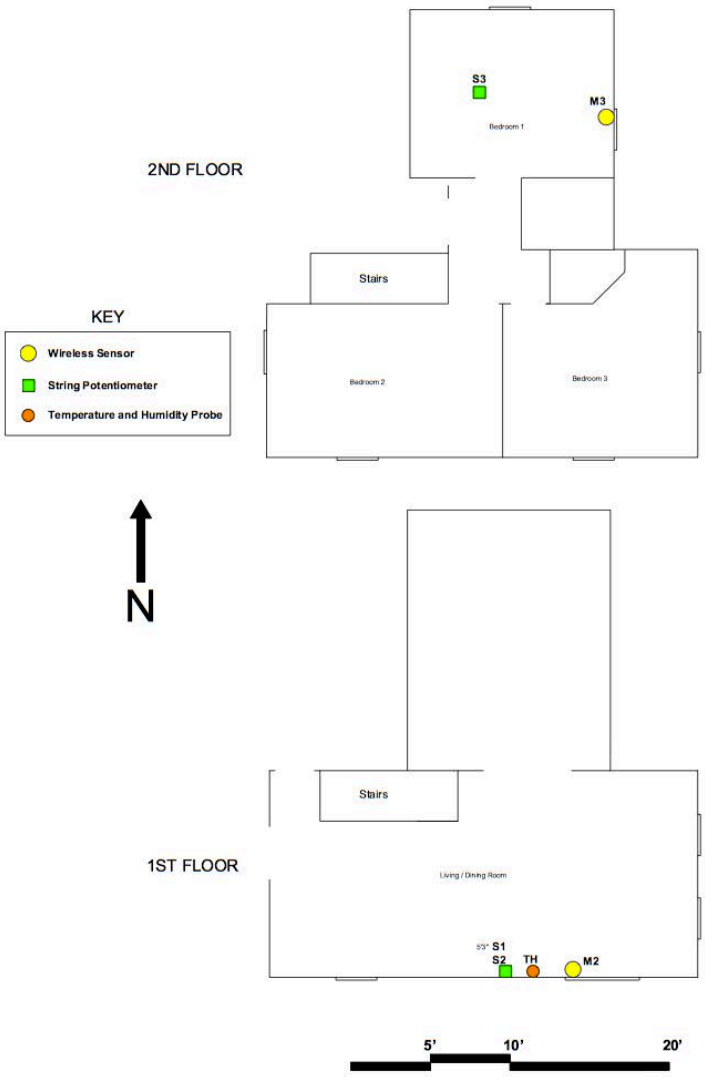

Figure E-4: Plan view of the first and second floors of the test house showing the location of the interior nodes (yellow) Temperature and humidity sensors (red) and crack sensors (green: 1 & 2 on south wall and 3 on second floor ceiling).

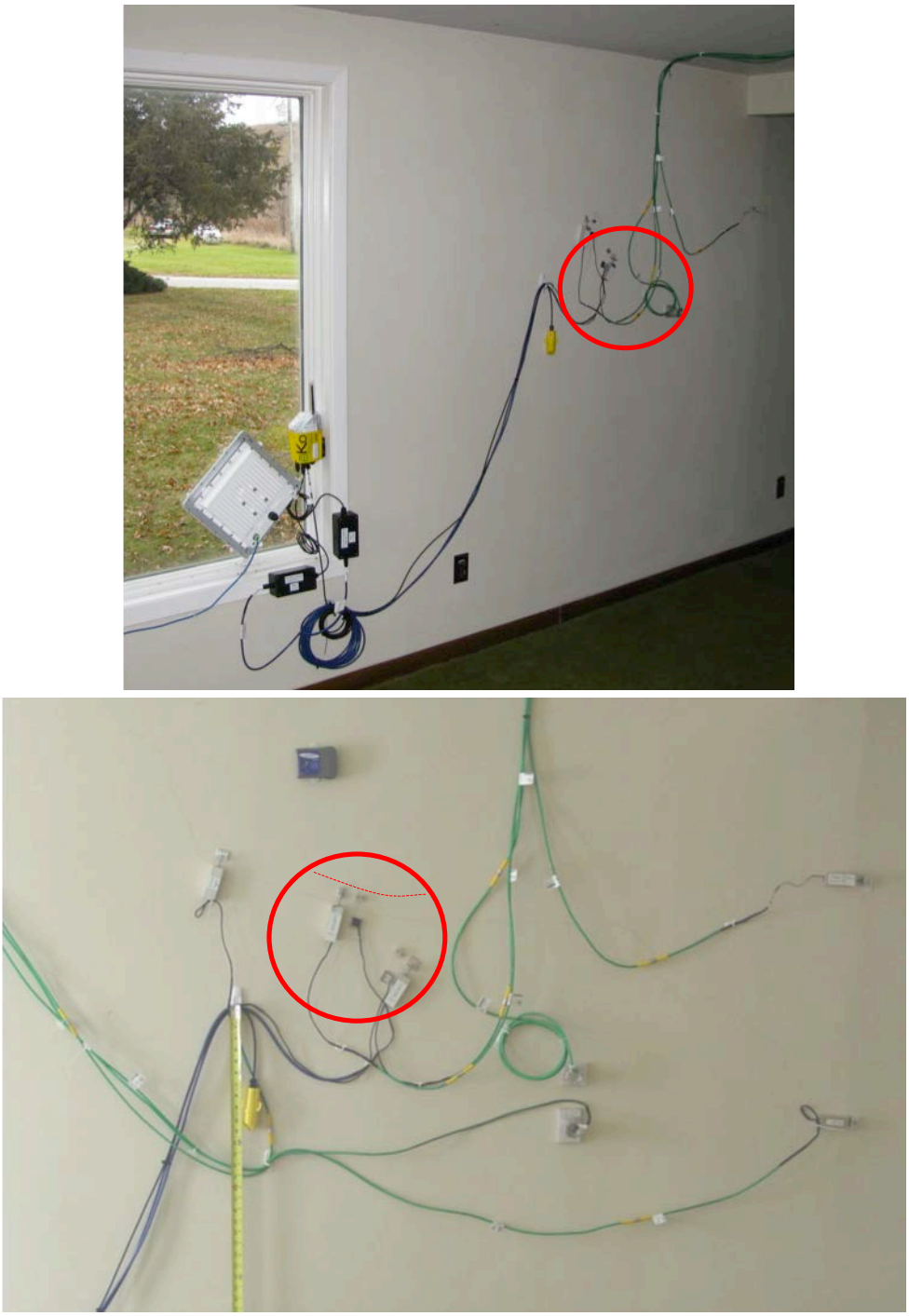

Figure E-5: Context of south wall installation: wireless node on window frame, signal conditioners (black boxes immediately below the node on window frame) on lines leading to sensors (temperature & humidity and crack sensors. Red circle encircles the potentiometer crack sensors attached to wireless node by blue lines. The crack, which transects the upper two displacement sensors in the inset red circle, is underlined by a dashed line.

Figure E-6: Context of node 3 and ceiling crack sensor. A close-up photograph of the ceiling crack and potentiometric proximity sensor is shown in Figure E-8.

Figure E-7. Wireless node weatherproof enclosure and access ports.

Figure E-8: Details of the potentiometric proximity sensor spanning the ceiling crack

System Components

The example wireless system employed in this comparison with research grade wired systems is designed for environmental and agricultural monitoring. Each node is water and dust resistant, capable of operating in wide temperature and humidity ranges, and is advertised to operate for over five years with sufficient sunlight. Its weatherproof design makes it an attractive platform for deployment in exterior as well as interior locations.

Nodes are the principal components of the Wireless Sensor Network (WSN). Its energy-efficient radio and sensors are designed for extended battery-life and performance, and integrates IRIS family processor/radio board and antenna that are powered by rechargeable batteries and a solar cell. A node is capable of an outdoor radio range of 500ft to 1500ft depending on deployment. Since the nodes form a wireless mesh network, the range of coverage can be extended by simply adding additional nodes. The nodes come pre-programmed and configured with a low-power networking protocol.

The base station, which must be connected to 110 V AC power and a network connection, can transmit e-mail alerts when sensor readings cross-programmable thresholds. Though the base station can be connected directly to the Internet, the test deployment described herein employed a secure virtual private networking system to traverse corporate firewalls and protect the system and the data. A point-to-point wireless Ethernet system was employed to connect the base station to an Internet connection located in an adjacent building.

The base station provides multiple methods for viewing and manipulating recorded data: One may use the base stations built-in web interface to perform simple plotting operations. One may also connect to the base station using FTP or SFTP to retrieve raw data for further, more sophisticated processing and Web display. The latter method was employed in the described test deployment.

A unique feature of this system is that the node end-user need not manually program the system to function properly, which is attractive to those with normal computer skills. The nodes

record data every thirty seconds for the first hour after activation. Thereafter they record once every fifteen minutes. These data are automatically stored, retrieved once daily, processed, and graphically displayed on a secure Web site.

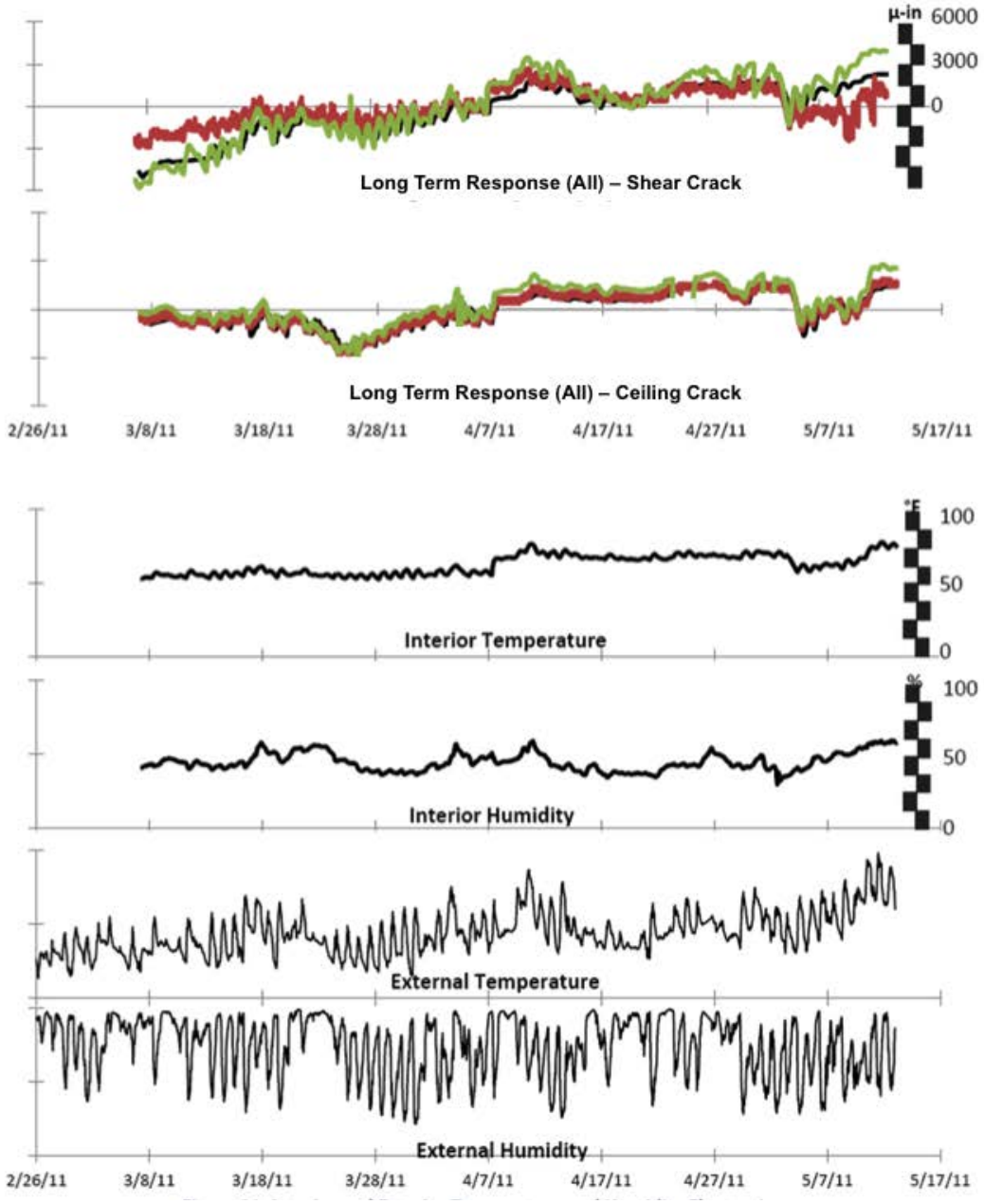

Figure E-9: Comparison of long-term response of the three systems with temperature and humidity.

During every sampling cycle, each node records its internal temperature, battery voltage, and solar input voltage, along with data from up to four external sensors to which it is attached. For instance, external temperature and humidity, soil moisture, and other agriculturally interesting phenomenon can be recorded using sensors supplied by the manufacturer. Two nodes

in this demonstration were fitted with temperature and humidity probes supplied by the manufacturer, as shown in the left photograph in Figure E-3.

Nodes that were deployed to measure crack response were supplemented with a signal conditioning board, available from the manufacturer, to amplify excitation voltage and sensor output voltage, effectively increasing the resolution of the system. As configured by the manufacturer, the signal conditioning board increases the resolution of the crack displacement sensor by approximately ten times. Unfortunately, the module is sold without a weatherproof enclosure and the black temporary housings shown dangling from the yellow node in the lower left of the lower photograph in Figure E-5 was constructed using non-weatherproof components to facilitate indoor deployment.

Crack response was determined by measuring the opening and closing of cracks with a miniature string potentiometer, shown in Figure E-8. Potentiometer-based displacement sensors with their very low power consumption, no warm up time, and excitation voltage flexibility are prime candidates for wireless structural health monitoring. The batteries in typical nodes have limited energy density, which eliminates the usage of more power-hungry linear-variable differential transformer (LVDT) and eddy current sensors that have been used for many years in crack monitoring. As compared to these sensors, power consumption of the potentiometer is considerably smaller and thus prolongs the battery life of this system in periods of prolonged absence of sunlight.

The potentiometer chosen for wireless sensing is a subminiature position transducer. The sensor consists of a stainless steel extension cable wound on a threaded drum coupled to a rotary sensor, all of which is housed in a plastic block. The cable is anchored on the opposite side of the crack. Displacement of the crack extends the cable, which rotates the drum and changes the sensor output linearly between ground and the excitation voltage. This potentiometer is capable of measuring dynamic response (Ozer, 2005). However, as with all other wireless systems, there is insufficient battery life to maintain the 1000 samples per second operation necessary to capture dynamic events (Kotowsky, 2010).

As with the LVDTs, the more standard crack displacement sensor no additional electronics are required, which simplifies installation. While specifications indicate that this potentiometer's operational temperature range is –65 to +125° C, it has been qualified in a un-moderated garage with humidity's between 60 to 90% and temperatures between 10 to 30° C. As of the writing it has not been employed outside, where it can be exposed to rain.

As with other sensors, theoretical resolution can be calculated directly from sensor range and the specifications of the analog-to-digital converter employed in the sensor node. Full-scale range of the string potentiometer is 3.8 centimeters and the node utilizes a 10-bit analog-to-digital converter, rendering an effective resolution of .0038 centimeters. With the signal conditioner installed, the effective resolution is increased by a factor of approximately 10, for about 3.8 μm, implying that the sensing system is approximately 38 times less sensitive than a system employing an LVDT.

Results

Results will be described in terms of field qualification, which, as introduced above, are 1) fidelity of the measured crack response, 2) ease of installation, 3) resolution of the SHM

measurement, micro-meter opening and closing of cracks, and 4) duration of operation under a variety of conditions without intervention.

1) Fidelity of Crack Response

Fidelity of crack response will be determined by comparison of long-term response, e.g. response that is monitored with timed measurements at specific intervals. At this time wireless systems are capable of measuring responses as long as they only need to sense a few times every hour, which allows them to operate in a low-power mode for most of their deployment life. Because continuous sensing to record random dynamic response would cause the node to remain in a high-power-usage state, wireless systems are only capable of monitoring in this mode for periods no longer than a couple of hours.

In order to assess fidelity of the measurement of crack response by the wireless system, its measurements must be compared to those made by another system. During qualification of this system, two other systems were measuring response of the living room shear and bedroom ceiling cracks. These systems will be referred to as Wireless 1 (W1) and Wireless 2 (W2). The W2 is the standard system employed by the majority of past autonomous crack measurement (ACM) research. The W1 system is a newly developed, lower cost version of the ACM system based (Koegel, 2011). In this test house, one of each of these systems are deployed using LVDTs to measure micrometer response of cracks to both long term and dynamic phenomena. Space does not permit a detailed discussion of these systems, but they are described in detail in internal ITI reports (Koegel 2011).

Crack response measurements over a two-month period returned by these three systems are compared in Figure E-9. Responses, in micrometers, measured by the three systems are plotted on top of each other for each crack with time along the horizontal axis. These long-term responses are the aggregation of measurements made autonomously every hour by the W1 and W2 and every 15 minutes by the wireless nodes

The three systems return the same response over time for the crack in the interior, second floor ceiling. If the crack response is the same at all gauge locations, the systems are expected to return the same measurement. This expectation is verified by previous work comparing response of LVDT and potentiometer gauges (Ozer, 2005)

There is a difference in the responses of the three systems for the shear crack on the south facing exterior wall. The differences occur mainly at the beginning and end of the observation period. Over the two-month observation period, the gauge attached to the wireless node responds less than the other two. The W1 LVDT is to the left of the red circle and the node potentiometer and W2 LVDT are in the circle.

Detailed fidelity of the wireless system is good on a daily basis as shown by the comparison of the potentiometer response with that of the LVDT response in Figure E-10 This figure displays the same information as in Figure E-9 only separated and in more detail. In addition to the overall similarity, two areas called out by the vertical lines describe areas that demonstrate fidelity in both long term and daily responses. The daily responses are the oscillations with a return period of one day in the left vertical line and the longer lasting drop on the right is the result of a longer-term climatological influence.

While the object of this report is not a study of crack response, a brief discussion places this study in context. In Figure E-9 crack responses (at the top) are compared to the changes in exterior and interior temperature and humidity at the bottom. As can be seen, the rise in external

temperature beginning in April induces a consistent change in both cracks. This rise in external temperature is accompanied by an increase in interior temperature and humidity. This change in humidity causes the wood in the house to swell and shrink, which induces large changes in crack width. Over the course of these observations, the two cracks changed width by some 75 micrometers several times. In contrast, a quarry blast with peak particle velocities between 5 and 15 millimeters per second (mmps) only produced dynamic crack displacements of 1.5 to 3.1 micrometers at the shear crack and 3.1 to 6.4 micrometers at the ceiling crack. This dynamic response is an order of magnitude less than that produced by climatological changes.

While this and most wireless system measure long term, climatological crack response well (1 to 4 samples per hour), they cannot measure short term, dynamic response (1000 samples per second) during long time intervals. This generic deficiency is the result of the lack of power provided by batteries small enough to be compatible with the small size of wireless systems. Dynamic events require continuous operation and thus quickly deplete battery power, whereas long term data can be captured by powering up only at selected times, say one can hour. In particular, dynamic events are captured by continuously recording at a high data rate and saving records that contain a data that exceed a threshold. Thus they must continuously record.

The long term data, which are measured once an hour, can provide dynamic response information by comparison of before and after blast crack width measures. For instance, a change in the long-term cyclical pattern of crack response after a dynamic event would indicate some change induced by the event. Only changes in pattern are diagnostic. Given the large crack change in crack response shown in Figures E-9 & E-10 produced by long-term environmental factors during an hour without a dynamic event, these changes would have to be large to be significant.

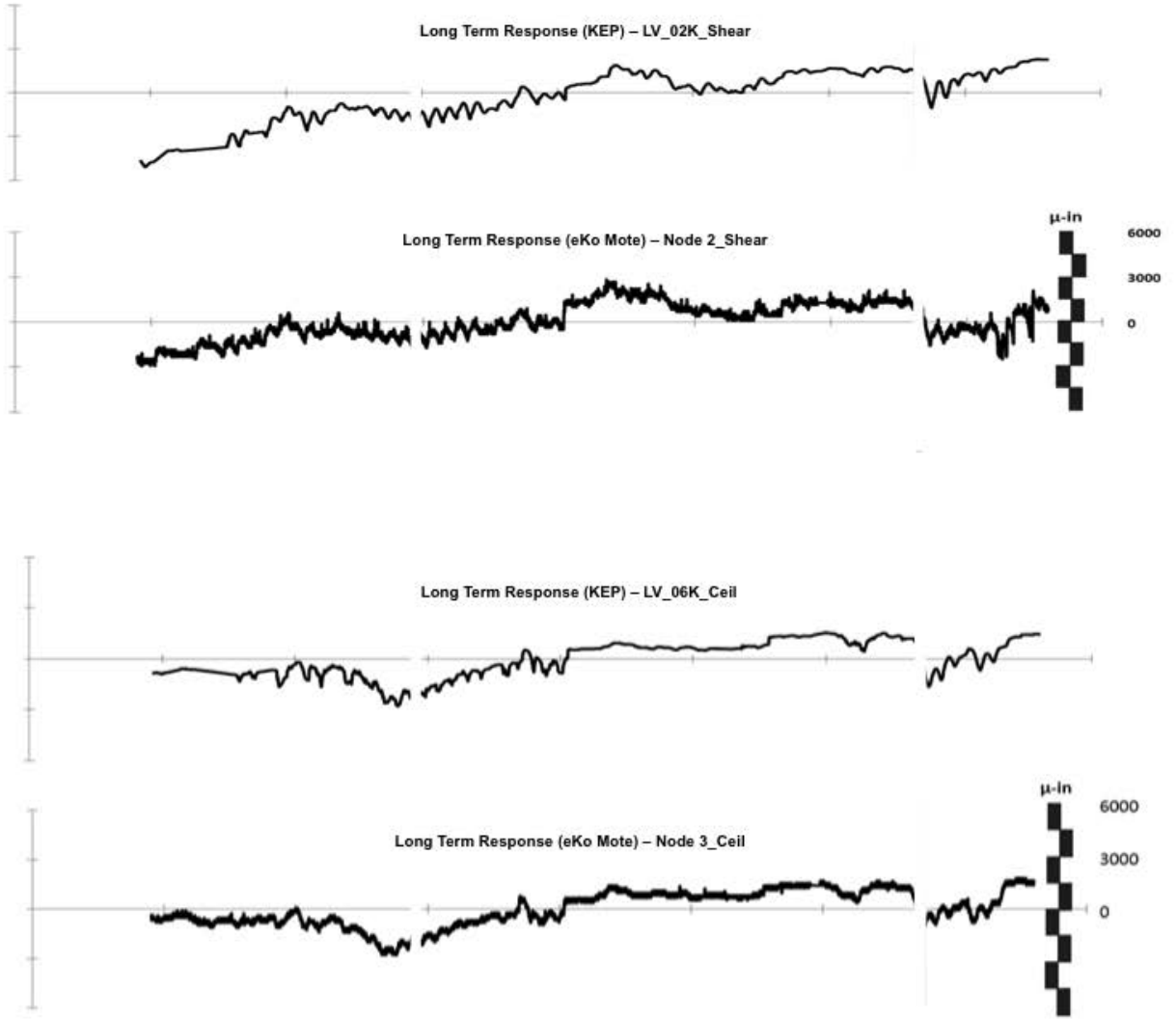

Figure E-10: Comparison of the long-term responses of the shear and ceiling cracks as provided by the W1 and wireless node systems.

2) Installation

A discussion of the installation differences will be divided into three components: complexity, ease of installation, and cost. Comparison will be based on installation of two similar systems, which differ mainly in their wiring and power, and distribution of sensing activities; the wireless sensor system and the wired W2 .The systems will both monitor 3 crack and null sensors (for a total of 6) and 2 sets of indoor and outdoor temperature and humidity gauges (for a total of 4 more and a grand total of 10 channels of data. While the W2 has a greater capability, the comparison will be made on the basis of a need for only 10 channels. As described below the main differences are the lower node costs and lower wiring costs of the wireless system.

Complexity can be assessed by considering the sensors, their physical nature and the installation procedure, as well as the integration of the systems with the internet. The attachment process for the displacement transducers is basically the same. While differing slightly in size

they both consist of a component glued to the wall on either side of the crack. The sensor output wires for the wireless system only need to be connected to the nearest node, while the sensor output wires for the W2 system need to be strung all the way back to the single, centrally-located W2. Both require an internet connection: the wireless base station and the W2 have standard Ethernet ports with statically or dynamically-assigned IP addresses. The main operational difference in sensor installation between these two systems is the process of zeroing the sensor. The W2's high sample rate and real-time display capabilities allow sensor zeroing to be completed in under two minutes per sensor.(the time necessary for the glue to cure), whereas the process requires some 10 or more minutes for each sensor connected to a wireless node because of the 15-second data acquisition interval during the first hour after each node is powered on.

Ease of installation can be assessed by considering wiring, power, sensor power requirements, and location restrictions. Wired systems can require up to 10 person-hours to run the wires to the sensors, often requiring drilling through walls, while the wireless system wiring time is part of the transducer installation. Thus wired systems require some ten hours of additional installation time. Both systems require standard household power. The wired W2 and its associated support electronics supply power to the transducers, while the wireless nodes supply transducer power from their own batteries. The wireless nodes should be placed by windows for solar power or if possible supplemented with a panel in a sunny location. This location requirement complicates the placement of the nodes.

Finally, cost can be determined by considering the wiring, transducers, data loggers, and internet connection. Research grade instrumentation wire and its associated modular connectors cost approximately $5.00 per meter. A typical house could require some 90 meters of instrumentation cable costing some $300 to $500 for a wired W2 system, but less than $100 for the wireless nodes. The transducer costs are similar ~ $200 for each of the displacement transducers or a cost of $2000 for each type of system. The main equipment cost difference is the cost of the systems: A 3 node wireless system with base station might cost ~ $3,500, whereas the W2 system might cost as much as $ 10,000.

3) Resolution of SHM measurement

Resolution of the base mote-based system needed to be improved with the signal conditioner module as introduced in the instrumentation section. This enhancement was needed to increase the resolution of the measurement of crack responses. Since a wireless node has only a 10-bit analog-to-digital converter, it can only divide the measurement range into 2^{10} or 1024 subdivisions. Because the excitation voltage is the same as the maximum voltage measureable by the analog-to-digital converter, the mote will always divide the entire 3.8 centimeter range of the potentiometer by 1024, yielding an effective resolution of approximately 0.0025 centimeters

The signal conditioner module improves resolution in two ways: it increases the excitation voltage supplied to the potentiometer and it amplifies the output signal from the string potentiometer as it is fed back into the mote's analog-to-digital converter. Because the range of the analog-to-digital converter is not increased, this effectively decreases the range of the sensor by a factor of 10, but also increases the resolution by a factor of 10. Resolution can be further increased, at the expense of total sensor range, by performing hardware modifications to the signal conditioner module. These modifications were not made for this experiment.

The effect of the improved resolution is shown in the comparison of the long term response the shear crack (from node 2) before and after installation of the signal conditioner in

Figure E-11. During similar transitions between heating and cooling seasons (September before and May after) the variability produced by the daily swings is more prominent after the addition of the signal conditioner.

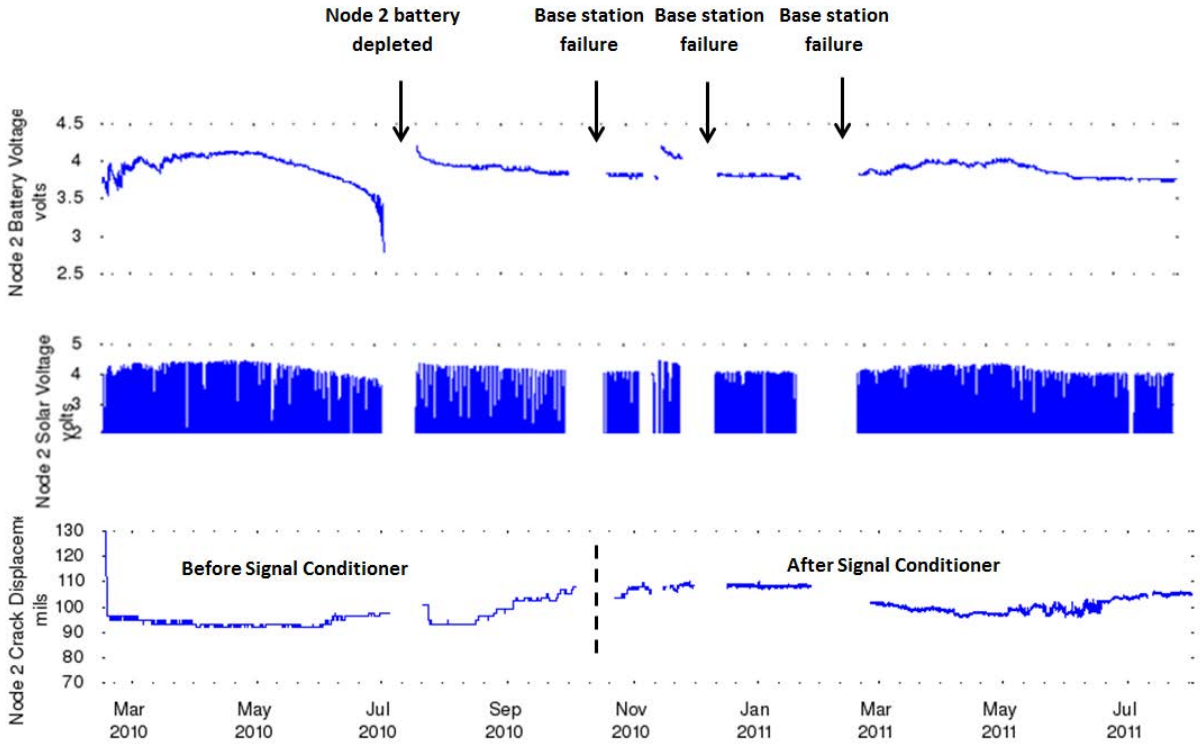

Figure E-11: Top: Comparison of wireless system's battery life during one year of operation. Upper graph: Node 2 depletion occurred because of the leaf induced shading of the window in which the node was installed. Middle: Solar voltage shows fluctuations increasing after leaves blossomed. Bottom: Comparison of the crack displacements recorded by the same node before (left) and after (right) addition of the signal conditioning board to amplify the signal.

4) Duration of operation

Duration of operation is controlled predominantly by the battery life and ease of recharging. Recharging capability is function of exposure to sun light, and exposure is a complex mixture of location and angle between sun and photovoltaic cells. Locations of nodes 2 and 3 present different exposure environments. Node 3 faces east and generally receives less sunlight than node 2. However, both are shadowed by trees, so the density of the leaves as a function of the season also affects the ability of the nodes to recharge. Figure E-11 compares solar voltage and battery voltage for the two nodes. First ignore system failures induced by failure of the base station. Node 3's battery died (lack of signal after fall in voltage) twice and node 2 only once. All node failures occurred during the summer when the leafy trees shadowed both windows.

While not shown here, nodes 4 and 5 (the nodes deployed outdoors and away from trees) did not fail during the one and a quarter year of observation.

The base station failures are not related to solar recharging as it operates with 110 v AC power. These failures are a result of long-term instability of the manufacturer-supplied software that runs the base station. This instability has been largely improved by upgrades supplied by the manufacturer.

5) Ease of Operation

The wireless node system includes its own graphical display interface, a screen shot of which is shown in Figure E-12. As long as the smallest sample interval needed is 15 minutes, this preprogrammed graphical interface can be employed with minimal learning. The crack response as well as the temperature, humidity and battery condition can all be tracked in real time (+/- 15 minutes) .

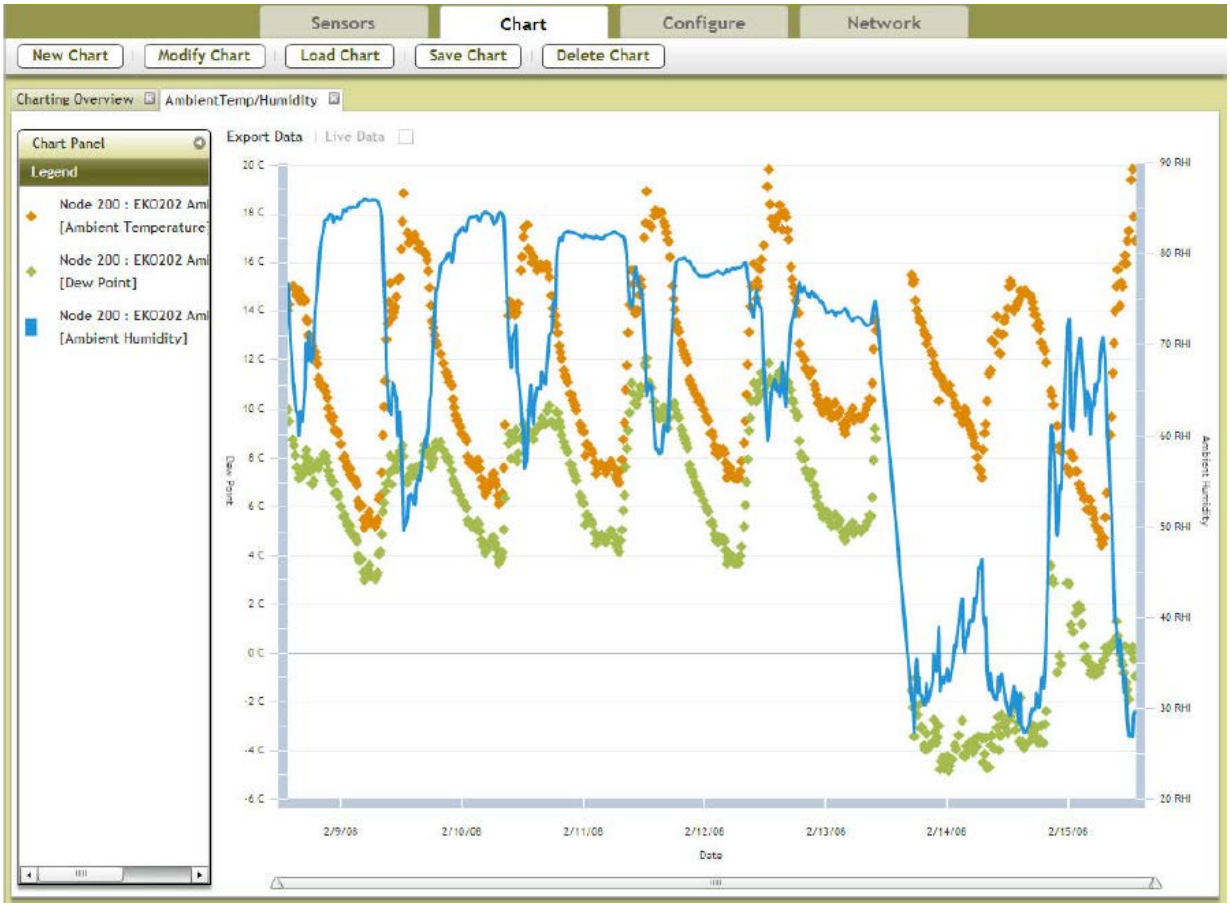

Figure E-12: Preprogrammed graphical users interface supplied by the wireless system's manufacturer. Data can be either plotted in their raw point form (triangles) or interpolated line form (solid). (Manufacturer's Users Manual-Meissner, 2010)

Phase E Findings & Conclusions

This study was undertaken to qualify the use of a wireless "node" system to track crack responses (changes in crack width) to climatological effects. Systems like this can be employed to monitor performance of any component of a constructed facility that involves cracking or relative displacements. Qualification was assessed by comparison of responses of the same crack as measured by the wireless "node" system compared to two wired systems, W2 and W1. In addition the ease and cost of installation of the wireless system was compared with that for the wired W2. The following conclusions were reached within the scope of the comparisons made. Since the wireless, "node" system is typical of such systems, these conclusions can be extrapolated to the class. If better performing equipment were available, it would have been employed. Of course as development continues with the typical speed of digital electronics, one should expect some of the observations to become dated. The wireless "node" system:

1) measures the long term crack response as well as the wired system(s),
2) has less crack response resolution than does the wired system even if a signal-conditioning unit is installed,
3) cannot capture dynamic responses directly, but can provide indirect detection if large changes in the cyclic response patterns occur at a time of a dynamic event,
4) is easier to install and less complex than wired systems,
5) is less costly (half the cost of a wired system),
6) operates autonomously as doses the wired system,
7) graphically displays long term crack responses autonomously over the internet as do wired systems,
8) can operate for intervals of time approaching a year provided that the nodes are placed near windows that are not shaded by deciduous trees.

MEMS Micro Electro-Mechanical Systems for Wirelessly Monitoring the Health of Transportation Related Structures:

References

Baillot, R. (2004). Crack response of a historic structure to weather effects and construction vibrations. Master's Thesis, Northwestern University, Evanston, IL.

Bourns, I. (2006). 4600X Series - Thick Film Conformal SIPs.

Crossbow Technology, Inc. (2007a). MDA300CA Data Acquisition Board. http://www.xbow.com/Products/Product pdf files/Wireless pdf/ MDA300CA_Datasheet.pdf.

Crossbow Technology, Inc. (2007b). MPR-MIB Users Manual. http://www.xbow.com/Support/Support pdf files/MPR-MIB Series Users Manual.pdf.

Crossbow Technology, Inc. (2007c). MTS/MDA Sensor Board Users Manual. http://www.xbow.com/Support/Support pdf files/MTS-MDA Series Users Manual. pdf.

Crossbow Technology, Inc. (2007d). Stargate Gateway. http://www.xbow.com/Products/Product pdf files/Wireless pdf/Stargate Datasheet.pdf.

Crossbow Technology, Inc. (2007e). XMesh Users Manual. http://www.xbow.com/Support/Support pdf files/XMesh Users Manual.pdf.

Crossbow Technology, Inc. (2009a).eko pro series data sheet. http://www.xbow.com/eko/pdf/eKo pro series Datasheet.pdf.

Crossbow Technology, Inc. (2009b). eKo pro series users manual. http://www.xbow.com/eko/pdf/eKo Pro Series Users Manual.pdf. Crossbow Technology, Inc. (2009c). ESB developer's guide.

Crossbow Technology, Inc. (2009d). MIB 510 Serial Interface Board. http://www.xbow.com/Products/Product pdf files/Wireless pdf/ MIB510CA Datasheet.pdf.

Crossbow Technology, Inc. (2009e). MICA2 Wireless Measurement System. http://www.xbow.com/Products/Product pdf files/Wireless pdf/ MICA2 Datasheet.pdf.

Dowding, C. H. (1996). Construction Vibrations. Prentice Hall, Upper Saddle River, New Jersey.

Dowding, C. H., Kotowsky, M. P., and Ozer, H. (2007). Multi-hop wireless system crack measurement for control of blasting vibrations. In Proc. 7th Int'l Symposium on Field

Mea- surements in Geomechanics, Boston, Massachusetts. American Society of Civil Engineers.

Energizer Holdings, I. (2010a). Product datasheet: Energizer e91. http://data.energizer.com/PDFs/E91.pdf.

Energizer Holdings, I. (2010b). Product datasheet: Energizer l91. http://data.energizer.com/PDFs/l91.pdf.

Firstmark Controls (2010). Data sheet - series 150 subminiature position transducer. http://www.firstmarkcontrols.com/s021f.htm.

for Testing, A. S. and Materials (2006). Standard Test Method for Determination of Resistance to Stable Crack Extension under Low-Constraint Conditions. ASTM E2472.

Geo Space Corporation (1980). GEO GS-14-L3 28 HZ 570 OHM. Part number 41065.

Geo Space Corporation (1996). HS-1-LT 4.5Hz 1250 Ohm Horiz. Part number 98449.

Hopwood, T. (2008). Personal communication with University of Kentucky researcher.

Hopwood, T. and Prine, D. (1987). Acoustic emission monitoring of in-service bridges Technical Report UKTRP-87-22, Kentucky Transportation Research Program, University of Kentucky, Lexington, Kentucky.

ITW CHEMTRONICS (2009). CircuitWoprks Conductive Pen TDS Num. CW2200.

Jevtic, S., Kotowsky, M. P., Dick, R. P., Dinda, P. A., and Dowding, C. H. (2007a). Lucid dreaming: Reliable analog event detection for energy-constrained applications. In Proc. IPSN-SPOTS 2007, Cambridge, Massachusetts. Association for Computing Machinery / Institute of Electrical and Electronics Engineers.

Jevtic, S., Kotowsky, M. P., Dick, R. P., Dinda, P. A., Dowding, C. H., and Mattenson, M. J. (2007b). Lucid dreaming: Reliable analog event detection for energy-constrained applications. Poster presented during live demonstration.

Kaman Measuring Systems (2009). Sensor data sheet: SMU-9000. http://www.kamansensors.com/html/products/pdf/wSMU9000-9200.pdf.

Koegel, T. (2011) Comparative Report, Internal Report for the Infrastructure Technology Institute, Northwestern University, Evanston, IL, and archived in the Northwestern University Transportation Library.

Kosnik, D. E. (2007). Internet-enabled geotechnical data exchange. In Proc. 7th Int'l Symposium on Field Measurements in Geomechanics, Boston, Massachusetts. American Society of Civil Engineers.

Kotowsky, M. (2010) "Wireless Sensor Networks for Monitoring Cracks in Structures", Master's Thesis, Department of Civil Engineering, Northwestern University, Evanston, IL.

Kotowsky, M. P., Dowding, C. H., and Fuller, J. K. (2009). Poster summary: Wireless sensor networks to monitor crack growth on bridges. In Proceedings, Developing a Research Agenda for Transportation Infrastructure Preservation and Renewal Conference, Washington, DC. Transportation Research Board.

Louis, M. (2000). Autonomous Crack Comparometer Phase II. Master's Thesis, Northwestern University, Evanston, IL.

Macro Sensors (2009). Macro sensors LVDTs: DC-750 series general purpose DC-LVDT position sensors. http://www.macrosensors.com/lvdt macro sensors/ lvdt products/lvdt position sensors/dc lvdt/free core dc/dc 750 general purpose.html.

Marron, D. R. (2010). Personal communication with Chief Research Engineer at the Infrastructure Technology Institute at Northwestern University.

Maxim Integrated Products (2003). SOT23, Dual, Precision, 1.8V, Nanopower Comparators With/Without Reference. Part number MAX9020EKA-T.

Maxim Integrated Products, Inc. (2009). 1024-bit, 1-wire eeprom data sheet.

McKenna, L. M. (2002). Comparison of measured crack response in diverse structures to dynamic events and weather phenomena. Master's Thesis, Northwestern University, Evanston, IL.

Meissner (2010) "Installation report for Sycamore test house" Internal Report for the Infrastructure Technology Institute, Northwestern University, Evanston, IL, and archived in the Northwestern University Transportation Library.

Moxa, Inc (2010). UC-7410/7420 Series. http://www.moxa.com/doc/specs/ UC-7410 7420 Series.pdf.

Ozer, H. (2005) "Wireless Crack Measurement for the control of construction vibrations", Master's Thesis, Department of Civil Engineering, Northwestern University, Evanston, IL. .

Puccio, M. (2010). Personal communication with Application Engineer of Macro Sensors.

Siebert, D. (2000). Autonomous Crack Comparometer. Master's Thesis, Northwestern University, Evanston, IL.

Snider, M. (2003). Crack response to weather effects, blasting, and construction vibrations. Master's Thesis, Northwestern University, Evanston, IL.

SOLA HD (2009). SCL Series, 4 and 10 Watt CE Linears. http://www.solahd.com/products/powersupplies/pdfs/SCL.pdf.

SoMat, Inc. (2010). eDAQ Simultaneous High Level Layer. http://www.somat.com/products/edaq/edaq simultaneous high level layer_html#tabs-1-2.

Speckman, G. M. (2010). Personal communication with Regional Sales Manager of Kaman Sensors.

Stolze, F., J.Staszewski, W., Manson, G., and Worden, K. (2009). Fatigue crack detection in a multi-riveted strap joint aluminium panel. In Kundu, T., editor, Health monitoring of structural and biological systems, volume 7925. Bellingham, Wash. : SPIE.

Switchcraft Inc. (2004). EN3™ Cord Connector.

The Sherwin-Williams Company (2019). MACROPOXY 646 FAST CURE EPOXY.

United States Department of Transportation: Federal Highway Administration (2006). Bridge Inspector's Reference Manual, volume 2. National Highway Institute.

Vishay Intertechnology, Inc. (2008). Special use sensors - crack propagation sensors.

Waldron, M. (2006). Residential crack response to vibrations from underground mining. Master's Thesis, Northwestern University, Evanston, IL.